Studies on the mechanism of the mammalian sex determination with XX masculinized gonads

(XX 精巣化性腺を用いた哺乳類の性分化機構に関する研究)

Kyoko Harikae

張替　香生子

Department of Veterinary Anatomy

Graduate School of Agricultural and Life Sciences

The University of Tokyo

CONTENTS

General Introduction

Why are there two types of humans? In other words, men and women. This has been the basic question since the ancient era. For not only humans but also all animals, sex is one of the most important factors. Precise sex determination is the key to precise reproduction and survival of species. Once, it had been thought that children's sex is dependent on environment, such as nutrition, temperature or parents' age. In 1902, Edmund B. Wilson demonstrated the sex determination of insects, which had XX sex chromosomes for female and XY or XO for male (Wilson, 1902), and established the concept that sex is determined by specific nuclear component. Fifteen years later, Frank R. Lillie explained that gonads had identical characteristics in both XX and XY until a certain stage, and differentiated into each sex by zygotic and hormonal factors (Lillie, 1917). In 1947, Alfred Jost removed undifferentiated fetal rabbit gonads and found that even in XY rabbits, they became a female phenotype. Although Jost observed only genitalia and ductal systems, female state had been regarded as the "default" of the male for a long time (Jost, 1947). That is to say, if male factor had not affected undifferentiated gonads, ovary was thought to spontaneously develop.

Until now, sex-determining gene on Y chromosome, *SRY*, was discovered in 1990 and its many up- and down-stream gene cascades have been revealed (Sinclair et al., 1990; Koopman et al., 1991). Gonads arise as a bipotential state in regardless of XX or XY, and they have the potency to differentiate into both testes and ovaries. Male sex determination starts first at these gonads during the specific fetal period by "male genes" like *SRY*, Sry-box containing 9 (*SOX9*), Fibroblast growth factor 9 (*FGF9*), Anti-Müllerian hormone (*AMH*), Doublesex and mab-3 related transcription factor 1 (*DMRT1*) and so on (Figure of General Introduction) (Behringer et al., 1990; Kent et al., 1996; Colvin et al., 2001; Matson et al, 2011). After gonads differentiate into testes, hormones produced by testes masculinize the other internal

and external reproductive organs. Contrary to male, it remains to be known how ovaries develop from undifferentiated gonads. Recently, it has been reported that bipotential gonads originally have the bias primed with female (Jameson et al., 2012). This fact partially supports "ovary default hypothesis", but some experiments raise question toward it. First, as Lillie indicated in his paper in 1917, morphological XX masculinization like bovine freemartin syndrome is observed in nature. Almost all XX bovines born with XY co-twins cause freemartin syndrome, probably because of the exposure of male hormones to XX fetuses, and thus XX freemartin calves are suspected to have no ectopic male genes. However, in freemartin gonads, degenerated ovaries or even seminiferous tubule-like structures are observed. Such XX masculinization without any male-specific genes clearly suggests the presence of genes essential for ovarian differentiation. The precise molecular level of masculinization in freemartin syndrome is not known, though. Second, it is during only limited period that enforced expression of *Sry* on XX gonads is able to cause XX sex reversal (Hiramatsu et al., 2009). From embryonic day 11.0 (E11.0) to 11.25, during only 6 hours, forced *Sry* induces XX gonads to become complete testes. After this period, XX gonads differentiate into ovaries even under *Sry* expression. These experiments clearly demonstrate the presence of unknown *positive* ovary-determining pathway, rather than *passive* default ovarian pathway. At present, some candidates for *positive* ovary-determining genes like wingless-related MMTV integration site 4 (*WNT4*), Forkhead box protein L2 (*FOXL2*) and estrogen receptors (*ER*α/β) are found because of their XX sex-reversal phenotypes in case of lacking each gene (Couse et al., 1999; Vainio et al., 1999; Uda et al., 2004; Uhlenhaut et al., 2009). However, importantly, aberrant ovarian phenotype is only observed from post-natal periods. Therefore, it is still mystery how ovary differentiates and/or maintains itself during fetal periods.

In this study, by means of bovine and mouse XX masculinized gonads, I challenged to clarify the novel mammalian sex determination system, especially ovarian sex determination. In Chapter 1, I report a case of freemartin calf, which had almost complete testes with XX sex chromosomes, and showed the bovine XX sex-reversal without *SRY*. In Chapter 2, through analyses of developing XX ovaries with forced expression of *Sry*, I demonstrate the small population of ovarian granulosa cells with sexual bipotency present from fetal to post-natal periods, and indicate that ovarian sex determination is associated with high heterogeneity and sexual bipotency. In addition, I succeeded to identify the novel candidates for presumptive ovary-determining genes. In Chapter 3, I define how XX sex reversal occurs in both morphological and genetical aspects, and suggest the presence of testis forming pathway conserved among vertebrates by using experimental XX sex reversal models. My findings should be an important guide for future researches on mammalian sex determination.

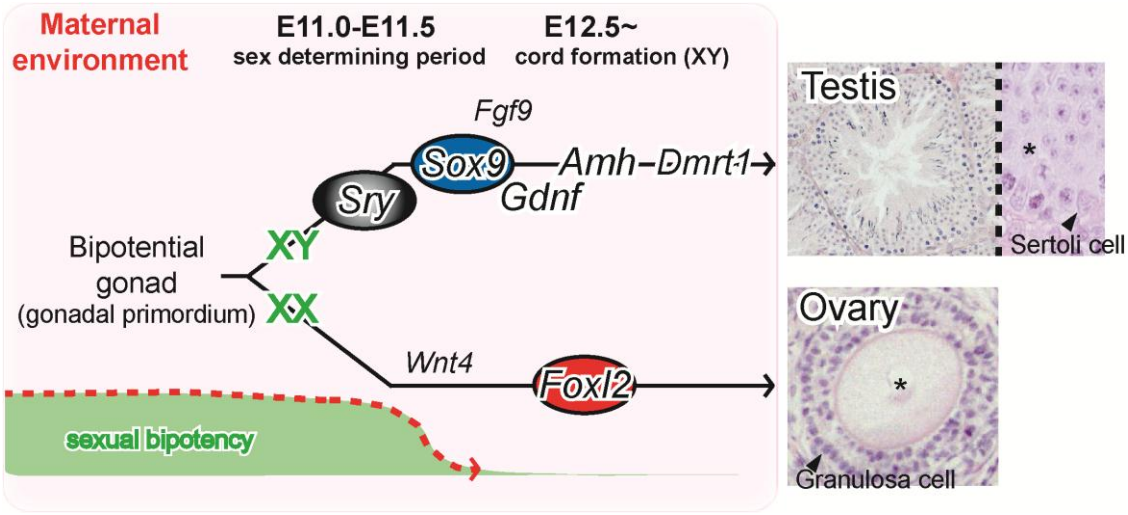

FIGURE OF GENERAL INTRODUCTION

Figure of General Introduction: Schematic view of mouse sex determination

Gonads arise with high sexual bipotency around embryonic day 10.5 (E10.5: embryonic day corresponds to days after fertilization) during pregnancy (under maternal environment). From E11.0, sex-determining gene on Y chromosome, *Sry* starts testis differentiation in somatic cells of XY gonads. *Sry* induces its downstream factors such as *Sox9, Fgf9* and *Gdnf* at around E11.5, *Amh* at E12.5 and *Dmrt1* at E13.5. These factors contribute to functional differentiation of Sertoli cells (somatic/supporting cells in XY testis) and morphological formation of testis cords. On the other hand, in XX gonads, few genes and morphological changes involving ovarian sex determination/differentiation are known. From around E11.5, XX-specific *Wnt4* expression begins, and *Foxl2* starts its expression at E12.5 in pre-granulosa cells (somatic/supporting cells in XX ovary). Follicle formation in XX ovaries are observed after birth. Along with sex determination, it is thought that sexual bipotentiality in somatic cells disappears.

Chapter 1

Evidence for almost complete sex-reversal in bovine freemartin gonads: formation of seminiferous tubule-like structures and transdifferentiation into typical testicular cell types.

Abstract

During mammalian sex determination of XY fetuses, SRY induces SOX9 in Sertoli cells, resulting in formation of testes with seminiferous tubules, interstitial Leydig cells and peritubular myoid cells. Meanwhile XX fetuses without *SRY* develop ovaries. In cattle, most XX heifers born with a male twin, so-called freemartins, develop nonfunctioning ovaries and genitalia with an intersex phenotype. Interestingly, freemartins sometimes develop highly masculinized gonads with seminiferous tubule-like structures despite the absence of *SRY*. However, in these cases, the degree of masculinization in each gonadal somatic cell type is unclear. Here, I report a rare case of a freemartin Japanese black calf with almost complete XX sex reversal. Gross anatomical analysis of this calf revealed the presence of a pair of small testis-like gonads with rudimentary epididymides, in addition to highly masculinized genitalia including a pampiniform plexus, scrotum and vesicular gland. Histological and immunohistochemical analyses of these masculinized gonads revealed well-defined seminiferous tubule-like structures throughout the whole gonadal parenchyma. In epithelia of these tubules, SOX9-positive supporting cells (i.e., Sertoli cells) were found to be arranged regularly along the bases of tubules, and they were also positive for GDNF, one of the major factors for spermatogenesis. 3β-HSD-positive cells (i.e., Leydig cells) and SMA-positive peritubular myoid cells were also identified around tubules. Therefore, for the first time, I found the transdifferentiation of ovarian somatic cells into all testicular somatic cell types in the XX freemartin gonads. These data strongly support the idea of a high sexual plasticity in the ovarian somatic cells of mammalian gonads.

Introduction

In mammals, the sex determination of gonads plays a pivotal role in the development of internal and external genitalia, secondary sexual characteristics and sexual behavior. Gonads arise in an undifferentiated state during the fetal period, as both Sertoli cells in the testes and granulosa cells in the ovaries develop from a common supporting cell precursor (Albrecht and Eicher, 2001). A sex chromosome genotype of XY leads to the development of a sex-determining region on the Y chromosome (*SRY*) gene, which induces downstream factors such as Sry-box containing gene 9 (*SOX9*), anti-Müllerian hormone (*AMH*) and glial cell line-derived neurotrophic factor (*GDNF*) in Sertoli cells to differentiate bipotential gonads into testes (Behringer et al., 1990; Koopman et al., 1990; Meng et al., 2000; Sekido and Lovell-Badge, 2008). Without *SRY*, XX gonads normally develop into ovaries, which comprise granulosa cells as supporting cells and theca cells as interstitial cells. Of the many factors involved in sex determination, *SOX9* is essential for both testicular differentiation and maintenance. Indeed, similar to *SRY*, gain- or loss-of-function of *SOX9* leads to sex reversal (Foster et al., 1994; Wagner et al., 1994; Vidal et al., 2001).

Testes are composed of seminiferous tubules containing germ cells and Sertoli cells within the epithelia. Surrounding the tubules, peritubular myoid cells support the basement membrane. Leydig cells produce steroid hormones via enzymatic activity such as 3β-HSD in the interstitial areas among seminiferous tubules. At puberty in XY males, these hormones secreted from testes lead to the development of secondary sexual characteristics such as accessory reproductive glands (vesicular, prostate, and bulbourethral glands), the pampiniform plexus and the scrotum.

As mentioned previously, mammalian sex determination is highly controlled by genetic programming. However, animals exhibiting XX sex reversal (XX maleness) without *SRY* are sporadically reported.In particular, freemartin syndrome, which is exhibited in XX female fetuses with male twins, has been recognized among farmers and researchers for centuries (Marcum, 1974; Capel and Coveney, 2004). It is reported that calves with freemartin syndrome exhibit varying degrees of female-to-male sex reversal, mainly of internal and external genitalia, by histological or anatomical methods. For example, Ghanem et al. (2005) and Payan-Carreira et al. (2008) showed case reports of gonads of new-born freemartin calves with abnormal genital tracts and ovarian dysplasia (i.e., no ovarian structures in gonads) (Ghanem et al., 2005; Payan-Carreira et al., 2008). Jost et al. (1972) examined 48 freemartin fetuses and also observed inhibition of ovarian growth and dysplasia of Müllerian ducts in all fetuses, although there were no seminiferous tubules (Jost et al., 1972). On the other hand, Dominguez et al. (1990) reported rows of cells resembling seminiferous epithelia and Leydig-like cells in some cases of over 70-day-old freemartin fetuses (Dominguez et al., 1990). Although the causes of freemartin syndrome remain debated, AMH (anti-Müllerian hormone) has been identified as one of the major candidate causal agents. In more than 90% of heterosexual twin pregnancies, common vascular connections form between the placentas of the female and male fetuses; XX/XY chimerism in blood cells is used to diagnose freemartin syndrome (Jost et al., 1972; Padula, 2005). Thus, it is hypothesized that hormones from the male co-twin, including AMH, cause the XX female co-twin to experience female-to-male sex-reversal during development (Vigier et al., 1984; Cabianca et al., 2007). Indeed, bovine AMH causes sexreversal-like freemartin syndrome in rat ovaries (Vigier et al., 1987). Despite this extensive research into the causes and anatomical aspects of freemartins,

there are no analyses of the expression patterns of proteins related to sexual development and the degree of masculinization in freemartin gonads.

Here, I report one rare case of a freemartin calf exhibiting severe masculinization of both external and internal genitalia. I demonstrate the presence of highly differentiated Sertoli cells positive for SOX9 and GDNF, peritubular myoid cells and 3β-HSD-positive Leydig cells in these freemartin gonads. This study clearly confirms the transdifferentiation of ovarian somatic cells into all types of testicular somatic cells, Sertoli, Leydig and peritubular myoid cells, in a freemartin calf. My findings have important implications, as they reveal that mammalian XX ovaries have a high potential for sexual plasticity.

Materials and methods

Animals

Spayed gonads were obtained from a 6-month-old female Japanese black calf (*Bos taurus*) that was born in Kagoshima, Japan, with a male twin. Blood and hair follicles were obtained for polymerase chain reaction (PCR) analysis. I used the castrated gonads of a 5-month-old male Holstein calf born in Gunma, Japan, as a control.

PCR

Genomic DNA was amplified using the following PCR profile for 35 cycles: denaturation at 94 ^{o}C for 30 sec, annealing at 60 ^{o}C for 60 sec, and extension at 72 ^{o}C for 60 sec. The amelogenin (Miller and Koopman, 1990) primers were used for detection of the X and Y chromosomes, and BOV97M (Ghanem et al., 2006) was used for the Y chromosome. The PCR products were visualized by gel electrophoresis on a 2% TBE agarose gel stained with SYBR Green.

Histology and immunohistochemistry

The removed gonads were immediately fixed in 4% paraformaldehyde (4% PFA) on ice and transported to the laboratory for further examination. After fixation, they were embedded in paraffin, and 7 μm sections were cut. Deparaffinized sections were subjected to hematoxylin-eosin (H-E) staining and immunohistochemical staining.

For immunohistochemical staining, sections were incubated with anti-DDX4/MVH (1:7,500 dilution) (Toyooka et al., 2000) (kindly provided by Dr. Toshiaki Noce, Advanced Research Centers, Keio University, Japan), anti-SOX9 (1:150 dilution) (Kidokoro et al., 2005),

anti-GDNF (1:200 dilution; Santa Cruz Biotechnology, Santa Cruz, CA, USA), anti-α-Smooth Muscle Actin (1:5,000 dilution; Clone number 1A4; Sigma Chemical Co, St. Louis, MO, USA) (Devkota et al., 2006), anti-SF1/Ad4BP antibody (1:10,000 dilution) (kindly provided by Dr. Ken-ichirou Morohashi, Department of Molecular Biology, Graduate School of Medical Sciences, Kyushu University, Japan) (Hatano et al., 1994), anti-3β-HSD (1:200 dilution; sc-30821; Santa Cruz Biotechnology) (Aponte et al., 2008) and anti-AMH (1:200 dilution; sc-6886; Santa Cruz Biotechnology) at 4 C^{o} for 12 h. The reaction was visualized with biotin-conjugated secondary antibody in combination with an Elite ABC Kit (Vector Laboratories, Burlingame, CA, USA)

Results

Diagnosis of freemartin syndrome by PCR

The genomic DNA was PCR-screened using specific primers for amelogenin, which is located on the X (DNA amplified fragment size is 280 base pairs [bp]) and Y chromosomes (217 bp amplicon), and Bov97M, which is found on the Y chromosome (157 bp amplicon). Blood and hair follicle samples were obtained from the heterosexual twin calf for the diagnosis of freemartin syndrome by PCR (Fig. 1-1A). At the same time, I tested samples from normal male and female calves as a control. For the hair follicle samples, PCR analysis of the heterosexual twin showed the presence of only the X chromosome and the absence of a Y chromosome (Fig. 1-1A), while bands for both the X and Y chromosomes were detected in the normal male calf, as expected. Conversely, like the normal male calf, the blood samples from the heterosexual twin revealed X and Y chromosomes (Fig. 1-1A). These results indicate that XX/XY chimerism developed as a result of the vascular connections between the male and female fetuses and that this twin can be diagnosed as a freemartin.

The masculinization of the freemartin calf in gross anatomical appearance

To assess the level of masculinization in gross anatomical appearance, I examined the internal and external genitalia of the freemartin calf. Vaginal length was 4.5 cm, whereas that of a normal 6-month-old female calf is 13–15 cm (Padula, 2005). Long hair, similar to that seen on a male, was present around the vulva, and a prominent clitoris was also found (1.1 cm). No uterus was detected on palpation. In addition, scrota-like structures were present in the abdomen of the calf (Fig. 1-1B), and small descended gonads resembling testes were observed within that structure (Fig. 1-1C, open arrowheads). On the left gonad, I detected an

epididymis-like structure (Fig. 1-1C, black arrowhead), while a concentrated blood vessel resembling a pampiniform plexus was present on the right gonad (Fig. 1-1C, arrow). I also noticed some accessory glands on the gonads, and H-E staining confirmed that they were vesicular glands characterized by the presence of tubules with a layer of smooth muscles (Fig. 1-1D, E arrowhead) and secretions in their lumina (Fig. 1-1D). None of their epithelia, however, exhibited a columnar shape, and there were fewer fat droplets than are present in mature males (Fig. 1-1E arrows) (Khan and Foley, 1994). These gross anatomical observations from internal and external genitalia demonstrate remarkable masculinization of this freemartin calf.

Seminiferous tubule-like structures in freemartin gonads shown by histological analysis

To further examine the level of masculinization, I performed histological analysis of the gonads. H-E staining of the gonads showed the presence of seminiferous tubule structures (Fig. 1-2A, B), as seen in control XY testes (Fig. 1-2C). Tubules with a round or elliptical shape were found in both gonads equally, and no ovarian follicles were detected. In addition, cell clusters were frequently seen in the large interstitial region of the freemartin gonads (Fig. 1-2B open arrow, compared with C). These tubules of the freemartin calf appeared to lack lumina (Fig. 1-2D) compared with those of XY gonads (Fig. 1-2F). On closer inspection of both samples, layers of epithelia consisting of cells with round nuclei were observed (Fig. 1-2E, G, black arrowheads). In XY testes, abundant long and slender cells identified as peritubular myoid cells were present around the tubules (Fig. 1-2G, open arrowheads). Also in the freemartin gonads, slender peritubular cells were detected along the outer wall of the seminiferous tubule-like structures (Fig. 1-2E, open arrowheads), although this cell layer appears to be discontinuous. Cells with round nuclei and relatively large amounts of

cytoplasm were seen in the interstitial area, especially near capillaries (Fig. 1-2H, I, black arrows).

SOX9 and GDNF expression in epithelial cells in freemartin gonads detected by immunohistochemical analyses

Given that the morphological observations of the freemartin gonads revealed both extremely masculinized features and ambiguous ones, in order to determine the level of masculinization more precisely, next I performed immunohistochemical analyses to determine the expressions of proteins related to testicular development. First, I examined whether there were germ cells in the seminiferous tubule-like structures of the freemartin gonads, because loss of germ cells is a characteristic histological feature among female-to-male sex-reversed gonads in mammals (Jost et al., 1972; Dominguez et al., 1990; Pailhoux et al., 2001). Staining with the antibody anti-DDX4 (formal name; also known as mouse vasa homolog (MVH), ATP-dependent RNA helicase), which is specific for germ cells (Fig. 1-3B), clearly confirmed no positive cells in the freemartin gonads (Fig. 1-3A). Next, I tested the cells within a layer in the seminiferous tubule-like structures with antibodies specific for Sertoli cells, i.e., anti-SOX9 (a marker for Sertoli cell nuclei) and anti-GDNF (a marker for secreted proteins from Sertoli cells that is known for its important role in spermatogenic stem cell maintenance) (Meng et al., 2000). For the SOX9 antibody, the interstitial cells were negative, while the round nuclei of all the cells in the epithelia were positive in both the freemartin gonads (Fig. 1-3C, arrowheads) and control XY testes (Fig. 1-3D, arrowheads). For the GDNF antibody, the basal cytoplasm of cells in the epithelia was positive in the freemartin and control gonads (Fig. 1-3E, F). It was previously reported that adult testes lacking germ cells have a high intensity of GDNF signals (Sato et al., 2011). Although I could not recognize apparent differences between them, it

might be because of immature Sertoli cells in both the freemartin and control XY testes. These data provide evidence of the presence of Sertoli–like cells positive for SOX9 and GDNF in these XX freemartin gonads.

Expression of SF1/Ad4BP and 3β-HSD in interstitial Leydig cells in freemartin gonads

H-E staining revealed that there were a few slender cells around the seminiferous tubule-like structures in the freemartin gonads. To confirm these cell types, staining was performed with an α-smooth muscle actin (SMA) antibody, which is normally present in the peritubular myoid cells in XY testes and the external theca cells in XX ovaries. In the control XY testes, SMA-positive myoid cells were detected and formed a thick layer surrounding the seminiferous tubules (Fig. 1-4B). Perivascular smooth muscle cells were also found around the capillaries in the interstitial region (Fig. 1-4B, asterisks). In the freemartin gonads, far fewer SMA-positive cells were observed (Fig. 1-4A) with the exception of strong expression around the capillaries similar to that founds in the XY testis (Fig. 1-4A, asterisks). However, it should be noted that there were several slender peritubular cells along the tubules that were stained positive with SMA in the freemartin gonads (Fig. 1-4A), suggesting a partial and discontinuous formation of the peritubular myoid cell layer around these seminiferous tubule-like structures.

Next, I performed staining with SF1/Ad4BP, which is a marker for nuclei of cells that secrete steroids (Sertoli cells and Leydig cells in XY and granulosa cells and internal theca cells in XX) (Hatano et al., 1994). In the control XY testis, positive cells were observed both within the Sertoli cells in the seminiferous tubules (Fig. 1-4D) and within the interstitial Leydig cells (Fig. 1-4D arrow). Similarly, in the freemartin gonads, SF1/Ad4BP was detected within both the Sertoli-like cells and Leydig-like cells (Fig. 1-4C). Interestingly, in the

peritubular region, the SF1-positive slender cells were found (Fig. 1-4C, arrowhead), in addition to SF1-positive Leydig-like cells with round nuclei and large amounts of cytoplasm (Fig. 1-4C, arrow).

Finally, I stained the cells with 3β-HSD, which is specific for the cytoplasm of Leydig cells. 3β-HSD-positive cells were detected in control XY testes (Fig. 1-4F, arrow) and also in the freemartin gonads. In addition, these cells were abundant near the capillaries and had large amounts of cytoplasm. However, in the freemartin gonads, 3β-HSD-positive cells were scattered, and their signals were weaker than in the control (Fig. 1-4E, arrow, compared with F). These data provide evidence of the presence of Leydig–like cells positive for SF1/Ad4BP and 3β-HSD in this XX freemartin gonad.

Discussion

Based on gross anatomical appearance, the external and internal genitalia of the freemartin calf appeared to be masculinized. A short vaginal length, large clitoris, and unpalpable uterus are typical in freemartin syndrome; indeed, these features are used to diagnose the syndrome. Although remnants of seminal glands are observed sporadically, the presence of a scrotum, an epididymis, or a pampiniform plexus is rarely reported. Given the vast phenotypic diversity among freemartin calves (Jost et al., 1972; Ghanem et al., 2005; Payan-Carreira et al., 2008), the anatomical characteristics of this calf strongly support the classification of the freemartin calf as highly masculinized.

The histological reports of most freemartin gonads showed only hypoplastic ovaries or streak gonads. In this study, I revealed apparent seminiferous tubule-like structures (i.e., rows of Sertoli-like cells) like those found in a rare case of freemartin gonads examined previously. However, I also found some ovarian characteristics remained even in these freemartin gonads; for example, by analyses of 30 serial sections, clusters of cells, which are observed more frequently in freemartin gonads, revealed the blind ends of seminiferous tubule-like structures (Fig. 1-2B, arrow; data not shown). This strongly suggests that these seminiferous tubule-like structures were originally derived from ovarian follicles and caused the lumina to fill with secretions. Actually, it has been reported that gonads of freemartin fetuses have only ovarian characteristics until 40 or 60 –days old (Jost et al.,1972; Dominguez et al., 1990). Meanwhile, immunohistochemical analysis with the DDX4/MVH antibody did not reveal any positive cells, which are the main cause of sterility (Padula, 2005). These histological features are concordant with the few previous reports of freemartin gonads being highly masculinized

(Jost et al.,1972; Dominguez et al., 1990). I did not know exactly why such a severe masculinization occurred, but Dominguez et al. (1990) demonstrated that the gonads of an 80-day-old freemartin fetus, which showed severe phenotype like the present study, had a large amount of testosterone (Dominguez et al., 1990). Because of this report, it is speculated that exposure to a high dose of male hormones (e.g., testosterone or AMH) during pregnancy caused the present severe phenotype in this freemartin calf as well.

In this paper, I confirmed the cell type of immature Sertoli-like cells, Leydig-like cells and peritubular cells. Because other reports on freemartin gonads observed only morphologic features, I examined immunohistochemical staining. Indeed, based on the results of SOX9 and GDNF staining, I can conclude that the freemartin calf possessed differentiated Sertoli cells. Considering the fact that ovarian characteristics remained in these freemartin gonads and the histological analyses reported previously, this is the first report indicating that XX ovarian somatic cells in bovine freemartin gonads can transdifferentiate into Sertoli cells at the molecular level. It should be noted that the immature shape of these cells may not be due to freemartin syndrome but could reflect the prepubescent nature of this calf (Curtis and Amann, 1981; Sinowatz and Amselgruber, 1986). I also performed staining them with an antibody against AMH, another marker for immature Sertoli cells, but no AMH-positive cells were detected in both control testes and freemartin gonads (data not shown), probably because of decreased AMH level in even normal XY Sertoli cells after birth. This is consistent with the fact that the AMH activity was too low to be detected in the 6-month-old freemartin calf (Rota et al., 2002).

Given the extensive masculinization of the supporting cells, I hypothesized that the Leydig

cells and peritubular myoid cells would also differentiate. Actually, staining with both anti-3β-HSD and anti-SF1/ Ad4BP antibodies showed that there were interstitial Leydig cells with round nuclei positive for these markers. In addition, surprisingly, I also observed slender cells positive for α-SMA that appeared to be differentiated peritubular myoid cells. However, because some of them seemed to be also positive for SF1/Ad4BP and they were discontinuous around the tubules, I suggest that this freemartin calf exhibits incomplete sexreversal in terms of the interstitial cell lineage. Although it has been reported in ovine testicular-type freemartins that there are gonads with 3β-HSD-positive interstitial cells (Smith et al., 2003), this is apparently the first report to show the presence of both 3β-HSD- and SF1/Ad4BP-positive differentiated Leydig cells and SMA-positive peritubular myoid cells in the freemartin calf. In mammalian gonadogenesis, testicular supporting cells appear to differentiate first, after which interstitial cells arise (Schmahl et al., 2000). Thus, the process of female-to-male sex reversal might also occur first in the supporting cell lineage and then in the interstitial cell lineage. This apparent incomplete sexreversal of the interstitial cells explains the low postnatal testosterone activity even in such a severely masculinized freemartin calves (Rota et al., 2002).

In conclusion, I suggest that this freemartin calf exhibited almost complete testes and transdifferentiation of ovarian somatic cells into Sertoli, Leydig and peritubular myoid cells.

Congenital or experimental XX sex-reversal cases have been reported sporadically not only in cows or ewes but also in mice (Ottolenghi et al., 2007a; Uhlenhaut et al., 2009). Most of these cases represent loss of germ cells accompanied by the formation of seminiferous tubule-like structures resembling freemartins (Guigon and Magre et al., 2006), which is in accordance with the current data as well. Conversely, varying levels of differentiation of

Sertoli or Leydig cells are reported in XX sex reversal. With the exception of genetic mutants (Koopman et al., 1990; Ottolenghi et al., 2007b; Hiramatsu et al., 2009), SOX9 expression is rarely detected. The expression of only SOX9 was reported previously in mouse ovaries transplanted under renal capsules (Morais da Silvia et al., 1996). Therefore, the present freemartin gonads are also a very rare case of genetically non-mutated mammalian XX sex-reversed gonads.

In mouse models, it has long been speculated that there remains an unknown testis-forming pathway that is not mediated by the mammalian-specific testis-determining gene *Sry* (Ottolenghi et al., 2007b). Indeed, nonmammalian species such as birds, fish and reptiles exhibit numerous testis-determining mechanisms that are independent of *Sry* (Matsuda et al., 2002; Yao, 2005; Smith et al., 2009). Because it was suggested that freemartin syndrome was caused by AMH from male fetuses (Padula, 2005), AMH is thought to have a key role in such a testis-forming pathway. Indeed, it is reported that the teleost fish Patagonian pejerrey has *amhy* (duplication of *amh* on Y chromosome) as the master testis-determining gene (Hattori et al., 2012). Given the almost complete bovine testes in the XX individual in this study, my results strongly support the presence of AMH-mediated unknown testis-forming pathways in mammals. Moreover, my results firmly demonstrate that mammalian ovaries possess much more extensive sexual plasticity than previously expected.

Figures and Legends

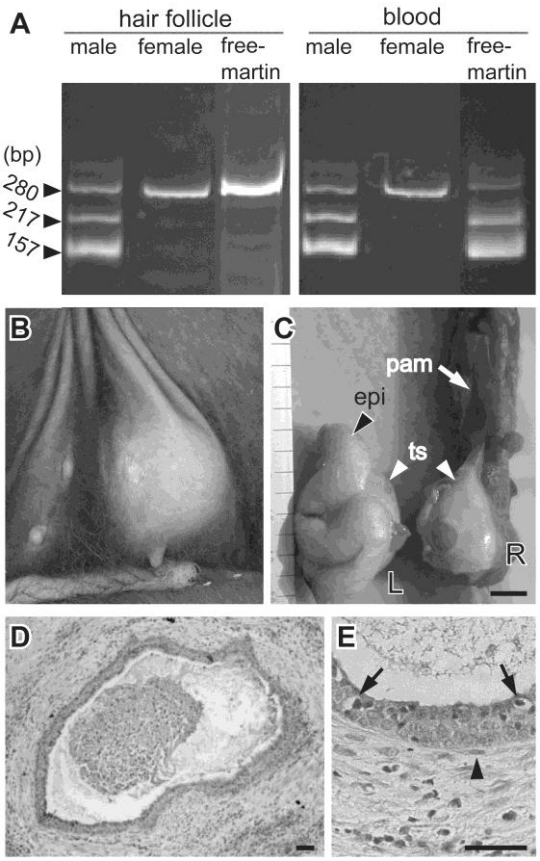
A
hair follicle
male
female
free-martin
blood
male
female
free-martin
(bp)
280
217
157
B
C
pam
epi
ts
R
L
D
E

FIGURE 1-1

Fig. 1-1. Diagnosis of freemartin syndrome by PCR and observation of gross anatomical appearance. (**A**) Hair follicle samples of the heterosexual twin calf showed only one band at 280 bp for amelogenin on the X chromosome, as in a normal female. For the blood samples, bands of 280 bp and 217 bp for amelogenin on the Y chromosome and 157 bp for BOV97M on the Y chromosome were detected. Thus, the presence of both X and Y chromosomes was clear. (**B**) Observation from the ventral view. Scrota-like structures were detected. (**C**) Gonads present within the scrota (open arrowheads; ts). On the left gonad (L), an epididymis-like structure was observed (black arrowhead; epi), whereas on the right gonad (R), blood vessels similar to a pampiniform plexus were observed (open arrow; pam). (**D**) H-E staining of the vesicular gland-like structures showed secretions in their lumina. (**E**) Gland-like structures were surrounded by smooth muscle (arrowhead), as typically seen in normal male vesicular glands. Some cells contained fat droplets, although a columnar shape was not observed (arrows). Scale bars: 30 μm (bars in C, 1 cm).

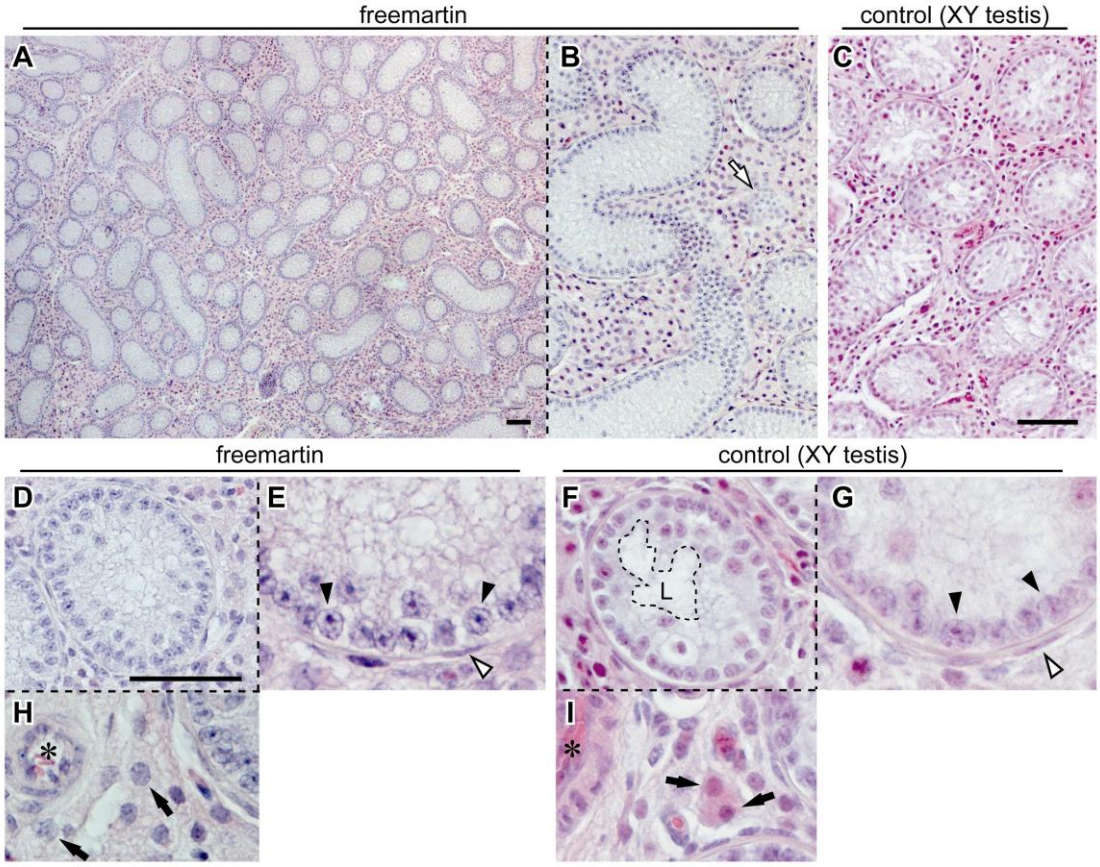
freemartin
control (XY testis)
A
B
C
freemartin
control (XY testis)
D
E
F
G
L
H
I
*
*

FIGURE 1-2

Fig. 1-2. Histological analysis of 6-month-old freemartin gonads and 5-month-old XY testes by H-E staining. (**A**) In the freemartin gonads, apparent seminiferous tubule-like structures were observed throughout the whole gonads, and no follicle-like structures could be seen. (**B**, **C**) Freemartin gonads had a relatively large interstitial area compared with control testes. In addition, clusters of cells were detected in the freemartin gonads (open arrow in B) but not in the control testis. (**D**, **F**)Lumina were identified in each tubule in the control ("L"), but not in the freemartin gonads. (**E**, **G**) High-magnification images of the regions surrounding the tubules revealed the presence of epithelial cells similar to immature Sertoli cells (black arrowheads), fusiform cells in the freemartin gonads (open arrowhead in E), and peritubular myoid cells in the XY testis (open arrowhead in G). (**H**, **I**) The interstitial area contained interstitial cells with large amounts of cytoplasm resembling Leydig cells (black arrows), especially near the capillaries (asterisks). Scale bars: 100 μm.

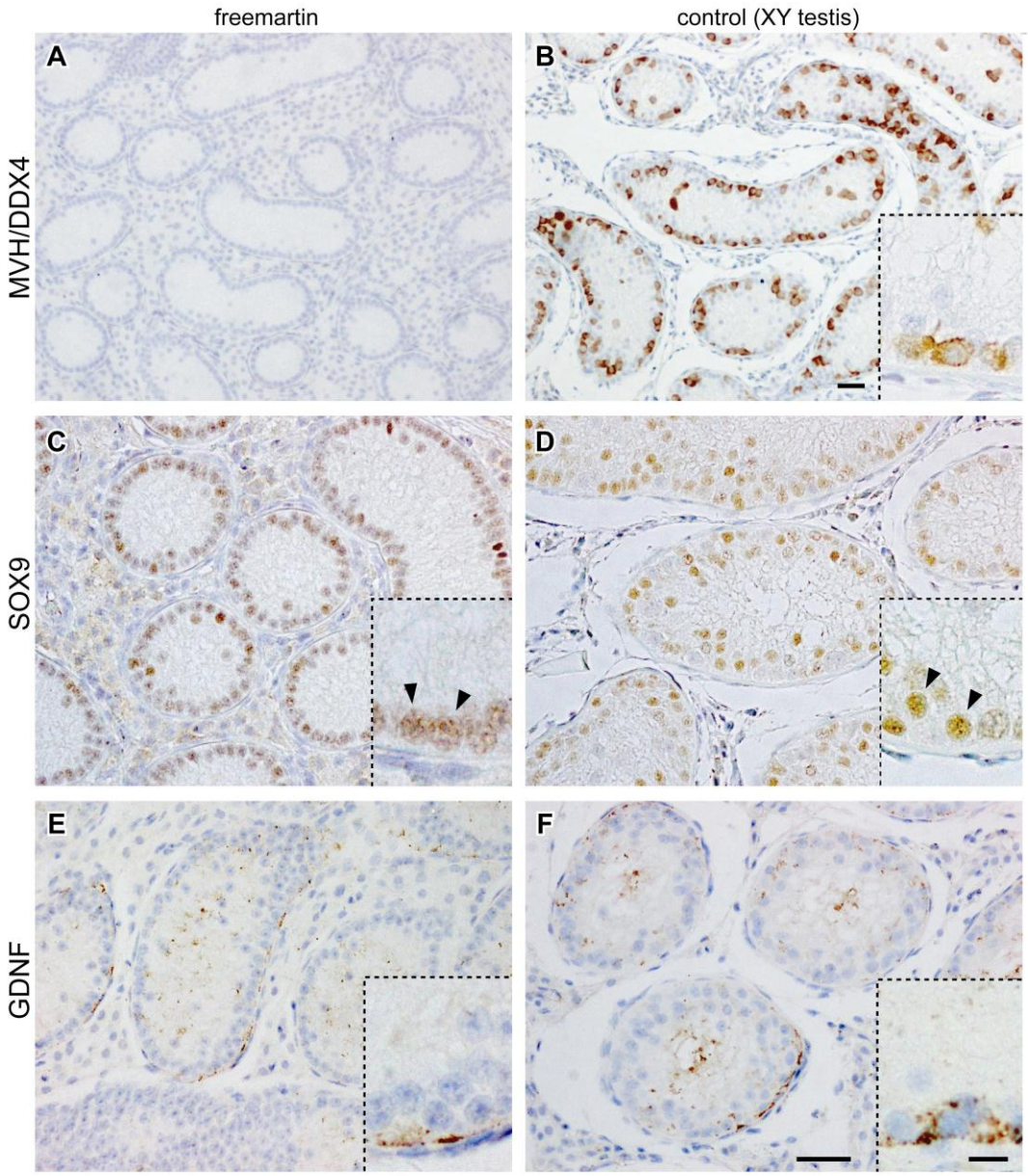

FIGURE 1-3

Fig. 1-3. Evidence of the formation of seminiferous tubule-like structures without germ cells, but with SOX9- and GDNF-positive epithelial cells in freemartin gonads. (**A**, **B**) Immunohistochemistry for the DDX4/MVH antibody. No positive cells were detected in the freemartin gonads, whereas they were observed inside tubules in the controls. DDX4/MVH was present within the cytoplasm of germ cells. (**C**, **D**) Immunohistochemistry for SOX9 antibody. SOX9 was detected in round nuclei of epithelial cells of the tubules (arrowheads). (**E**, **F**) Immunohistochemistry for GDNF antibody. Positive signals were observed within the cytoplasm of cells in the epithelia. Scale bars: 100 μm (bar in insets in F, 10 μm).

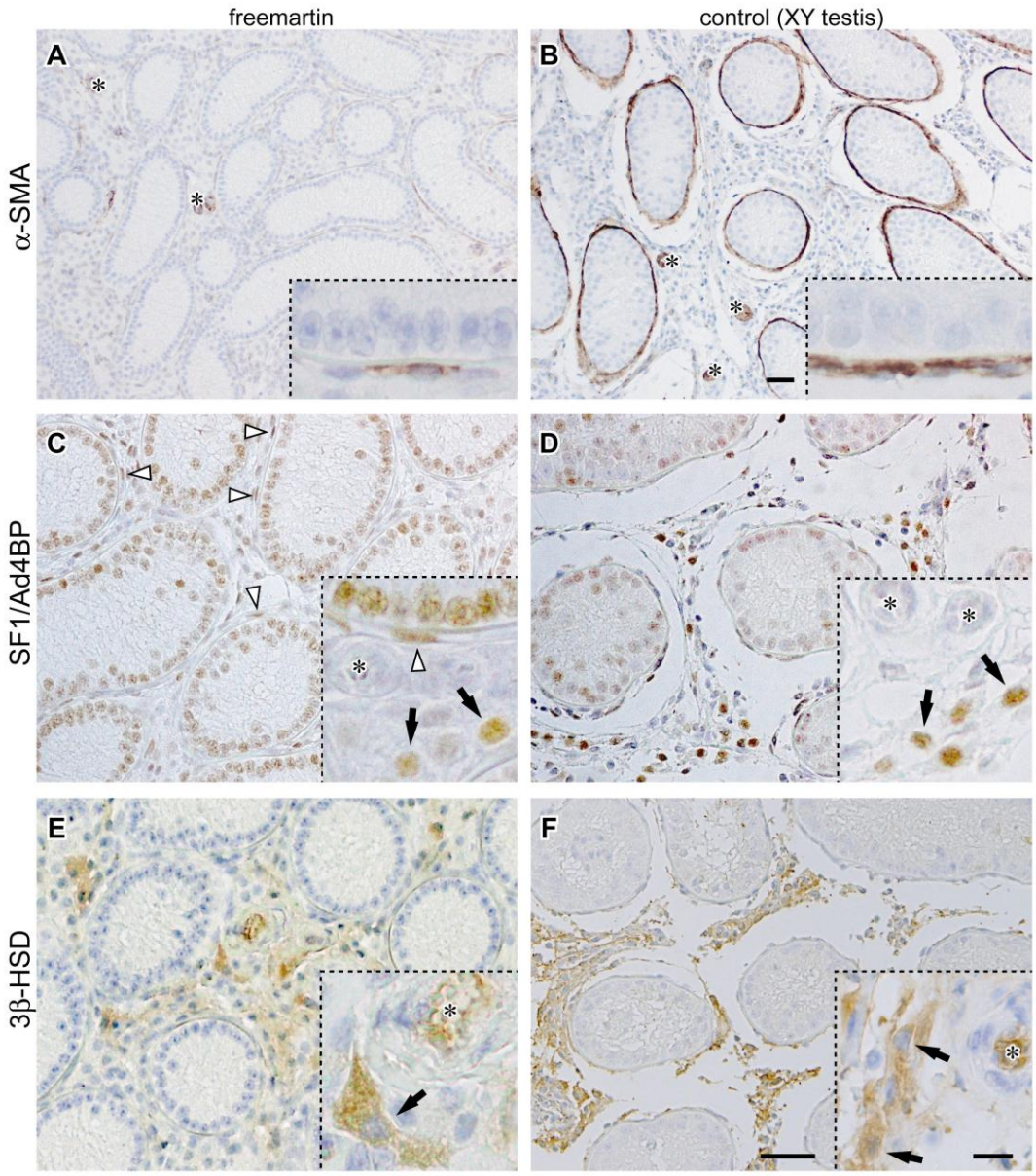

FIGURE 1-4

Fig. 1-4. Presence of α-SMA-, SF1/Ad4BP- and 3β-HSD-positive cells in the interstitial area. (A, B) Immunohistochemistry for α-Smooth muscle actin (α-SMA). Smooth muscle cells around the capillaries were positive for α-SMA (asterisks). In the freemartin gonads, some thin cells positive for SMA were detected. SMA-positive peritubular myoid cells around the seminiferous tubules were clearly present in the control testes. (**C**, **D**) Immunohistochemistry for SF1/Ad4BP. SF1/Ad4BP was detected in both the freemartin gonads and the control testes. In the freemartin gonads, positive cells were seen in the epithelia, interstitial cells with round nuclei (arrows in C) and thin cells around the seminiferous tubules (arrowheads in C). In the control testes, round cells were present in the epithelia and interstitial area (arrows in D). The thin cells positive for SF1/Ad4BP (arrowheads in C) appeared to be the same cell lineage as the SMA-positive cells (A). (**E**, **F**) Immunohistochemistry for 3β-HSD. 3β-HSD-positive interstitial cells were detected in both the freemartin gonads and the control testes (arrows in E, F). These positive cells were mainly located near capillaries (asterisks). The 3β-HSD-positive interstitial cells in the freemartin gonads appeared to be the same cell lineage as the SF1/Ad4BP-positive cells (arrows in C). Asterisks: capillaries. Scale bars: 100 μm (bar in insets in F, 10 μm).

Chapter 2

Heterogeneity in Sexual Bipotentiality and Plasticity of Granulosa Cells in Developing Mouse Ovaries

Abstract

In mammalian sex determination, SRY directly activates the *SOX9* gene encoding the central factor of Sertoli cell differentiation, leading to testis formation. When, where and how granulosa cells are determined to differentiate in developing ovaries, however, remains unclear. By monitoring SRY-dependent SOX9-inducibility in a *Sry*-inducible mouse system, here I show spatiotemporal changes in the sexual bipotentiality/plasticity of ovarian somatic cells throughout a life. The early pre-granulosa cells maintain SRY-dependent SOX9-inducibility until 11.5 dpc, after which most pre-granulosa cells rapidly lose this ability by 12.0 dpc. Unexpectedly, I found a subpopulation of the granulosa cells near ovarian medulla that continuously retains SRY-dependent SOX9-inducibility throughout fetal and early postnatal stages. After birth, these SOX9-inducible granulosa cells contribute to the initial round of folliculogenesis by secondary follicle stage. In experimental sex reversal of 13.5-dpc ovaries grafted into adult male nude mice, the differentiated granulosa cells reacquire SRY-dependent SOX9-inducibility before other signs of masculinization. Furthermore, by microarray analysis, I identified ovarian genes responsible for loss or reaquirement of SRY-dependent SOX9-inducibility. My data provide direct evidence of an unexpectedly high sexual heterogeneity of granulosa and coelomic epithelial cells in developing mouse ovaries in a stage- and region-specific manner. Discovery of such sexually bipotential granulosa cells and expected anti-testis/ovarian genes have implications for their potential contribution to XX masculinization and suggest their importance in normal ovarian development.

Introduction

In mammalian gonadogenesis, both testicular Sertoli cells and ovarian granulosa cells develop from a common supporting cell precursor (Albrecht and Eicher, 2001) which arises from the coelomic epithelium (Karl and Capel, 1998; Schmahl et al., 2000; Schmahl and Capel, 2003; Sekido et al., 2004). In XY males, *Sry* is transiently (11.0-12.0 days post coitum [dpc]) activated in a center-to-pole wave-like pattern along the anteroposterior (AP) axis of the indifferent XY gonads (Harikae et al., in press). In these bipotential supporting cells, SRY directly up-regulates another, autosomal *Sry*-box gene, *Sox9* (Sekido and Lovell-Badge, 2008), and *Sox9* induces *Fgf9* expression in a similar center-to-pole pattern (Kim et al., 2006; Hiramatsu et al., 2010). FGF9 signals, in turn, up-regulate SOX9 expression, resulting in the maintenance of high-level SOX9 expression in Sertoli cells.

In contrast, without *Sry* expression, the bipotential supporting cells become granulosa cells, leading to follicle formation. Similar to SRY/SOX9 expression in Sertoli cell differentiation, ovarian differentiation is marked by early female-specific expression of several genes including *Wnt4* (Vainio et al., 1999), *Rspo1* (Parma et al., 2006) and *FoxL2* (Uda et al., 2004; Ottolenghi et al., 2005). The enforced expression of either FOXL2 or active β-catenin disrupts testis development in XY gonads (Ottolenghi et al., 2007; Maatouk et al., 2008**;** Garcia-Ortiz et al., 2009). In contrast, ovarian development in XX gonads lacking a single gene among them is not severely affected (Vainio et al., 1999; Uda et al., 2004*;* Chassot et al., 2008; Tomizuka et al., 2008; Liu et al., 2009). Even in *Wnt4/Foxl2* double-null embryos, female-to-male sex reversal starts to occur at the perinatal period (Ottolenghi et al., 2007).

Therefore, it remains unclear how many other ovarian genes are involved in the switch from the sexually bipotential state to an ovarian fate (Nef et al., 2005; Beverdam and Koopman, 2006; Garcia-Ortiz et al., 2009; Munger et al., 2009; Chen et al., 2012; Jameson et al., 2012). It is also unclear when, where and how granulosa cell fate is determined in developing fetal ovaries.

Previously, it have been demonstrated that in XX *Sry* transgenic (Tg) gonads, forced ubiquitous SRY expression in the entire gonadal area from earlier stages resulted in neither any advance in timing nor ectopic activation of *Sox9* expression in developing gonads (Kidokoro et al., 2005). This finding indicates that SRY-dependent *Sox9*-inducibility is tightly regulated in gonadal precursor cells, and that only supporting cells which correspond to *Sry*-expressing pre-Sertoli cells in XY gonads achieve a competent state to respond to SRY action in XX gonads. Moreover, my laboratory has developed a novel *Sry*-inducible transgenic (*Hsp-Sry*) system to induce XX testis sex reversal (Hiramatsu et al., 2009). In this *Hsp-Sry* system, heat shock (HS) treatment induces ectopic *Sry* expression, leading to transient *Sox9* induction in XX supporting cells. When the *Hsp-Sry* transgene was induced during the critical time window of 11.0-11.25 dpc (i.e. 12-14 tail somites [ts]), *Sox9* expression was not only transient but maintained at high levels, resulting in testis formation of XX gonads. After this critical time period, ectopic *Sry* induction initially induced SOX9 expression in most supporting cells by 11.5 dpc, however, *Sox9* expression was not maintained, resulting in ovarian differentiation (Hiramatsu et al., 2009). In fetal ovaries at 12.0-12.5 dpc, HS-dependent *Sry* expression did not induce ectopic SOX9 initiation in most ovarian cells, suggesting that the loss of SOX9-inducibility is one of the earliest key events in granulosa cell differentiation. Hence, I hypothesized that the loss and reacquisition of the

potency to initiate SRY-dependent *Sox9* activation can be used to monitor the sexually bipotential states in ovarian development under normal and aberrant conditions.

By using *Hsp-Sry* mouse system, this study is the first to visualize spatiotemporal changes in SRY-dependent SOX9-inducibility in developing granulosa cells of normal and masculinized ovaries.

Materials and methods

Animals

The inducible *Sry* transgenic line #44 (with the *HSP-Sry* [*Hsp70.3* promoter-driven murine *Sry*] transgene; ICR/C57BL6[B6]-mixed background; Hiramatsu et al., 2009), *Wnt4* mutant line (129svJ/ICR-mixed background; Vainio et al., 1999) and XO/Eda^{Ta} line (Background strain is unknown; Probst et al., 2008) were used in this study (Kidokoro et al., 2005; Mizusaki et al., 2003). Male nude mice (8 weeks old; BALB/c, nu/nu, SLC Japan) were used as host mice for the transplantation of fetal ovaries.

Transplantation of Fetal Mouse Ovaries

Transplantation of fetal ovaries was carried out by the previously reported procedure (Taketo et al., 1984; Taketo et al., 1986). In brief, fetal ovaries (without mesonephroi) were isolated from XX Tg and wild type embryos at 13.5 dpc (some ovaries were depleted of germ cells by busulfan pre-treatment), and transplanted beneath the kidney capsule of male nude mice. Transplants were dissected from host animals on days 4~20 post-transplantation.

Heat shock (HS) Treatment in Vitro and in Vivo

For in vitro HS treatment, embryos were collected from pregnant female mice at various stages (11.0-18.5 dpc). From 10.5 to 12.5 dpc, the tail somites of each embryo were counted for accurate staging. Using tail somite stages, 11.0 dpc corresponds to approximately 12 ts, 11.5 dpc to 18 ts, 12.0 dpc to 24 ts, and 12.5 dpc to 30 ts. Genital ridges and ovaries were isolated from the embryos, pups (1, 3, 7, 14 and 21 dpp) and adult females (7 weeks old) in cold Dulbecco's Modified Eagle's Medium (DMEM; Sigma). One genital ridge of each pair

was subjected to HS treatment (43˚C for 10 min) in a 0.2 ml thin-wall PCR tube as described previously (Hiramatsu et al., 2009). In most cases, the other genital ridge was used as non-HS control. In some experiments of postnatal and adult ovaries, the ovaries were fragmented into small pieces before HS treatment. Fetal ovary transplants and fragments of postnatal and adult ovaries were HS-treated under the same conditions (43˚C for 10~15 min). All samples were cultured for 9 hours before SOX9 expression was detected immunohistochemically.

For in vivo HS treatment, the postnatal and adult ovaries were surgically separated from the mesovarium. Then, the left ovaries, complete with oviducts and uterine horns, were gently extracted from the abdominal cavity and immersed in pre-warmed DMEM (43˚C) in a 0.5-ml tube for 15 min under anesthesia (right ovaries were used as a non-treated control).

Organ Culture

All ovarian samples were cultured on ISOPORE membrane filters (Millipore) in DMEM containing 10% horse serum at 37˚C for appropriate periods (2 hours to 3 days). Some genital ridges were cultured in 10% horse serum-DMEM supplemented with FGF9 (Sigma; 100 ng/ml). The segment culture assay using anterior, middle and posterior segments of the genital ridge (Hiramatsu et al., 2003) and the gonad culture without adjacent mesonephros (Matoba et al., 2005; 2008) were also initiated from the XX Tg gonads at 14-15 ts.

Histology and Immunohistochemistry

The samples were fixed in 4% PFA-PBS at 4^{o}C for 4 hours, dehydrated, and then embedded in paraffin. Serial sagittal sections (approximately 4 μm in thickness) were cut in the middle portion including the largest area and then every 10th section of the samples was principally analyzed by anti-SOX9 immunostaining, while adjacent section was used for immunostaining

for other markers as described below. The sections were incubated with anti-AMH (1:200 dilution; Santa Cruz), anti-Laminin (1:400 dilution; ICN Pharmaceuticals), anti-DAX1 (1:500 dilution; Ikeda et al., 2001); anti-DMRT1 (1:100 dilution; Santa Cruz), anti-EMX2 (1:1,000 dilution; Kusaka et al., 2010), anti-FOXL2 (1:200 dilution; Uda et al., 2004; 1:200 dilution [goat antibodies for double-staining with SOX9], Abcam), anti-Heparan Sulfate (1:200 dilution; 10E4 epitope; Seikagaku Corporation, Japan), anti-IRX3 (1:200 dilution; Abcam), anti-PCNA (1:1,000 dilution; PC10; DAKO), anti-SF1/Ad4Bp (1:1,000; Ikeda et al., 2001), anti-SOX9 (1:250 dilution; Kidokoro et al., 2005; Kent et al., 1996), anti-SPRR2d (1:300 dilution; Alexis Biochemicals), or anti-SRY (1:10 dilution; Wilhelm et al., 2005) at 4 °C for 12 hours. The reaction was visualized with biotin-conjugated secondary antibody in combination with Elite ABC kit (Vector Laboratories) or by Alexa-488/594 conjugated secondary antibodies (Invitrogen).

For whole mount immunohistochemistry, the PFA-fixed samples were treated with 0.5% Triton X-100 for 15 min at 4°C, and then incubated with rabbit anti-SOX9 and mouse anti-ZO1 (1:400 dilution; Invitrogen) antibodies at 4°C for 12 hours. The reaction was visualized with Alexa-488/594 conjugated secondary antibodies. After the mesonephric tissue was removed, they were mounted mesonephric side down (coelomic epithelium side up) using an antiphotobleaching medium. Finally, I calculated the total number of the SOX9/ZO1-double positive cells located within the coelomic epithelium (total 8 explants).

For quantitative analysis of SOX9-inducible cells, I calculated the number of SOX9-positive cells located in regions I~V (see right lower plate in Fig. 2-12D) of three~five longitudinal sagittal sections per explant (the section containing the largest area in the middle position of the gonad, and two sections before and behind it at an interval of approximately 50 μm). The

area of each region was also measured using the ImageJ program (Ver. 1.44). Finally, the cell number per area (mm^2) was separately estimated in each region of XX gonadal explants.

For the number of SOX9-inducible cells in postnatal ovaries and grafted ovarian transplants, I separately counted the numbers of each primary, primordial or secondary follicle in three~five longitudinal sagittal sections per ovary. I also counted the numbers of SOX9-positive and –negative granulosa cells per each follicle. After counting the numbers in each section, the total number of oocytes was counted in each section image. Finally, relative numbers of SOX9-positive follicle relative to total follicle number (i.e., total oocytes number) and relative SOX9-positive granulosa cells in each follicle were estimated in postnatal ovaries at P3~P21 and in grafted ovaries at day 10 post-transplant.

For the PCNA-positive index of the SOX9-inducible cell population, SOX9-positive cells and PCNA/SOX9-double positive cells were separately estimated in three longitudinal sagittal sections per explant (n= 4, 6, 4 and 4 ovaries at E12.5, E17.5, P3, and P14, respectively).

Whole-mount in situ hybridization

Whole-mount in situ hybridization was performed using 4% PFA-fixed explants (n=6) as described previously (Hiramatsu et al., 2003).

Quantitative RT-PCR

Total RNA was reverse-transcribed using random primer with a Superscript-III cDNA synthesis kit (Invitrogen). Specific primers and fluorogenic probes for *Emx2* (Mm00550241_ml), *Dax1/Nr0b1* (Mm00431729_m1), *Irx3* (Mm00500463_m1), *Lzts1* (Mm01345507_m1), *Runx1* (Mm01213405_m1), *Sox9* (Mm00442795_m1), *Zbtb7c* (Mm02375515_s1) and *Gapdh* (Taqman control reagents) were purchased from Applied

Biosystems. PCR was performed using an Applied Biosystems Step One Real Time PCR System. The expression levels represented the relative expression levels of each marker gene per *Gapdh* amplicon ratio (mean ± standard error).

Microarray processing and analysis

Total RNA of all samples was purified by NucleoSpin RNA XS kit (Macherey-Nagel) and along the protocols in GeneChip 3' IVT Express kit (Affymetrix), fragmented aRNA was hybridized to mouse genome 430 2.0 arrays (Affymetrix). Chips were washed and stained in Fluidics Station 450 (Affymetrix). The arrays were scanned using a GeneChip scanner 3000 (Affymetrix) and the output was obtained by GeneChip Operating Software or Expression Console (Affymetrix). Data was normalized and further analyzed by RMA method using AltAnalyze software (http://www.altanalyze.org/). On unsupervised clustering, dChip was used (http://biosun1.harvard.edu/complab/dchip/). For getting 12.5 dpc somatic gene profiles and profiles of genes independent *Wnt4* or *Foxl2*, I used cell files of Bouma et al. (2010) and Garcia-Ortiz et al. (2009) supported by GEO (GSE18211, GSE12989).

Statistical Analysis.

Quantitative data (i.e., relative number of SOX9-inducible cells, real-time PCR data, and PCNA-positive index) were analyzed by Student's *t*-test. One-way analysis of variance (ANOVA) was also conducted to analyze significance of the regional difference of the SOX9-inducible cell number among wild type, *Wnt4*-heterozygous and *Wnt4*-null XX gonads.

Results

XX gonadal somatic cells rapidly lose SRY-dependent SOX9-inducibility in an anterior-to-posterior wave-like manner during 11.5 to 12.0 dpc.

First, I examined the onset of the loss of SRY-dependent SOX9-inducibility. In brief, XX Tg gonads were isolated at various tail somite stages, subjected to HS (43°C, 10min), and then cultured for 9 hours to allow immunohistochemical detection of SOX9-induced XX supporting cells (Fig. 2-1A). SOX9 immunostaining detected no positive signals in any non-HS treated XX explants ("-HS" in Fig. 2-1B). In 12-30 ts XX gonads, HS treatment induced ubiquitous SRY expression at 3 hours after HS (Fig. 2-2; Hiramatsu et al., 2009). In 12-18 ts XX gonads, ubiquitous SRY promoted SOX9 expression in most gonadal supporting cells approximately 9 hours after HS (upper plate in "15ts" of Fig. 2-1A), consistent with the fact that almost all XX gonadal somatic cells are sexually "bipotential" until 15ts (Hiramatsu et al., 2009). Interestingly, in 19-21ts XX explants, the somatic cells showed reduced levels of SOX9 induction in the anterior pole region, as compared to the center and posterior regions ("19ts" and "21ts" in Fig. 2-1B; see Fig. 2-12D). Subsequently, the number of SOX9-inducible ovarian cells in HS-treated explants was rapidly reduced in most somatic cells in XX gonads by 24-25 ts (Fig. 2-1B).

Two distinct populations of ovarian somatic cells retain SRY-dependent SOX9-inducibility in fetal mouse ovaries

Although there is a rapid loss of SOX9-inducibility in most XX gonadal cells by 12.0 dpc (24-25ts), interestingly, I have noticed the presence of two distinct populations of somatic cells that sustain SRY-dependent SOX9-inducibility even at 30 ts (12.5 dpc) (Fig. 2-1B-D). The first population consisted of coelomic epithelial and subepithelial cells located immediately beneath the coelomic epithelium (solid arrowheads in Fig. 2-1B; C), while the second population is the gonadal cells in the presumptive ovarian medullary region adjacent to the mesonephros (open arrowheads in Fig. 2-1B; D). Whole mount *in situ* hybridization of HS-treated XX Tg explants (12.5 dpc; 6-hour culture after HS treatment) also confirmed that the *Sox9*-positive signals were detected in the cells within the ovarian surface and the gonadal cells surrounding the germ cells near the mesonephric tissues (Fig. 2-1E, F).

In the coelomic epithelial and subepithelial regions, ectopic SOX9 activation was frequently found in HS-treated XX Tg explants isolated at 18 to 30 ts (with a peak between 19 and 24 ts; Fig. 2-1B), whereas only a few SOX9-positive cells were found within the coelomic epithelia at 13.0 dpc, and no SOX9-inducible cells were seen before 18 ts (“15ts” in Fig.2-1B) and after 13.5 dpc (not shown). By whole mount anti-SOX9/anti-ZO1 double-immunostaining of HS-treated ovaries at 12.5 dpc (28-30ts), the SOX9-inducible cells (a single cell or 2-3 clustered cells) were located throughout the gonadal surface along the anteroposterior (AP) axis at the level of average cell number 16.9 +/- 1.5 per gonad (n= 8; Fig. 2-1G). These SOX9-induced coelomic epithelial cells appeared to be positive for SF1/Ad4BP (a marker for gonadal somatic cells), but to be negative for FOXL2 (an early granulosa cell marker [Uda et al., 2004; Ottolenghi et al., 2005]) (Fig. 2-3A).

The second population that sustained SRY-dependent SOX9-inducibility in 12.5 dpc ovaries was the supporting cells that were located in the presumptive ovarian medullary region

adjacent to the mesonephros (open arrowheads in Fig. 2-1B; D, F "om"). In HS-treated XX Tg explants isolated at 30 ts, the SOX9-induced cells were closely connected with germ cells (Fig. 2-1D, F). In further analysis, they were found at the bottom of the ovarian medullary region with weak signals for anti-Heparin Sulfate Proteoglycans (HSPG) staining (Fig. 2-1H). Most interestingly, most of SOX9-induced ovarian cells near the mesonephric tissue were FOXL2 positive at 12.5 dpc (Fig. 2-1I). Moreover, some of these cells appeared to be positive for SPRR2d, another early granulosa cell marker (Lee et al., 2009; Bouma et al., 2010), in addition of SF1/Ad4BP (Fig. 2-3B). These data indicate that the SOX9-inducible population in the ovarian medulla is likely to be a subpopulation of FOXL2-positive granulosa cells.

Trans-differentiation of SOX9-inducible granulosa cells into Sertoli-like cells

It was previously reported that a high level of SOX9 expression is maintained by FGF9 signals, resulting in the establishment of Sertoli cells in XY gonads (Kim et al., 2006; Hiramatsu et al., 2010). Moreover, this action of FGF9 is antagonized by female-specific WNT4 signaling in developing ovaries (Kim et al., 2006). In order to reveal the further characteristics of SRY-inducible SOX9-expressing ovarian cells by using the "FGF9-WNT4 balance" model, XX Tg wild type and *Wnt4*-heterozygote ovaries at 13.0 dpc were treated with HS and cultured in the presence or absence of FGF9 (100ng/ml) for 12 to 72 hours (Fig. 2-4A). As anticipated, either exogenous FGF9 or reduced WNT4 activity resulted in the maintenance of SOX9 expression in a certain ovarian medulla subpopulation, albeit a small one, of granulosa cells even after 72 hours of culture (8/9 explants show maintenance of SOX9 expression in the presence of FGF9, 10/12 explants in $Wnt4^{+/-}$ background; Fig. 2-4B).

In particular, in FGF9-treated ovarian explants, some SOX9-positive cells in the ovarian medulla appeared to down-regulate FOXL2 and to up-regulate AMH, anti-Müllerian hormone secreted from differentiated Sertoli cells (5/6; Fig. 2-4C, D). These findings indicate that this ovarian medulla sub-population of granulosa cells can trans-differentiate into Sertoli cell-like population. Therefore, I can conclude that SRY-dependent SOX9-inducible ovarian medulla cells represent the sexual bipotentiality and/or plasticity.

The SOX9-inducible granulosa cell population contributes to the initial round of folliculogenesis

In order to map the cell fate of the SOX9-inducible subpopulation of granulosa cells in the developing ovarian medulla, I examined SRY-dependent SOX9-inducibility in the developing ovaries at the fetal and postnatal stages both in vitro (Fig. 2-5) and in vivo (Fig. 2-6).

In developing ovaries after 12.5 dpc, SRY-dependent SOX9-inducibility was maintained in a restricted population of granulosa cells in the ovarian medullary region throughout the fetal stages (Fig. 2-5A). Moreover, PCNA (a cell proliferation marker)/SOX9-double immunostaining (Fig. 2-7A-D) revealed poor proliferative activities in the ovarian medulla population in fetal ovaries at 12.5 dpc (percentage of PCNA-positive cells that are SOX9-inducible [PCNA index]: 14.2 +/- 6.2% [n=4]) and 17.5 dpc (5.6 +/- 3.2% [n= 6]), as opposed to a high PCNA-positive rate in the SOX9-inducible coelomic epithelial population at 12.5 dpc (91.7 +/- 8.3% [n=4]). After birth, at 3-14 dpp, SOX9-inducible cells were found in considerable numbers in developing ovarian follicles during the initial round of folliculogenesis (Fig. 2-5A,B; also see Fig. 2-11A) and only a small population of

FOXL2-positive basal granulosa cells maintained SRY-dependent SOX9-inducibility in primary and secondary follicles located in the centro-medullary region (Fig. 2-5A-C). SOX9-inducible cells became positive for anti-PCNA staining (PCNA index: 64.0 +/- 7.2% at 3 dpp [n=4] and 60.9 +/- 11.4% at 14 dpp [n=4], respectively; Fig. 2-7C, D). This finding is consistent with the recent cell-lineage tracing data showing a large contribution of *Foxl2*-positive granulosa cells at 12.5 dpc to the first follicular formation soon after birth (Mork et al., 2011). During the transition from the primordial to secondary follicular stages, SOX9-inducible granulosa cells did not appear to be increased in number and restricted to only a small population of basal granulosa cells in the secondary follicles (also see Fig. 2-11C). In ovarian surface epithelia and cortex regions, no SOX9-inducible granulosa cells were detected in the developing primordial and primary follicles (three lower right plates in Fig. 2-5B). Any SOX9-inducible granulosa cells were not found in the antral follicles at 14 dpp. Similarly, in adult ovaries, no SOX9-inducible granulosa cells were detected in both in vitro and in vivo HS-treatment experiments (data not shown). Therefore, it is likely that certain pre-granulosa cells in the spatially restricted domain of the ovarian medulla continuously retain SRY-dependent SOX9-inducibility throughout fetal stage. After birth, almost all of this population appear to contribute to the initial round of folliculogenesis, consequently leading to the complete loss of SOX9-inducibility during the transition from the secondary to antral follicle stages.

Reacquisition of SRY-dependent SOX9-inducibility in a partial sex-reversal model of the fetal ovaries grafted into adult male mice

It is well known that fetal ovaries grafted under the kidney capsule undergo partial sex-reversal (Morais da Silva et al., 1996; Sekido and Lovell-Badge, 2008). In particular, Taketo et al. (1984; 1986) reported a subset of granulosa cells near mesonephros (i.e., medullary region) transdifferentiate into SOX9-positive Sertoli-like cells around two to three weeks after transplantation (Taketo et al., 1984; Taketo et al., 1986; Morais da Silva et al., 1996). In order to examine the contribution of the SOX9-inducible granulosa cells in the ovarian medulla to this partial masculization and to observe spatiotemporal change of these cells in sex-reversal, fetal ovaries isolated from wild type and Tg embryos at 13.5 dpc were transplanted under the kidney capsule of male nude mice (7 weeks old). The grafted Tg ovaries were removed from the host kidney at 4 to 20 days after transplantation, treated with HS, and cultured for 9 hours to evaluate SOX9-inducibility (Fig. 2-8A). In non-HS treated control transplants of both wild type and Tg ovaries, some of the developing primordial follicle started to transform by day 7, leading to the partial formation of a testis cord-like structure by day 10 post-transplant (arrowheads in Fig. 2-9). At around days 12 to 14, most of the testis cord-like structures had become positive for DMRT1, an ancient, conserved factor of the vertebrate testis differentiation pathway (Matson et al., 2011) (Fig. 2-8B). At days 15 to 20, SOX9-positive/FOXL2-negative Sertoli-like cells were first detected in testis-cord like structures, and they were restricted to the ovarian medullary region (Fig. 2-8B-D), which is confirmed by brightly fluorescent DiI labeling in the plasma membrane of fetal ovaries before transplantation (Fig. 2-10).

During this process of granulosa cell transdifferentiation, I further analyzed SRY-dependent SOX9-inducibility in grafted ovarian explants at early stages of masculinization (i.e., days 7 and 10 post-transplant; no spontaneous SOX9 positive cells were detected in testis-cord like structures). At day 10 post-transplant, no SOX9-positive signals were detected in any

non-treated XX Tg (n=5; “-HS” in Fig. 2-8E) or HS-treated wild type explants (n= 11; figure not shown). While in HS-treated Tg ovarian transplants at early stages after transplantation, SOX9-inducibility was maintained in a subpopulation of granulosa cells, which was restricted to the presumptive ovarian medullary area (large open arrows in Fig. 2-8E, F). Surprisingly, I found that, at days 7 and 10 post-transplant, a considerable number of ovarian granulosa cells in not only the ovarian medullary region but also throughout the ovarian parenchyma gradually reacquired SRY-dependent SOX9-inducibility (arrowheads in Fig. 2-8E, G). Anti-PCNA/SOX9-double immunostaining revealed high proliferative activities in these SOX9-inducible granulosa cells of the follicular structures (PCNA index : 91.0 +/- 2.2% in primary and secondary follicular structures [n=4]; Fig. 2-7E, F). Moreover, these SOX9-inducible cells are FOXL2-positive/ DMRT1-negative granulosa cells, which are located in both follicular and testis-cord like structures (“DMRT1” in Fig. 2-8E; Fig. 2-8F, G). Quantitative real-time RT-PCR analysis also confirmed the reacquisition of SRY-dependent SOX9-inducibility in the XX Tg explants at days 7 and 10 post-transplant ($p<0.01$, Fig. 2-8H).

Moreover, I calculated both the relative numbers of the SOX9-inducible follicle per total number of all follicles and the relative numbers of the SOX9-inducible granulosa cell per total granulosa cells (in each SOX9-positive follicle) in the grafted ovaries at day 10 post-transplant, and then compared them with those in the postnatal ovaries at P3~21 (Fig. 2-11). In the grafted ovaries at day 10 post-transplant, relative number of the SOX9-positive follicle (“gray bar” in Fig. 2-11B) showed 52.8 +/- 10.3 % (38.4 +/- 6.3 % in primary follicles plus 14.6 +/- 6.3 % in secondary follicles [“orange bar” and “green bar” in Fig. 2-11B, respectively]). Each value in the grafted ovaries (Fig. 2-11B) showed significantly higher than each corresponding value in the postnatal ovaries at any stages of P3~P21 (Fig. 2-11A).

Moreover, in both primary and secondary follicle stages, the relative number of SOX9-inducible granulosa cells per follicle in the grafted ovaries (Fig. 2-11D) was significantly higher than each corresponding value in the postnatal ovaries at any stages of P3~P21 (Fig. 2-11C). These data imply that SRY-dependent SOX9-inducibility can be used as a functional marker for the earliest masculinization signs of granulosa cells. In summary, these data clearly demonstrate that SRY-dependent SOX9-inducible granulosa cells reduce their number with ovarian differentiation at the fetal stage, and reaquire it in postnatal sex-reversal. Therefore I could confirm that SRY-dependent SOX9-inducibility could be used as a functional marker for sexual bipotency or plasticity.

Neither WNT4 nor FOXL2 is responsible for the loss of SRY-dependent SOX9-inducibility in XX gonads

The mechanisms underlying the loss of SOX9-inducibility in the major population of XX supporting cells during fetal periods are still unclear. I hypothesized that the loss of SOX9-inducibility was caused by any ovarian factors and differentiaion of pre-granulosa cells, because SRY-dependent SOX9-inducibility was shown to be a functional marker for sexual bipotency. It was previously shown that fetal ovarian differentiation is promoted by the two major ovarian factors, transcription factor FOXL2 and soluble factor WNT4 (Vainio et al., 1999; Uda et al., 2004; Ottolenghi et al., 2005; Ottolenghi et al., 2007; Maatouk et al., 2008; Garcia-Ortiz et al., 2009; Liu et al., 2009).

To identify a possible link of the loss of SOX9-inducibility with WNT4 signaling, I crossed the inducible *Sry* Tg mouse line onto the *Wnt4*-mutant background and examined the

SOX9-inducibility in the HS-treated XX Tg explants in wild type, *Wnt4*-heterozygous and *Wnt4*-null background. No significant differences could be detected in the spatiotemporal patterns of the loss of SOX9-inducibility between *Wnt4* heterozygous and wild type XX Tg explants (Fig. 2-12A, B, D). In both XX Tg explants at 21 ts, the SOX9-induced gonadal cells in the anterior region were significantly lower in number than those in the posterior region (asterisks on the bars in Fig. 2-12D). In *Wnt4*-null XX Tg explants, the loss of SOX9-inducibility properly occurred in the anterior region at 20-21 ts (upper plates in Fig. 2-12C; Fig. 2-12D), albeit slight delay of the onset of loss of SOX9-inducibility and persistence of a small number of SOX9-positive cells even at 30 ts.

The female-specific FOXL2 expression started in the centro-medullary region near the adjacent mesonephros from around 24-26 ts in developing XX gonads in vivo (Fig. 2-13). The timing of the onset of the reduced SOX9-inducibility in the anterior region (19-20 ts) was approximately 8 hours earlier than the activation of FOXL2 in developing XX gonads in vivo. Interestingly, in HS-treated *Wnt4*-null XX Tg explants, female-specific FOXL2 expression appears to be delayed (lower plates in Fig. 2-12A,C), showing no appreciable FOXL2-positive cells in these *Wnt4*-null XX Tg gonads at 21-26 ts (i.e., a similar situation to *Wnt4/Foxl2*-double null XX gonads). Even in these XX explants missing both *Wnt4* and FOXL2 activities (n=4), the loss of SOX9-inducibility properly occurs in most of the gonadal cells by 26 ts (upper plates in Fig. 2-12C; right lower graph in Fig. 2-12D).

Next, I tested a possible contribution of the adjacent mesonephric tissue to the loss of SOX9-inducibility in developing XX gonads (Fig. 2-14A, B). I isolated XX genital ridge with or without adjacent mesonephros at 14-15 ts, cultured them for 14 hours until the stage corresponding to 21 ts, and then examined HS-treatment-induced SOX9 expression patterns

in these explants. Removal of the adjacent mesonephros from XX gonads at 14-15 ts did not have any appreciable effect in the anterior-to-posterior disappearance pattern of SOX9-inducibility in developing fetal ovaries (Fig. 2-14B), which was similar to the pattern observed in XX gonads isolated at 21 ts (Fig. 2-14A). Moreover, I tested a possible contribution of the anterior gonadal region to the loss of SOX9-inducibility in middle and posterior regions of developing XX gonads (Fig. 2-14C-E). I separated the XX genital ridges into three equal (anterior, middle or posterior) segments at 14-15 ts and cultured for 14 or 30 hours until the stage corresponding to 21 or 30 ts, respectively. Finally, I examined HS-treatment-induced SOX9 expression patterns in these explants (Fig. 2-14C). Separation of three segments from the XX genital ridge did not have any appreciable effect on the anterior-to-posterior disappearance pattern of SOX9-inducibility in developing ovarian segments (Fig. 2-14D, E).

All these data suggest that the unidentified ovarian factor(s) other than WNT4 and FOXL2 are responsible for the loss of the SRY-dependent SOX9 inducibility. In addition, it occurs tissue- and region-autonomous manner in developing XX gonads.

Identification of several ovarian factors whose expression negatively correlates with the loss and reacquisition of SRY-dependent SOX9-inducibility in developing granulosa cells.

In order to detect unidentified factors which lead disappearance of SRY-dependent SOX9-inducibility further, I decided to conduct comprehensive gene profile analysis by DNA microarray. As described above, in transplanted ovaries under male kidney capsule, SRY-dependent SOX9-inducibility was reaquired from day 0 to days 10 (Fig. 2-8E, H). On

the other hand, from 11.5 dpc to 12.5 dpc, SRY-dependent SOX9-inducibility disappeared (Fig. 2-1B). Therefore, genes down-regulated in days 10 transplants compared with day 0 and up-regulated in 12.5 dpc XX ovaries (i.e., genes negatively correlated with SRY-inducible SOX9-inducibility) could be unidentified genes I want to know (Fig. 2-15A). In transplants, I used busulfan-treated ovaries to eliminate the effect of oocyte-related genes as much as possible. For 12.5 dpc gonads, I used microarray data comparing *Sry*-EGFP positive XX cells with XY cells by Bouma et al. (2010).

As a result, unsupervised clustering among day 0, days 10 transplants, 12.5 dpc XX and XY somatic cells showed that days 10 transplants were clustered together with 12.5 dpc XY samples rather than XX, although the values in correlation matrix between days 10 transplants and 12.5 dpc XY samples seemed to be slightly low (Fig. 2-15B) (554 genes whose expression was changed in days 10 transplants compared with day 0 was used; log fold > 1, $p < 0.05$). On gene clustering, I found that genes were clustered into three types (Fig. 2-15C). In part of cluster-A, genes were down-regulated in days 10 transplants and up-regulated both in day 0 ones and 12.5 dpc XX somatic cells. In some part of cluster-B and C, genes were up-regulated both in days 10 transplants and 12.5 dpc XY somatic cells (Fig. 2-15C). Thus, I thought that unidentified genes I want were contained in cluster-A. In order to analyse genes in cluster-A further, next I performed supervised analyses. On comparing days 10 (expriment) with day 0 (baseline), GO analysis demonstrated that G1 to S cell cycle control pathways were changed, which is consistent with my observation of the change of PCNA index (Table 2-1, Fig. 2-7E, F). 787 genes were down-regulated (Fig. 2-15D; log fold < -1, $p < 0.05$) and among these, I found many genes which seemed to be related to experimental procedure or loss of oocytes rather than somatic sex reversal or reaquirement of SOX9 inducibility (e.g.

Hbb-y, *Hba-x*, *Hbb-bh1* might be associated with low-oxygen under kidney capsule, and *Sox2* has been reported to express highly in oocytes) (Avilion et al., 2003) (Table 2-2). In order to pick up more precise candidates, I crossed pre-granulosa cell specific 1116 genes at 12.5 dpc by Bouma et al. (2010) and got 236 genes (Fig. 2-15D, Table 2-3). Many known ovarian genes such as *Bmp2*, *Nr0b1/Dax1*, *Irx3*, *Fst*, *Wnt4* were found to be down-regulated (rank 56th, 70th, 98th, 119th, 173th, respectively) (Swain et al., 1998; Jorgensen and Gao, 2005; Kim et al., 2011; Ludbrook et al., 2012).

As described above, neither WNT4 nor FOXL2 is responsible for the loss of SRY-dependent SOX9-inducibility in developing ovaries at early stages (Fig. 2-12). Recently, Garcia-Ortiz et al. (2009) showed the ovarian transcriptome independent of *Wnt4* or *Foxl2* at 12.5 dpc. Among 236 genes I identified above, 113 genes were overlapped (Fig. 2-15D, Table 2-3). In particular, considering tissue- and region-autonomous disappearance manner of SRY-dependent SOX9-inducibility (Fig. 2-14) and nuclear localization of heat-inducible SRY protein (Fig. 2-2), I thought that genes which can work at nuclei seemed to be potential candidate genes. By Gene Ontology annotation, from 236 genes, I obtained 43 genes which had possibility to localize at nuclei (Table 2-4).

Next, in order to confirm the result of microarray analyses, I performed real-time RT-PCR analysis of candidate genes with grafted ovaries at early stages of masculinization (i.e., days 0, 7 and 10 post-transplant). Among these genes, *Irx3*, *Zbtb7c*, *Lzts1*, and *Nr0b1/Dax1* were found to be significantly down-regulated in ovarian transplants at day 7 post-transplant (Fig. 2-16A). Anti-IRX3, anti-DAX1 and anti-EMX2 immunostaining also confirmed reduced signals in the grafted ovarian transplants at day 10 post-transplant (data not shown). In fetal

ovaries at 12.5-13.5 dpc, anti-IRX3 staining showed a negative correlation of its expression with the SOX9-inducibility, i.e., very weak IRX3-positive signals in SOX9-inducible cells, but their strong signals in other SOX9-negative ovarian cells (Fig. 2-16B). This is clearly in contrast to strong DAX1- or EMX2-positive signals in both SOX9-inducible and non-inducible ovarian cells in the 12.5 dpc ovaries.

Therefore, these data suggest that several factors such as *Irx3* and *Zbtb7c* can be responsible for the disappearance of sexually bipotential granulosa cell population, i.e., SRY-dependent SOX9-inducible granulosa cells. In other words, several factors I identified here are implicated to be early ovarian markers that negatively correlate with sexually bipotential population of granulosa cells.

Discussion

By monitoring the SRY-dependent SOX9-inducibility, this study is the first to visualize dynamic changes in sexual bipotentiality in developing XX gonads, showing an unexpected wide range of bipotential states of granulosa cell lineage, from the precursor state in the coelomic epithelium/bipotential state of gonadal supporting cells in early XX gonads to the high level of sexual plasticity in granulosa cells of postnatal ovaries. First, the present study demonstrated that, in the majority of XX supporting cells, the loss of the SRY-dependent SOX9-inducibility occurs in an anterior-to-posterior wave-like pattern from 18 to 24 ts (around 11.5~12.0 dpc). In contrast to a rapid loss of SOX9-inducibility in most XX supporting cells, interestingly, here I have discovered two distinct populations of supporting cell lineage that sustain the SOX9-inducibility in fetal ovaries even at 12.5 dpc. One is a subpopulation of the coelomic epithelial and subepithelial cells that cover the surface area of ovarian parenchyma from 11.5 to 12.5 dpc. Since testis-specific recruitment of Sertoli cell precursor occurs in the proliferating coelomic epithelial cells from 14 to 18 ts (Karl and Capel, 1998; Schmahl et al., 2000, Schmahl and Capel, 2003; Colvin et al.,2001), this SOX9-inducible population in the ovarian coelomic epithelium may be homologous to the reserved pool of the supporting cell precursors, which are fated to become SRY-positive pre-Sertoli cells in developing testis.

Most interestingly, another SOX9-inducible population is identical to a subpopulation of differentiated granulosa cells that are restrictedly localized in the ovarian medullary region adjacent to the mesonephros. The present data revealed that this ovarian medulla population is

mitotically silent throughout the fetal life, and then soon after birth, contributes to the first wave of folliculogenesis at prepubertal stages. These data provide, for the first time to my knowledge, direct evidence showing the unexpected heterogeneity in the sexual bipotentiality/plasticity of granulosa cells in mouse postnatal ovaries. The existence of the granulosa cell population with sexual bipotentiality would explain the ovotestis-like phenotype in various partial XX sex reversal models such as the *Esr1/Esr2* (estrogen receptor α/β; Couse et al., 1999; Dupont et al., 2003), *Foxl2/Wnt4* (Schmidt et al., 2004; Uda et al., 2004; Ottolenghi et al., 2007) and *Rspo1* (Chassot et al., 2008)-null ovaries. For example, in *Foxl2/Wnt4*-double null newborn ovaries, it was reported that the testis cord-like tubules in the medullary region harbored well-differentiated spermatogonia, in contrast to the ovarian structures including oocytes in the cortex region (Ottolenghi et al., 2007). In *Esr1/Esr2*-double null prepubertal ovaries, it was also shown that the initial transdifferentiation into the seminiferous-like tubules with SOX9-positive Sertoli-like cells appears to be found in the first wave of folliculogenesis in the centro-medullary region (Dupont et al., 2003). The present data using a partial sex reversal model of the grafted ovaries also demonstrated that, in the wild type ovarian transplants, spontaneous transdifferentiation of granulosa cells into SOX9-positive Sertoli-like cells is restrictedly found in ovarian medullary region (Figs. 2-8C,D; 2-10). In addition, the loss of the SOX9-inducibility was reversible in the most of these cells of the grafted ovaries, showing reacquirement of this inducibility before the onset of a partial sex reversal (Fig. 2-8E-H). Taken together, these data therefore suggest that such SOX9-inducible granulosa cells in the medullary region cause or contribute to partial masculinization in various SRY-negative XX sex reversal cases.

Although FOXL2 was recently shown to be crucial for the maintenance of ovarian phenotype in the granulosa cells at the adult stage (Uhlenhaut et al., 2009), unfortunately, it was shown that either loss or reacquirement of the SOX9-inducibility in these cells occurs independently of FOXL2 expression in developing ovaries (Figs. 2-1I; 2-5C; 2-8F, G). By the contrast, in *Wnt4*-mutant embryos, it was shown that reduced *Wnt4* activity does not alter any reduced patterns of this SOX9-inducibility in developing XX gonads (Fig. 2-12). Moreover, the present data demonstrated that proper reduction of the SOX9-inducibility occurred even in the *Wnt4*-null XX gonads at 21-26 ts (before the onset of FOXL2 expression) where immunoreactive FOXL2 activity was almost abolished, similar to the situation seen in XX gonads of the *Wnt4/Foxl2*-double null embryos (Ottolenghi et al., 2007a) (Fig. 2-12C). Taken together, these data suggest that neither WNT4 nor FOXL2 is responsible for the loss of the SRY-dependent SOX9-inducibility in the majority of XX supporting cells. Since any appreciable changes in the disappearance pattern of SOX9-inducibility could not be detected in XX Tg explants (initiated at 14 ts) cultured in the presence of retinoic acid (2μM) or pan-RAR antagonist (7.5μM) (n= 4 for each; Harikae and Kanai, data not shown), these data clearly highlight the existence of other unidentified ovarian factor(s) which tissue- and region-autonomously antagonize(s) the SRY action in developing XX gonads.

From microarray analyses, I could gain some candidates for the cause of loss of SRY-dependent SOX9-inducibility. Considering my results, 113 ovarian genes independent of *Wnt4* and *Foxl2* might be the leading candidates (Table 2-3). Actually, expression and/or localization of transcripton factors, *Irx3*, *Zbtb7c* and *Emx2*, were found to be significantly decreased on the reaquirement of SRY-dependent SOX9-inducibility by transplanted ovaries (Fig. 2-16). Because SOX9 is known to be maintained by synergistic action of SRY and

SF1/Ad4BP on *Sox9* enhancer TESCO and the clear localization of SF1/Ad4BP and heat-induced SRY at nucleus was observed at the present study, I can suggest that the genes which can bind TESCO and antagonize SRY action might be the cause of the loss of SRY-dependent SOX9 inducibility (Sekido et al., 2008; Figs. 2-2, 2-3). Moreover, recently, I have crossed the inducible *Sry* Tg mouse line onto the XO/*Eda*^{Ta} mouse line which lacks one X chromosome spontaneously (Probst et al., 2008). Unfortunately, XO/*Eda*^{Ta} mouse line was very hard to breed in my laboratory and the number of mother mice ($X^{Ta}O$) available was limited, so I used new-born mice instead of 11.0 to 12.5 dpc fetuses. Surprisingly, in XO Tg new-born ovaries, I have found that high SOX9-inducibility were maintained not only in ovarian medullary region but throughout the ovarian parenchyma (n=2; Fig. 2-17). Therefore, it might be possible that genes on X chromosome (*Mbnl3* etc.) are the cause of loss of SOX9-inducibility. However, to define the cause and its relationship with ovarian differentiation precisely, I must conduct further experiment.

The identification of such population of sexually bipotential granulosa cells and the genes responsible for the loss of sexual bipotency (i.e., presumptive early ovary-determining/ differentiating gene) has important implications for their contribution to not only masculinization, but also aberrant folliculogenesis and granulosa cell tumorigenesis in immature ovaries.

Figures and Legends

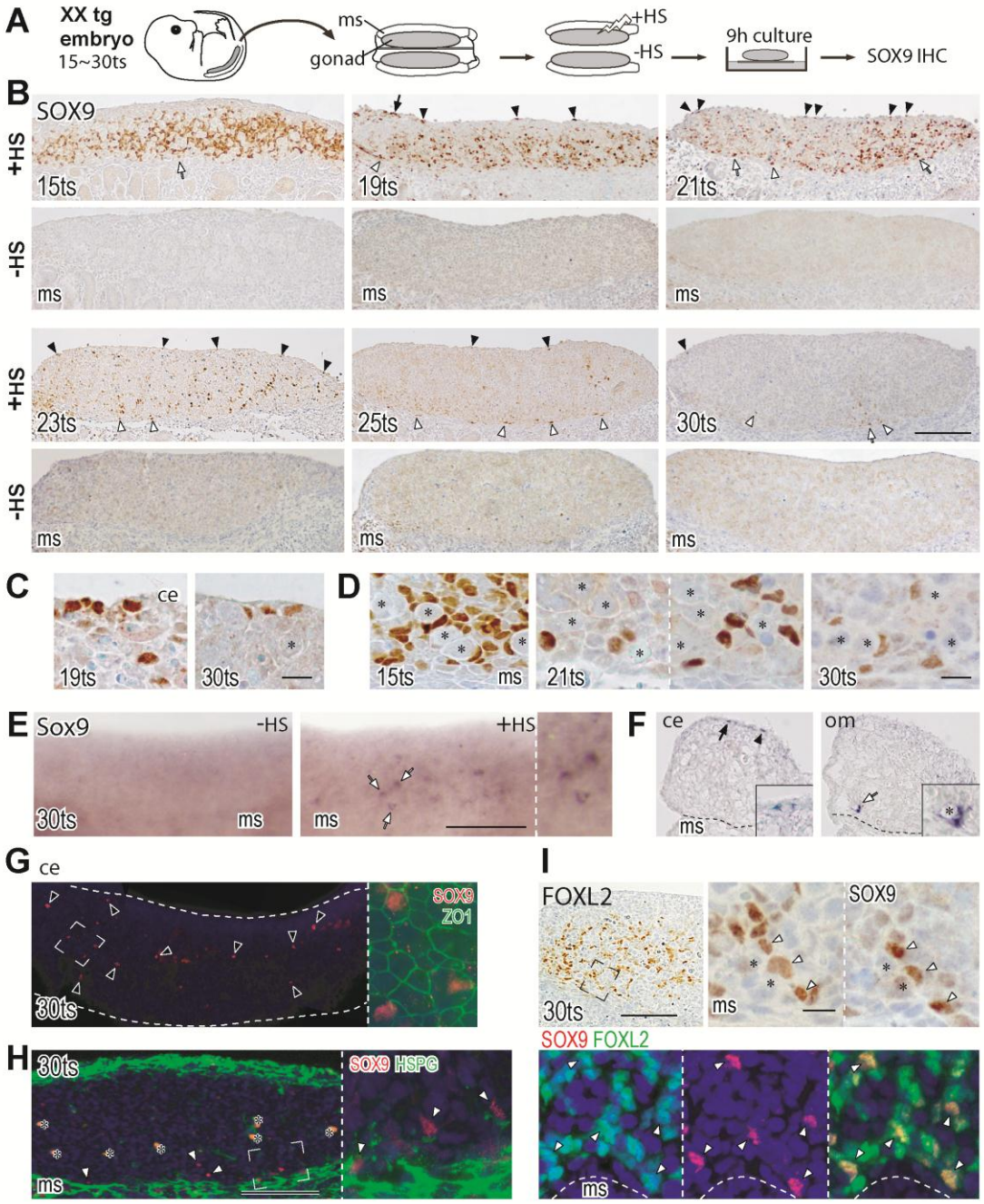
A
XX tg
embryo
15~30ts
ms
gonad
+HS
-HS
9h culture
SOX9 IHC
B
SOX9
+HS
-HS
15ts
19ts
21ts
23ts
25ts
30ts
ms
C
ce
19ts
30ts
D
15ts
ms
21ts
30ts
E
Sox9
-HS
+HS
30ts
ms
F
ce
om
ms
G
ce
SOX9
ZO1
30ts
I
FOXL2
SOX9
30ts
ms
SOX9 FOXL2
H
30ts
SOX9 HSPG
ms

FIGURE 2-1

Figure 2-1. Spatiotemporal changes in SRY-dependent SOX9-inducibility in developing XX gonads

(**A**) XX genital ridges were subjected to HS treatment (43°C, 10 min) to induce ectopic transient SRY expression and then cultured for 9 hours. (**B-D**) Anti-SOX9 immunostaining of HS-treated (+HS) and non-treated (-HS) ovarian explants initiated at various stages. SOX9-positive signals are found in the coelomic epithelial/subepithelial cells (solid arrowheads in B; C) and the presumptive pre-granulosa cells located in the ovarian medullary region (open arrowheads in B; D) even at 30 ts. (**E, F**) Whole mount in situ hybridization (E) and their sectioning images (F) of fetal ovaries at 30 ts showing ectopic *Sox9* expression in the coelomic epithelium (ce) and ovarian medullary region (om). (**G**) Whole mount anti-SOX9 (red)/ anti-ZO1 (green) double-immunostaining of the fetal ovaries at 30 ts, showing SOX9-induced cells in the ovarian surface (arrowheads). (**H**) Anti-SOX9 (red)/ anti-HSPG (green) double-immunostaining of the fetal ovaries at 30ts showing SOX9-induced cells at the bottom of HSPG-negative ovarian parenchyma (note: strong anti-HSPG-positive signals in ovarian surface region and in the border region along the mesonephros.) (**I**) Comparative anti-SOX9/ anti-FOXL2 staining of two consecutive sections (brown; upper plates) and anti-SOX9 (red)/ anti-FOXL2 (green) double-staining (DAPI, dark blue; lower plates) of the fetal ovaries at 30 ts (open arrowheads). Plates in C-D and insets in E-I show higher magnified images indicated by the arrows (B, E, F) or by broken rectangles (G-I). The anterior pole side is shown on the left in each plate. Asterisk, blood cells in H and germ cells in others; ce, coelomic epithelium; ms, mesonephros. Scale bar: 100 μm in B, E, H-I, and 10 μm in others.

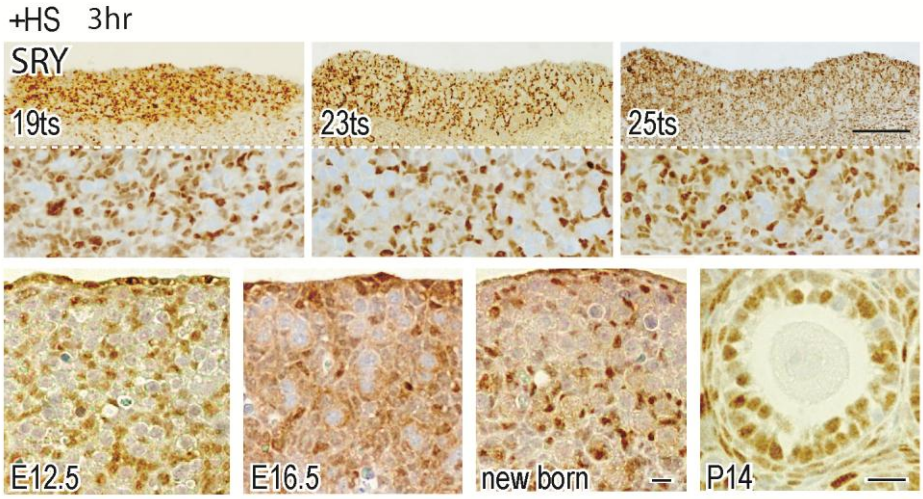

FIGURE 2-2

Figure 2-2. Ubiquitous SRY expression in HS-treated XX Tg ovarian explants

Anti-SRY immunostaining (brown staining) of ovarian explants (initiated at 19~25 ts, at 12.5 and 16.5 dpc, and at 0 and 14 dpp; 3-hour culture). Ubiquitous SRY expression is seen in ovarian somatic cells (albeit no SRY expression in germ cells). Upper three plates (19, 23 and 25 ts) include the insets showing higher magnified images of the nuclear staining. ms, mesonephros. Scale bar: 100 μm in upper plates and 10 μm in lower plates.

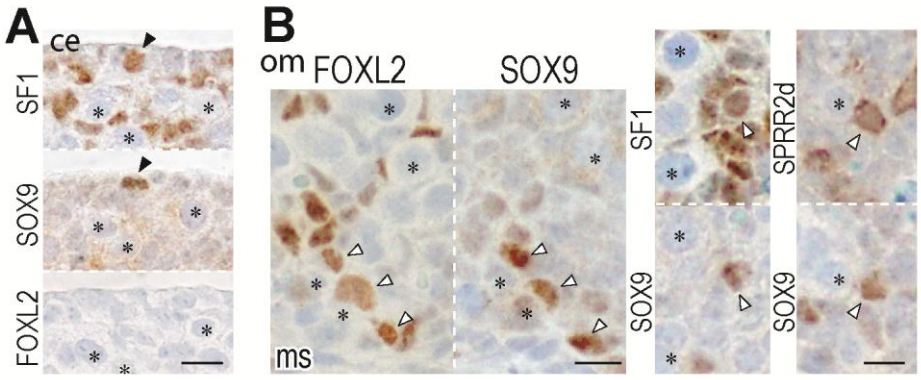

FIGURE 2-3

Figure 2-3. Comparative anti-SOX9 staining of three consecutive sections with anti-SF1/Ad4Bp, anti-FOXL2 or anti-SPRR2d staining in SRY-induced ovarian explants initiated at 30 ts (9-hour culture).

SOX9-inducible cells appear to be SF1-positive/FOXL2-negative signals in coelomic epithelia (solid arrowheads in A) and SF1-positive/ SPRR2d-positive in ovarian medullary region (open arrowheads in B). Asterisk, germ cells; ce, coelomic epithelium; ms, mesonephros. Scale bar: 10 μm

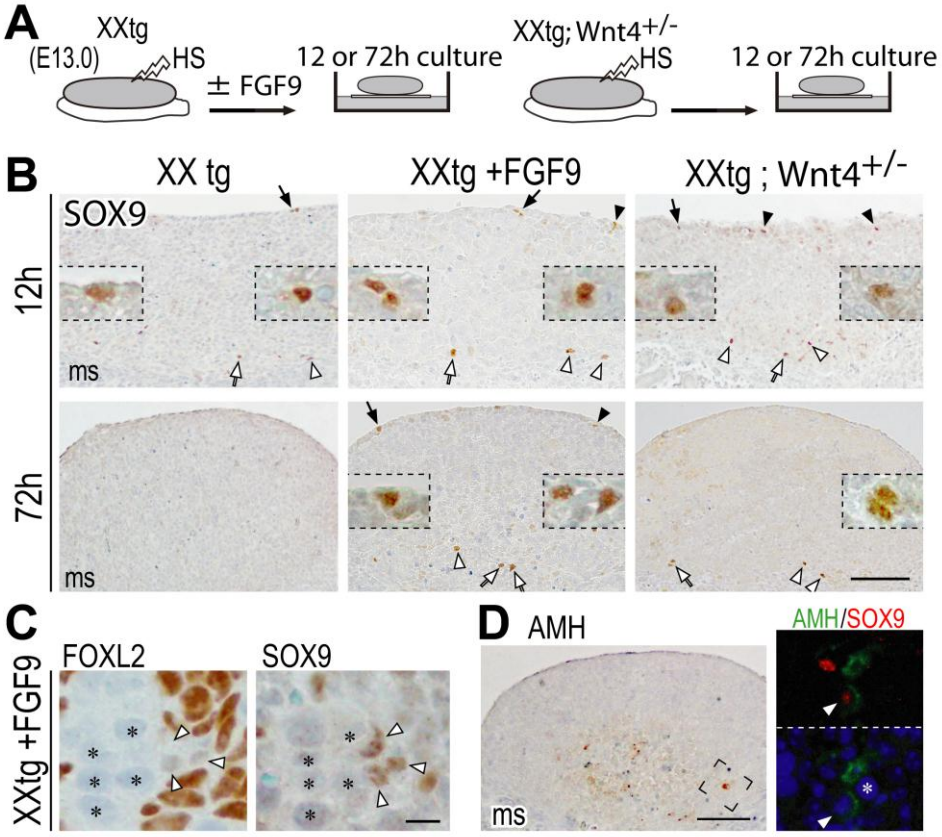
A
XXtg
(E13.0)
HS
± FGF9
12 or 72h culture
XXtg; Wnt4+/-
HS
12 or 72h culture
B
XX tg
XXtg +FGF9
XXtg ; Wnt4+/-
SOX9
12h
72h
ms
ms
C
XXtg +FGF9
FOXL2
SOX9
D
AMH
ms
AMH/SOX9

FIGURE 2-4

Figure 2-4. Trans-differentiation of SOX9-induced granulosa cells into Sertoli-like cells by a forced male-specific FGF9/WNT4 signaling state

(**A**) Wildtype and *Wnt4*-heterozygote XX Tg ovaries at 13.0 dpc were subjected to HS treatment and then cultured in the presence or absence of FGF9 (100 ng/ml) for 12 and 72 hours. (**B**) Anti-SOX9 immunostaining (brown) of SRY-induced ovarian explants showing that either exogenous FGF9 or reduced *Wnt4* activity induced sustained high levels of SOX9 expression in the ovarian medulla population (open arrowheads/arrows) in 72-hour culture. In the coelomic epithelial/subepithelial regions, SOX9 expression is maintained in only a few cells in FGF9-treated explants (solid arrowheads/arrows). Right or left insets show higher magnified images of the SOX9-induced cells in ovarian medulla (open arrows) or in coelomic epithelium (solid arrows), respectively. (**C**, **D**) Comparative anti-SOX9 staining of two consecutive sections with anti-FOXL2/ anti-AMH staining in FGF9-treated explants initiated at 13.0 dpc (72-hour culture). The SOX9-induced granulosa cells in the ovarian medulla are FOXL2-negative (C) and AMH-positive (D) Sertoli-like cells in 72-hour culture. In D, two consecutive sections were stained with anti-AMH staining (brown; left plate) and anti-AMH (green)/ anti-SOX9 (red)-double staining (right plate, which corresponds to the area indicated by a broken rectangle in the left plate). Asterisk, oocyte; ms, mesonephros. Scale bar: 10 μm in C, and 100 μm in others.

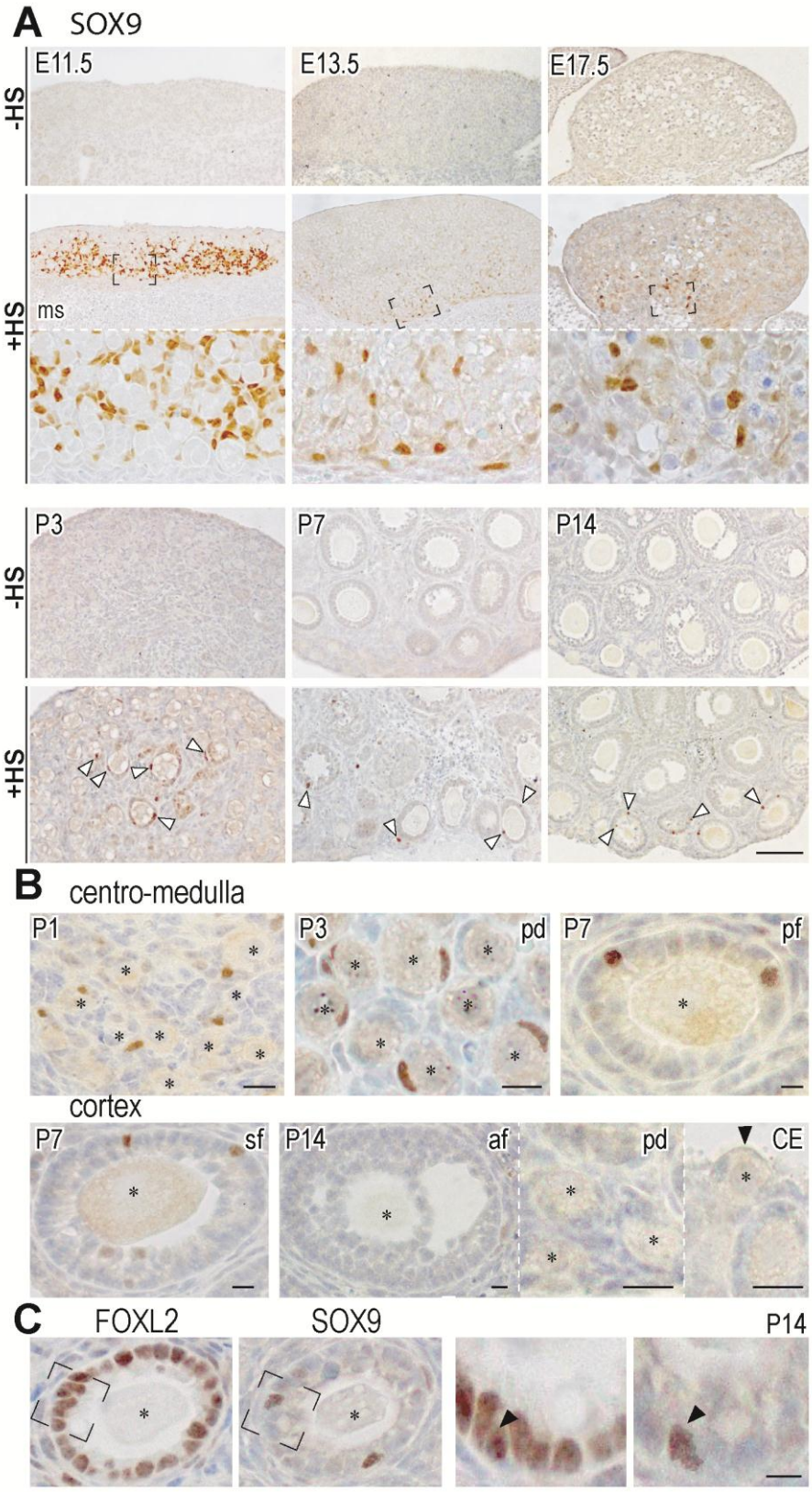
A
SOX9
E11.5
E13.5
E17.5
SH-
SH+
ms
P3
P7
P14
B
centro-medulla
P1
P3
pd
P7
pf
cortex
P7
sf
P14
af
pd
CE
C
FOXL2
SOX9
P14

FIGURE 2-5

Figure 2-5. SOX9-inducible granulosa cells in the ovarian medulla contribute to the first wave of folliculogenesis

Anti-SOX9 immunostaining (brown) of SRY-induced ovarian explants from various developmental stages of embryos (E) and pups (P) (9-hour culture). The SOX9-inducible granulosa cells are retained in the ovarian medullary region adjacent to the mesonephros during the fetal stages (broken rectangles in A). This population contributes to the initial round of folliculogenesis in postnatal ovaries (open arrowheads in A; B). In most-right lower plate of B, solid arrowhead indicates the ovarian surface epithelia. In C, comparative anti-SOX9/ anti-FOXL2 staining of two consecutive sections shows SOX9-inducibility in FOXL2-positive basal granulosa cells of the primary follicle at 14 dpp (solid arrowheads in C). In A and C, broken rectangles demarcate the areas magnified in the insets. Asterisk, oocyte; af, antral follicle; ce, coelomic (or ovarian surface) epithelium; ms, mesonephros, pd, primordial follicle; pf, primary follicle; sf, secondary follicle. Scale bar: 100 μm in A and 10 μm in B, C.

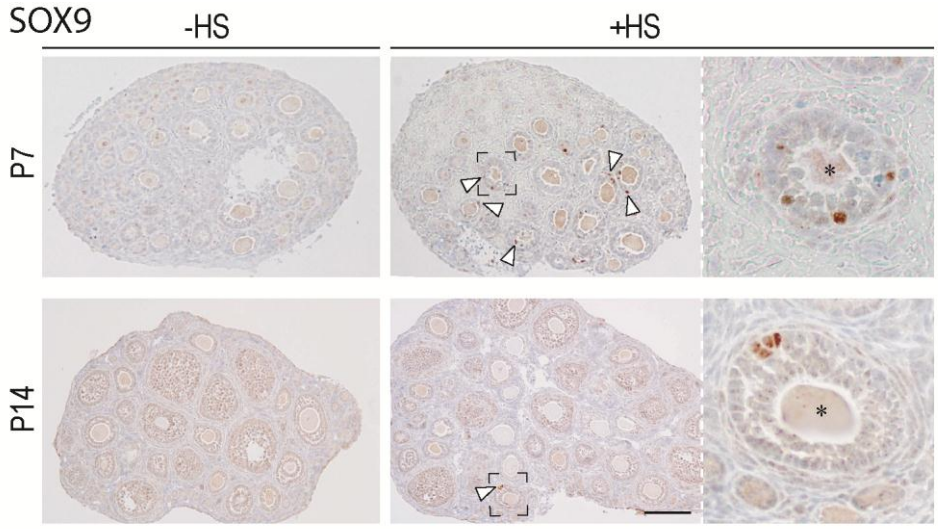

FIGURE 2-6

Figure 2-6. Detection of SOX9-inducibility in postnatal ovaries treated with heat shock in vivo.

Anti-SOX9 immunostaining (brown staining) of ovaries subjected to in vivo HS treatment at 7 (P7) and 14 (P14) dpp (9-hour recovery after HS treatment). In postnatal XX Tg ovaries, one of each pair (left ovary) was extracted from the abdominal cavity and immersed in pre-warmed DMEM (43 °C 15 min) in a 0.5 ml tube for 15 min under anesthesia. The other (right) ovary was used as a non-treated control. The HS-treated ovaries were returned to the original position and sutured, and the HS-operated mice were allowed to recover for 9 hours. In the HS-treated ovary (+HS), SOX9–positive cells are frequently found in primordial and primary follicles in the centro-medullary region at 7 and 14 dpp (open arrowheads), as in the in vitro HS-treatment experiments shown in Fig. 2-3. The SOX9-positive signals disappear in developing follicles during the transition into the secondary follicle stage at 7-14 dpp. No SOX9-positive cells are detected in non-treated ovaries (-HS). Inset plates show higher magnified images surrounded by broken rectangles. Scale bar: 100 μm.

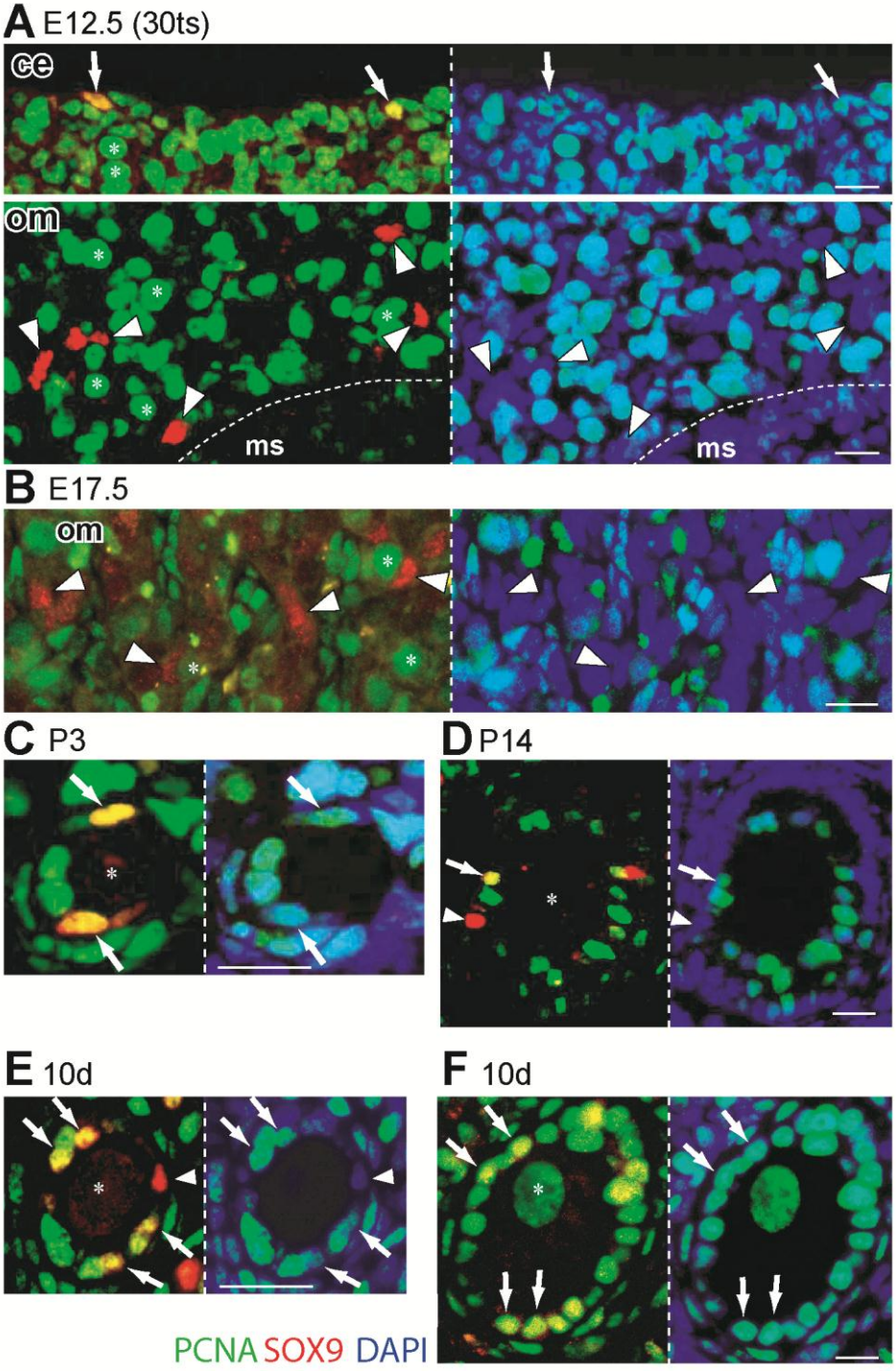
A E12.5 (30ts)
ce
om
ms
ms
B E17.5
om
C P3
D P14
E 10d
F 10d
PCNA SOX9 DAPI

FIGURE 2-7

Figure 2-7. Anti-PCNA staining showing proliferative activities of SOX9-inducible populations in developing ovaries (A-D) and ovarian transplants grafted (E, F). Anti-PCNA (green fluorescence) and anti-SOX9 (red fluorescence)-double staining (DAPI, dark blue) of HS-treated Tg ovarian explants initiated at 12.5 dpc (30 ts; **A**), 17.5 dpc (**B**), 3 dpp (**C**), and 14 dpp (**D**) (9-hour culture after HS treatment). In the coelomic epithelium (ce), many SOX9-inducible cells are positive for anti-PCNA staining (PCNA-positive index, 91.7 +/- 8.3%; arrows in A). In the ovarian medullary region (om), most of SOX9-inducible granulosa cells are negative for anti-PCNA staining at 12.5 dpc (arrowheads in A; PCNA-positive index, 14.2 +/- 6.2%) and at 17.5 dpc (arrowheads in B; PCNA-positive index, 5.6 +/- 3.2%). After birth, SOX9-inducible granulosa cells become PCNA-positive during the initial round of folliculogenesis (arrows in C, D; PCNA-positive index, 64.0 +/- 7.2% at P3 and 60.9 +/- 11.4% at P14, respectively). In the grafted ovarian transplants at day 10 post-transplant (**E**, **F**), SOX9-inducible granulosa cells are highly positive for anti-PCNA staining at presumptive primary and secondary follicle (PCNA-positive index, 91.0+/- 2.2% [n=4]; arrows in E). Each right plate shows a merged image of PCNA (green) and DAPI (blue). Broken lines mark the gonad/mesonephros border. ms, mesonephros. Scale bar: 10 μm.

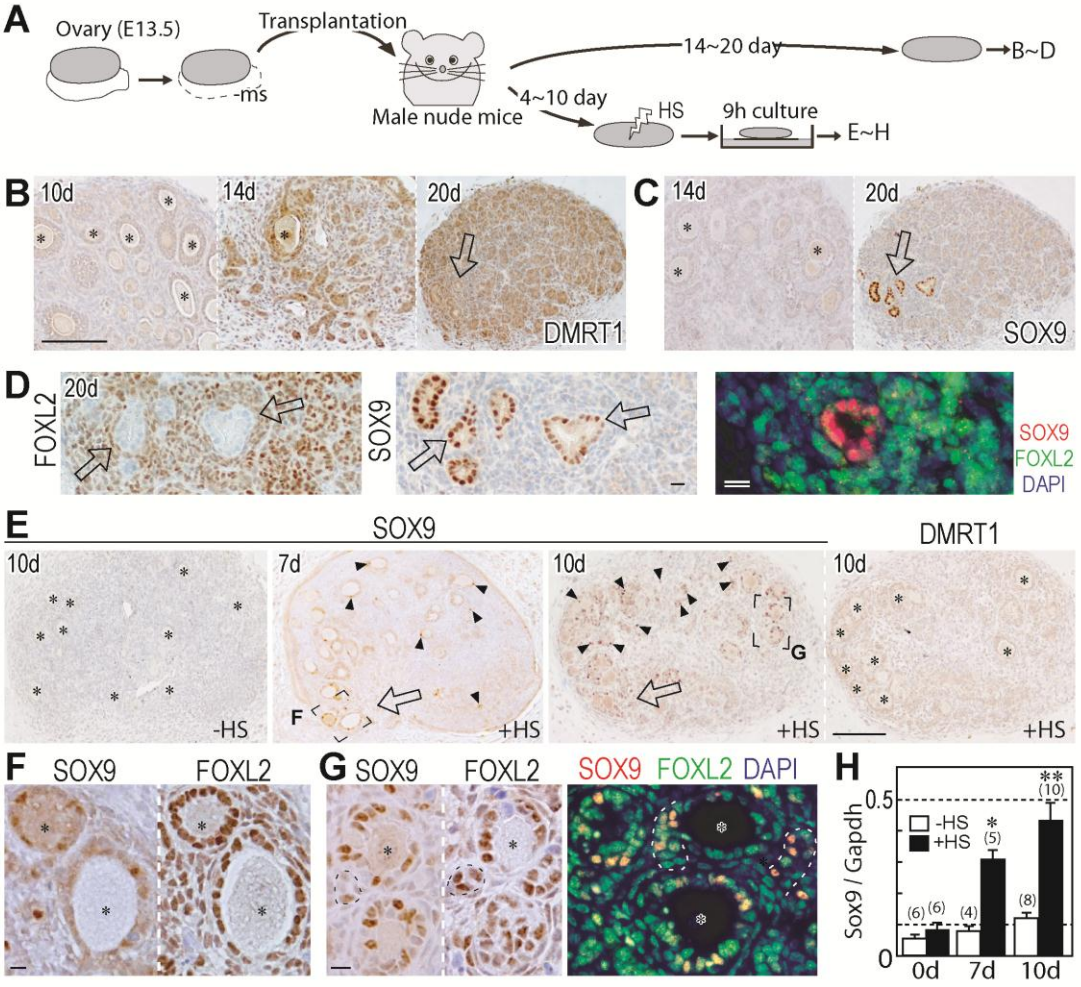
A
Ovary (E13.5)
-ms
Transplantation
Male nude mice
14~20 day
B~D
4~10 day
HS
9h culture
E~H
B
10d
14d
20d
DMRT1
C
14d
20d
SOX9
D
FOXL2
20d
SOX9
SOX9
FOXL2
DAPI
E
SOX9
DMRT1
10d
7d
10d
10d
-HS
+HS
+HS
+HS
F
G
F SOX9
FOXL2
G SOX9
FOXL2
SOX9 FOXL2 DAPI
H
Sox9 / Gapdh
0.5
0
-HS
+HS
(6) (6) (4) (5) (8) (10)
0d
7d
10d

FIGURE 2-8

Figure 2-8. Reacquisition of SRY-dependent SOX9-inducibility in granulosa cells during masculinization of grafted ovaries

(**A**) The fetal ovaries at 13.5 dpc were transplanted under the kidney capsule for 4 to 20 days, treated with or without HS treatment, and then cultured for 9 hours. (**B-D**) Comparative anti-SOX9 (C) staining with anti-DMRT1 (B) and anti-FOXL2 (D) staining in the consecutive sections of non-treated wildtype ovarian transplants. The spontaneous SOX9-positive/FOXL2-negative ovarian cells are detectable in the ovarian medullary region at day 20 post-transplant (large open arrow in C, D). (**E-G**) Anti-SOX9 immunohistochemical analysis of non-treated (-HS, most left plate in E) and HS-treated (+HS) ovarian explants at 7 and 10 days post-transplant, showing a considerable increase in numbers of SOX9-inducible cells (arrowheads) before the onset of high DMRT1 expression (E). In E, large open arrows indicate the presumptive SOX9-inducible populations that are maintained in the ovarian medullary region. In F and G, comparative anti-SOX9/ anti-FOXL2 staining of two consecutive sections shows SOX9-inducible/ FOXL2-positive granulosa cells located in ovarian follicles and testis cord-like structures (broken lines). The immunofluorescent images of anti-SOX9 (red) / anti-FOXL2 (green) double staining are also shown in D and G. (**H**) Real-time RT-PCR analysis showing *Sox9* transcript levels relative to *Gapdh* (the mean values ± standard error; n= 4~10) in the HS-treated and non-treated ovarian explants at days 0, 7 and 10 after transplantation. In the ovarian transplants, *Sox9*-inducible levels are significantly higher at days 7 and 10 post-transplant than that at day 0 post-transplant (**p<0.01). In H, two horizontal broken lines indicate *Sox9* transcript levels in the wildtype testes (0.50 +/- 0.20) and ovaries (0.10 +/- 0.01) at 13.5 dpc, respectively. Asterisk, oocytes; ms, mesonephros. Scale bar: 100 μm in B, E, and 10 μm in others.

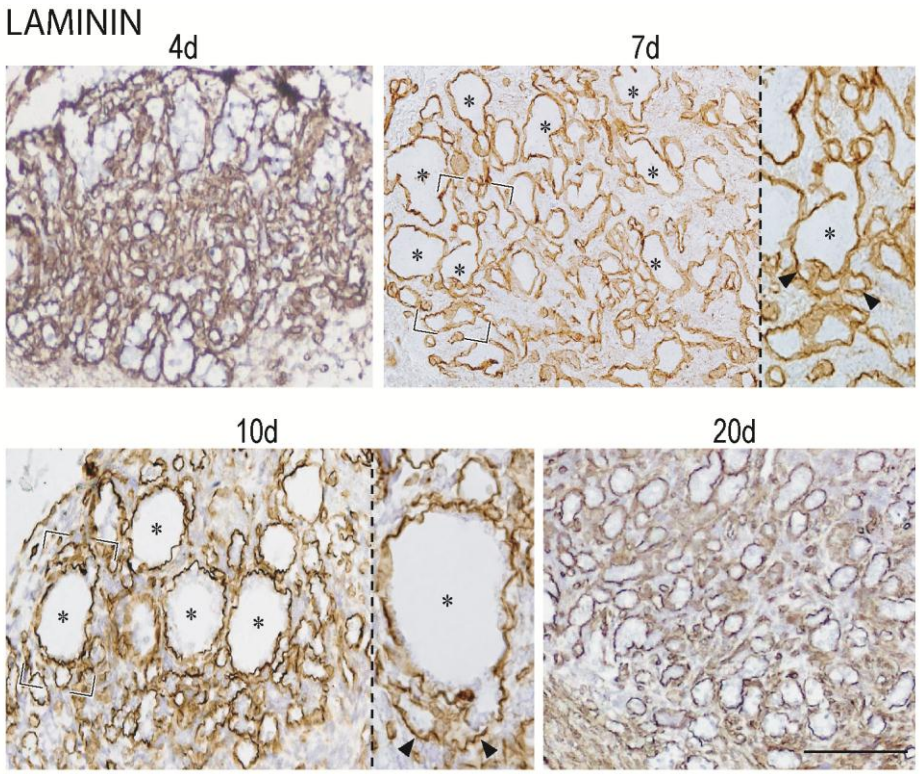

FIGURE 2-9

Figure 2-9. Formation of testis cord-like structures in ovaries grafted under the kidney capsule of nude male mice

The fetal ovaries from wild type embryos at 13.5 dpc were grafted under the kidney capsule for 4 to 20 days, and then analyzed by anti-Laminin immunostaining. Anti-Laminin staining visualized ovarian ovigerous cords in the ovarian parenchyma at day 4 post-transplant. At 7 to 10 days post-transplant, a part of the growing primordial and primary follicles (asterisks) starts to transform into a testis cord-like structure (arrowheads). At day 20, the testis cord-like structures are well developed throughout the ovarian parenchyma. Broken rectangles in left plates indicate the area highly magnified in right plates. Scale bar: 100 μm.

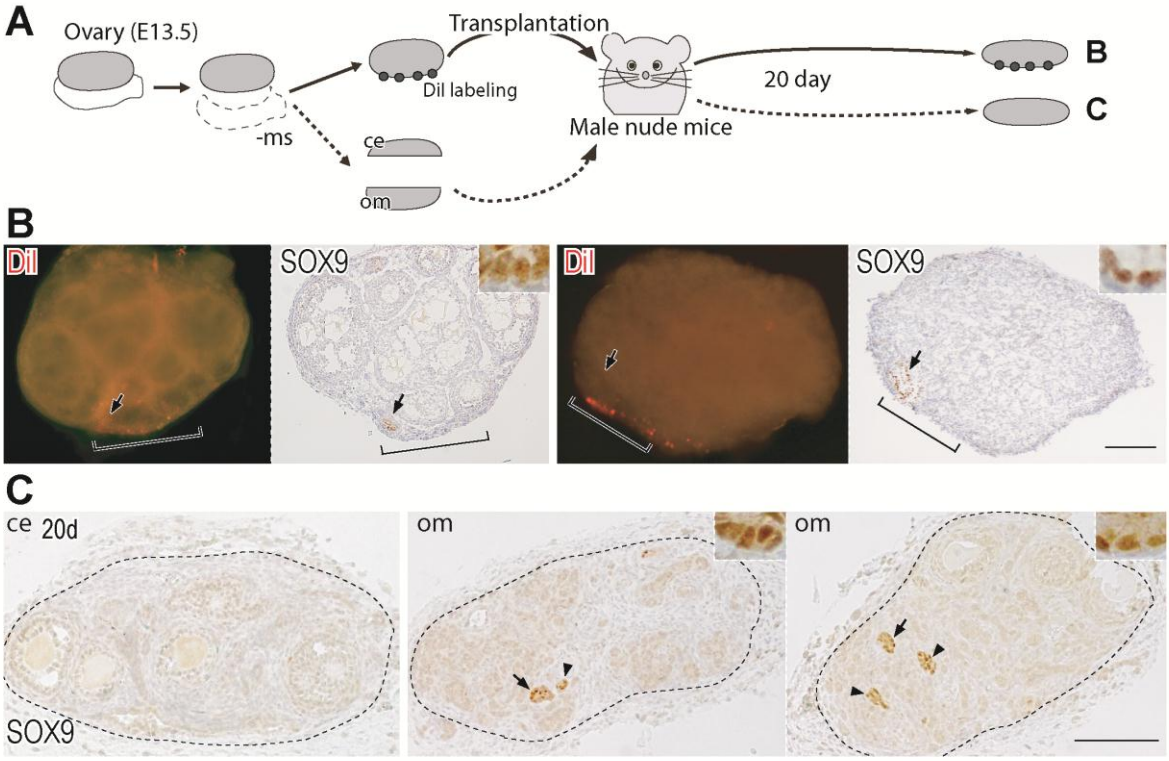
A
Ovary (E13.5)
-ms
Dil labeling
Transplantation
ce
om
Male nude mice
20 day
B
C
B
DiI
SOX9
DiI
SOX9
C
ce 20d
SOX9
om
om

FIGURE 2-10

Figure 2-10. Spontaneous appearance of SOX9-positive Sertoli-like cells in the ovarian medullary region in grafted ovaries

(**A**) The fetal ovaries from wild type embryos at 13.5 dpc were labeled with DiI at the mesonephric side, and then transplanted under the kidney capsule for 20 days. (**B**) Anti-SOX9 (brown staining; right in each plate) immunostaining of two DiI-labeled (red fluorescence; left in each plate) grafted ovaries at day 20 post-transplant. Almost all of SOX9-positive Sertoli-like cells (arrows; right upper insets) appear in the region near the DiI-labeled area of ovarian parenchyma. (**C**) Ovarian medulla (om) of fetal ovaries were separated from coelomic epithelium (ce) and each part were transplanted (A). Anti-SOX9 immunostaining show positive signals are only detecetd in ovarian medullary region. Most of transplants containing only coelomic epithelial region were degenerated. Scale bar: 100 μm.

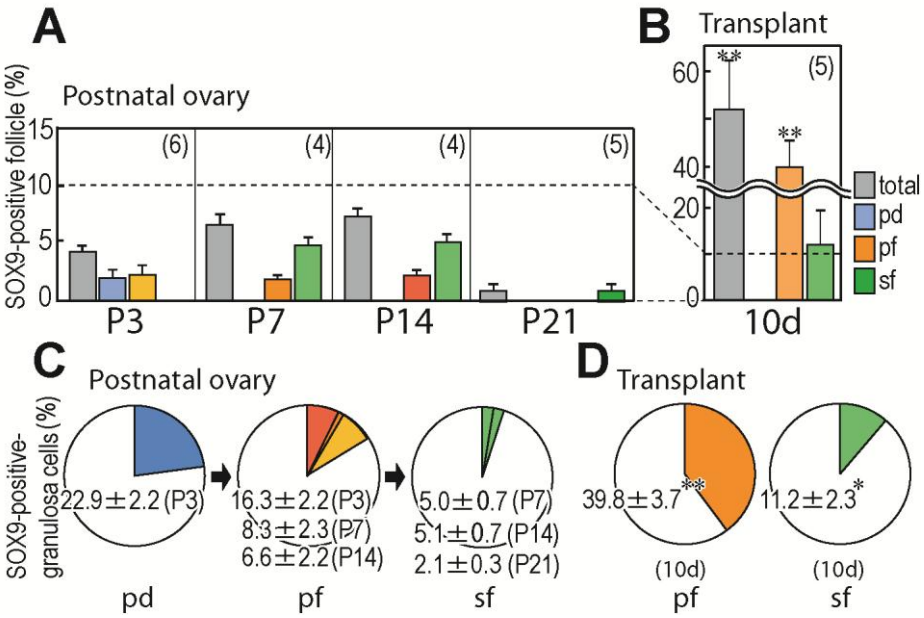
A
Postnatal ovary
SOX9-positive follicle (%)
15
10
5
0
(6)
(4)
(4)
(5)
P3
P7
P14
P21
B
Transplant
60
40
20
0
**
**
(5)
10d
total
pd
pf
sf
C
Postnatal ovary
SOX9-positive-granulosa cells (%)
22.9±2.2 (P3)
16.3±2.2 (P3)
8.3±2.3 (P7)
6.6±2.2 (P14)
5.0±0.7 (P7)
5.1±0.7 (P14)
2.1±0.3 (P21)
pd
pf
sf
D
Transplant
39.8±3.7**
11.2±2.3*
(10d)
(10d)
pf
sf

FIGURE 2-11

Figure 2-11. Changes in relative number of the SOX9-inducible follicles and SOX9-inducible granulosa cells in postnatal (P3~21; A, C) and grafted (day 10 post-transplant; B, D) ovaries The bar graphs showing relative numbers of the SOX9-inducible follicles per total follicle number at each stage (A, B). The circle graphs showing relative numbers of SOX9-inducible granulosa cells per total granulosa cells in each SOX9-induced follicle (C, D). All values in the grafted ovarian transplants are significantly (*$p<0.05$, **$p<0.01$) higher than each corresponding value in the postnatal ovaries at any stage of P3~P21. Each number in parenthesis in A and B represents total number of the explants used. pd, primordial follicle; pf, primary follicle; sf, secondary follicle.

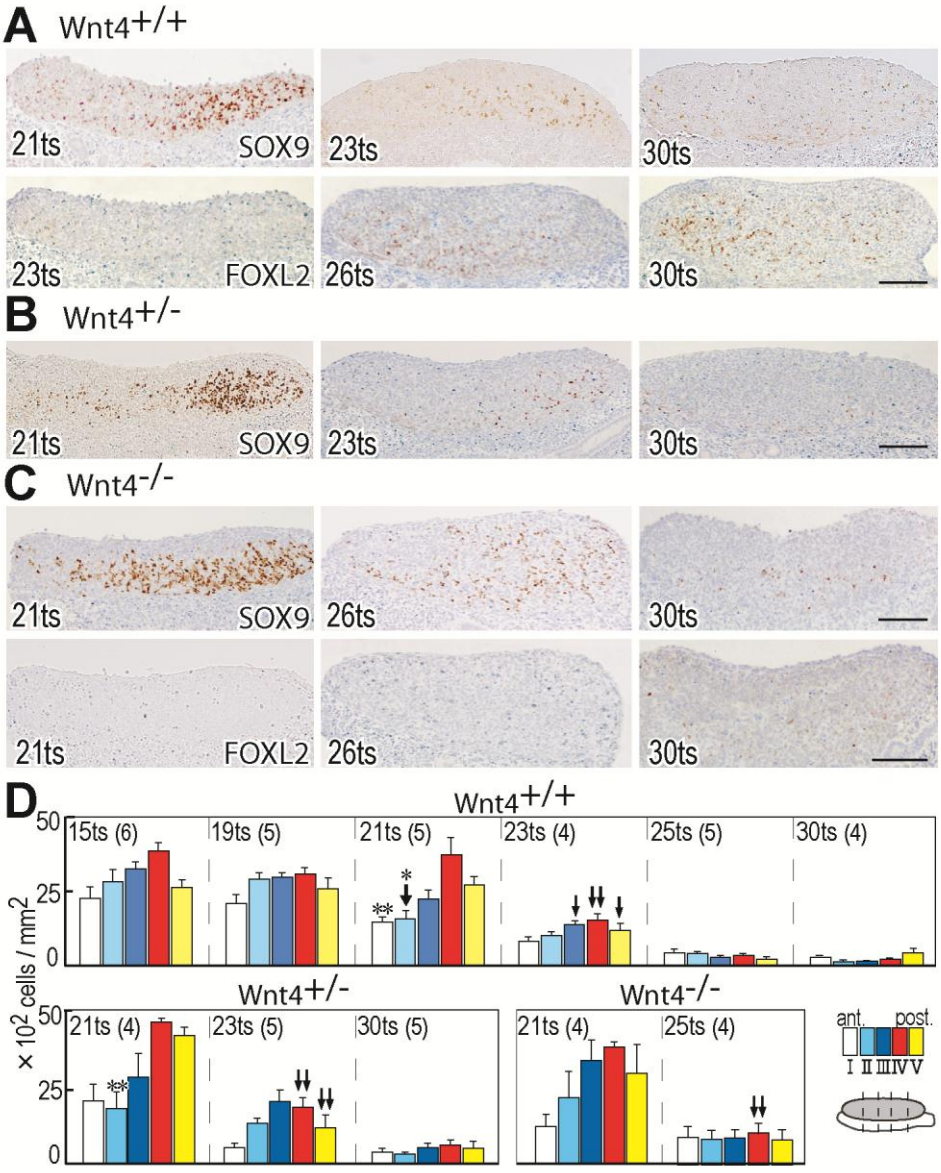
A Wnt4+/+
21ts
SOX9
23ts
30ts
23ts
FOXL2
26ts
30ts
B Wnt4+/-
21ts
SOX9
23ts
30ts
C Wnt4-/-
21ts
SOX9
26ts
30ts
21ts
FOXL2
26ts
30ts
D
Wnt4+/+
15ts (6)
19ts (5)
21ts (5)
23ts (4)
25ts (5)
30ts (4)
Wnt4+/-
21ts (4)
23ts (5)
30ts (5)
Wnt4-/-
21ts (4)
25ts (4)
× 10² cells / mm²
50
25
0
ant.
post.
I II III IV V

FIGURE 2-12

Figure 2-12. The loss of SRY-dependent SOX9-inducibility in *Wnt4*-mutant XX gonads (**A-C**) Anti-SOX9 (upper) and anti-FOXL2 (lower) immunostaining of two consecutive sections of HS-treated widltype (A), *Wnt4*-heterozygote (B) and *Wnt4*-null (C) ovarian explants (9-hour culture) initiated at 21-30 ts. The anterior pole side is shown on the left in each plate. (**D**) Quantitative data showing changes in the SOX9-induced cell number along AP axis of developing XX gonads in *Wnt4*-mutant background (each number in parenthesis indicates total number of the explants used). Vertical axis represents the SOX9-induced cell number per unit area, while horizontal axis represents regions I~V of the gonads. The significant reductions of SOX9-induced cell number are detected at 19-21 ts (region II) and 21-23 ts (regions III-V) in wildtype, at 21-23 ts (regions IV-V) in *Wnt4*-heterozygote, and at 21-25 ts (region IV) in *Wnt4*-null gonads ("↓" and "↓↓" indicate $p<0.05$ and $p<0.01$, respectively). In wildtype and *Wnt4*-heterozygote gonads at 21 ts, the SOX9-induced cell numbers are significantly lower in anterior regions than those in posterior regions (*$p<0.05$, **$p<0.01$, when compared between regions I and V or between regions II and IV). Any significant differences of the SOX9-inducible cell number in all regions (I~V) at 21ts could not be detected among wild type, *Wnt4*-heterozygote and *Wnt4*-null backgrounds by ANOVA analysis. Scale bar: 100 μm.

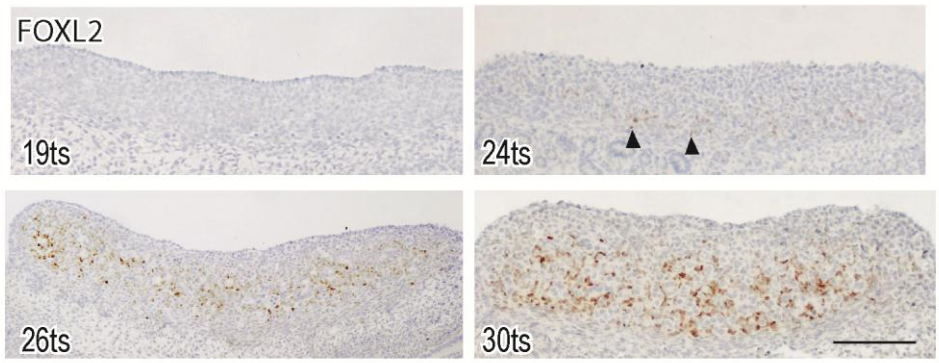

SUPPLEMENTAL FIGURE 2-13

Figure 2-13. FOXL2 expression patterns in developing XX gonads in vivo

Anti-FOXL2 immunostaining (brown staining; transverse section) of XX gonads at 19-30 ts, showing that FOXL2-positive signals are first detected in several gonadal cells near the mesonephros at 24 ts (arrowheads) and then expand into the whole ovarian parechyma at 30 ts. No FOXL2-positive signals are detected in the gonadal surface and subepithelial regions even at 30 ts. Scale bar: 100 μm.

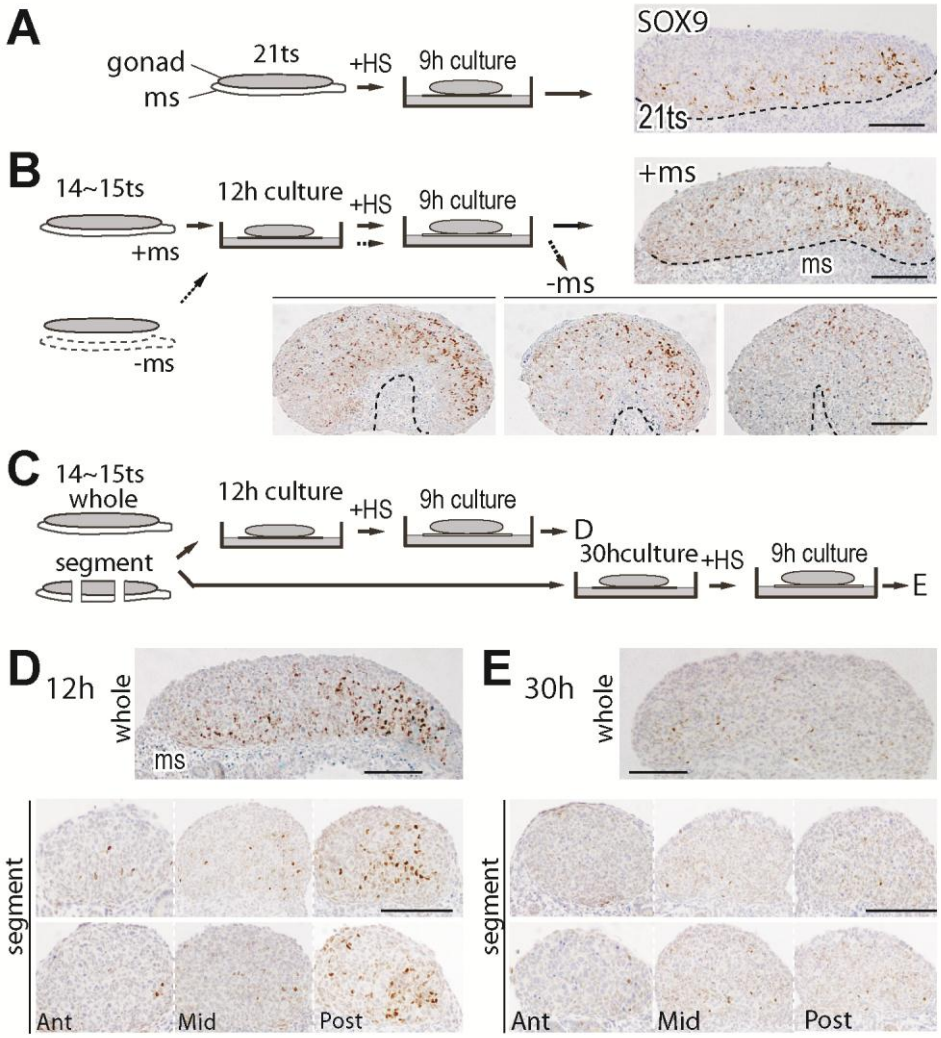
A
gonad
ms
21ts
+HS
9h culture
SOX9
21ts
B
14~15ts
+ms
12h culture
+HS
9h culture
-ms
+ms
ms
-ms
C
14~15ts
whole
segment
12h culture
+HS
9h culture
D
30hculture
+HS
9h culture
E
D 12h
whole
ms
E 30h
whole
segment
Ant
Mid
Post
segment
Ant
Mid
Post

FIGURE 2-14

Figure 2-14. The anterior-to-posterior loss of SRY-dependent SOX9-inducibility in XX gonads occurs in a tissue autonomous manner

(**A**) Anti-SOX9 immunostaining of HS-treated XX Tg explants (9-hour culture) initiated at 21 ts, demonstrating reduced SOX9-inducibility in an anterior region. (**B**) Anti-SOX9 immunostaining of XX genital ridge explants (initiated at 14 ts) with or without adjacent mesonephroi (HS treatment at 12 hours after culture initiation; total culture period: 21 hours). In A and B, a broken line marks the gonad/mesonephros border. (**C**) A whole genital ridge (whole) and three equally separated segments (i.e., anterior, middle and posterior) explants of XX genital ridge at 14 ts (HS treatment at 12 or 30 hours after culture initiation; total culture period: 21 or 39 hours). (**D, E**) Anti-SOX9 immunostaining of whole and segmented explants (HS treatment at 12 hours (D) and 30 hours (E)). The anterior pole side is shown on the left in each plate. ms, mesonephros. Scale bar: 100 μm.

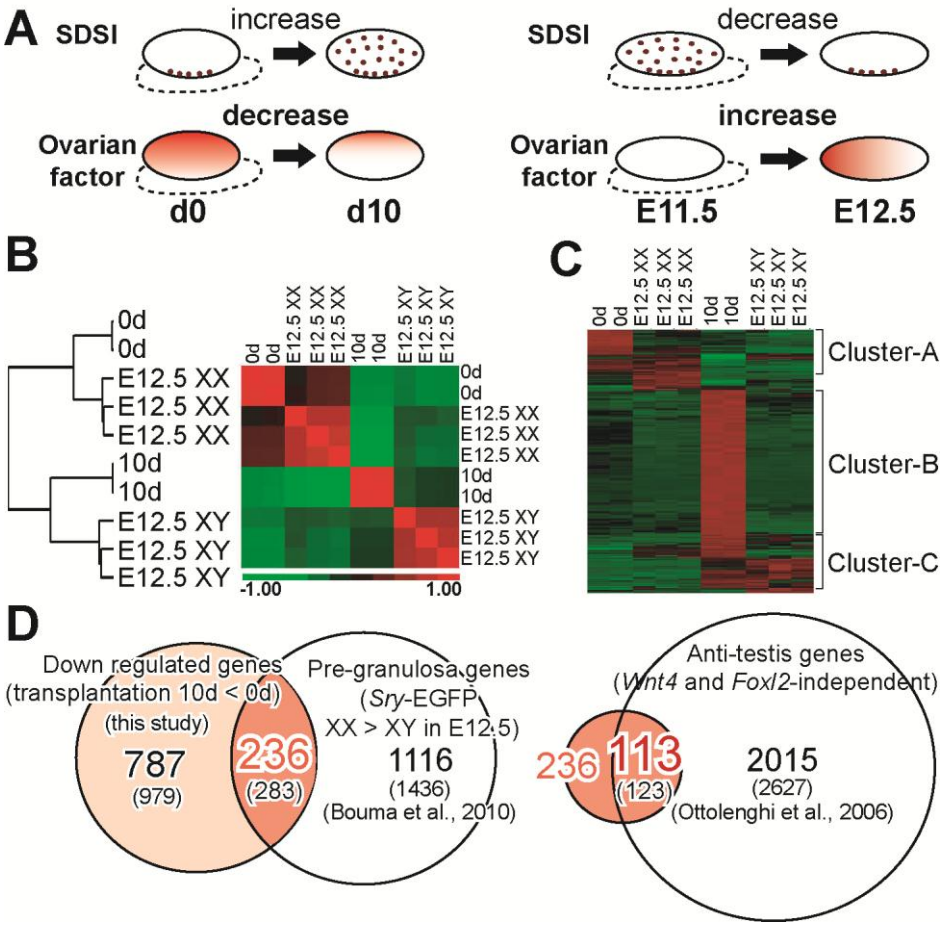
A
SDSI
increase
decrease
Ovarian factor
d0
d10
SDSI
decrease
increase
Ovarian factor
E11.5
E12.5
B
0d
0d
E12.5 XX
E12.5 XX
E12.5 XX
10d
10d
E12.5 XY
E12.5 XY
E12.5 XY
-1.00
1.00
C
Cluster-A
Cluster-B
Cluster-C
D
Down regulated genes
(transplantation 10d < 0d)
(this study)
787
(979)
236
(283)
Pre-granulosa genes
(Sry-EGFP
XX > XY in E12.5)
1116
(1436)
(Bouma et al., 2010)
Anti-testis genes
(Wnt4 and Foxl2-independent)
236
113
(123)
2015
(2627)
(Ottolenghi et al., 2006)

FIGURE 2-15

Figure 2-15. 236 genes identified by comprehensive gene profile analysis of grafted ovaries and fetal ovaires.

(**A**) During transplantation, from 0d to 10d, SRY-dependent SOX9-inducibility (SDSI) is reaquired (i.e., expression of candidates (presumable ovarian factors) are thought to be decreased). While, along with ovarian differentiation, SDSI is disappeared and conversely, expression of candidates are thought to be increased. (**B, C**) On genes significantly changed in 0d vs 10d, unsupervised sample clustering (B) and gene clustering (C) show transplanted ovaries are classified into the same group with XY testis and thus, proceeding sex-reversal. Part of cluster A contains presumptive candidates (C). (**D**) Common 236 genes (283 probe sets) significantly decreased in 10d compared with 0d and expressed in E12.5 ovarian somatic cells are obtained. Considering SOX9-inducibility did not change in *Wnt4*-null and FOXL2-abberant gonads, 113 genes (123 probe sets), whose expressions are independent of *Wnt4* and *Foxl2* are thought to be the leading candidates.

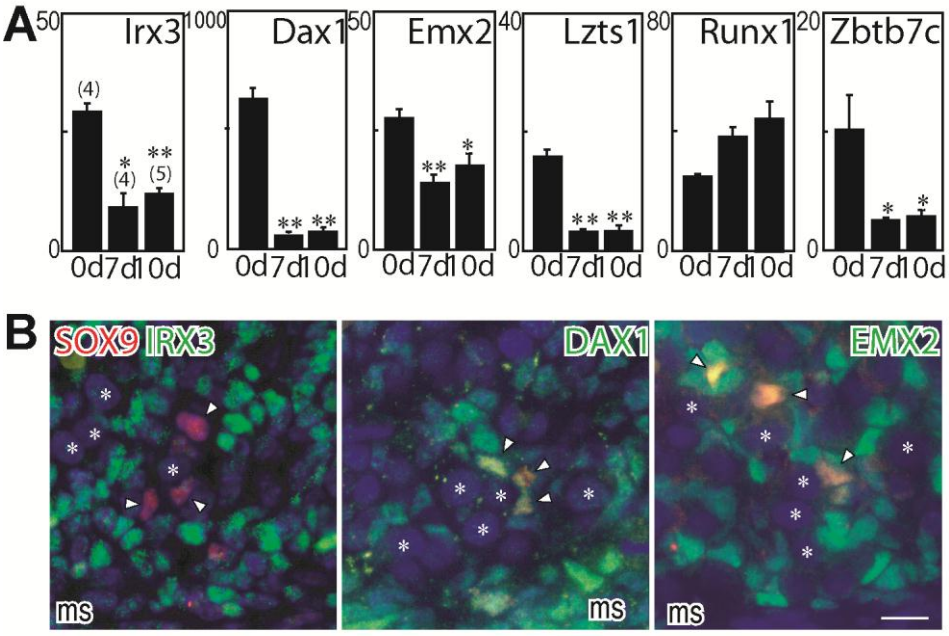
A
Irx3
Dax1
Emx2
Lzts1
Runx1
Zbtb7c
0d 7d 10d
B
SOX9 IRX3
DAX1
EMX2
ms

FIGURE 2-16

Figure 2-16. Expression of several early ovarian factors negatively correlates with the loss and reacquisition of SRY-dependent SOX9-inducibility

(**A**) Real-time RT-PCR analysis showing transcript levels of the *Irx3*, *Zbtb7c*, *Runx1*, *Lzts1*, *Dax1*, and *Emx2* genes relative to *Gapdh* (the mean values ± standard error; n= 4-5) in the HS-treated and non-treated ovarian transplants at days 0, 7 and 10 after transplantation (*$p<0.05$, **$p<0.01$, as compared with each transcript level at day 0). (**B, C)** anti-IRX3, EMX2 or DAX1 (green) staining showing a reduction of their signals in the grafted ovaries as compared with those of the ovaries at 12.5-13.5 dpc before transplantation. Anti-SOX9 (red)/ anti-IRX3, EMX2 or DAX1 (green) double-staining (DAPI, dark blue) (C) of the fetal ovaries at 12.5-13.5 dpc showing their non-overlapping expression profiles of IRX3 and DAX1 with SOX9-induced granulosa cells. Asterisk, oocytes; ms, mesonephros. Scale bar: 100 μm in B, E, and 10 μm in others.

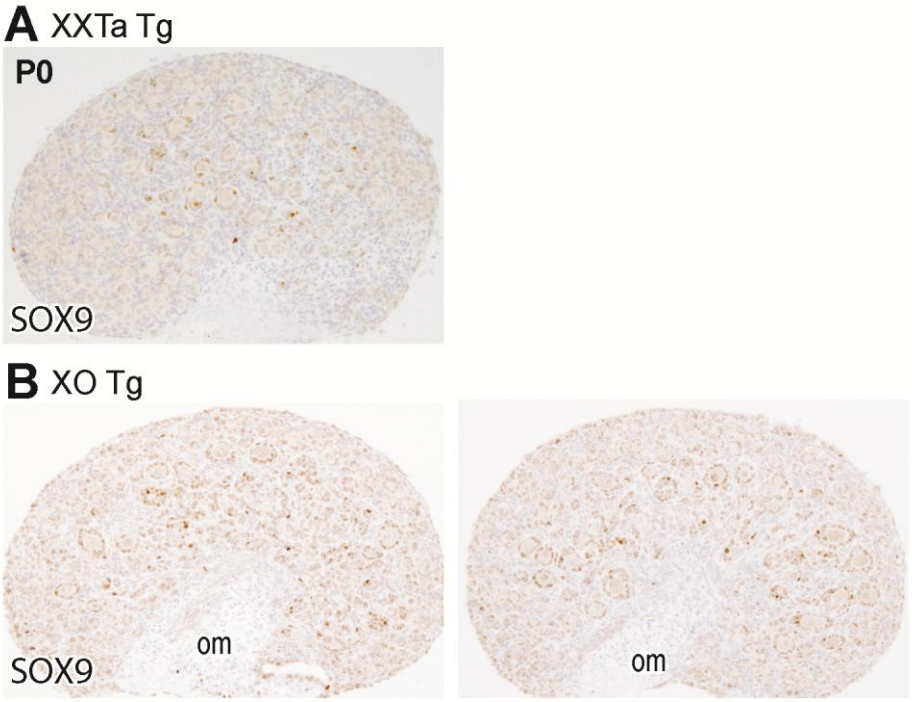

FIGURE 2-17

Figure 2-17. SRY-dependent SOX9-inducibility was widely maintained in XO Tg ovaries. Anti-SOX9 immunostaining (brown staining; transverse section) of XX^{Ta} and XO Tg new-born ovaries. (**A**) In XX^{Ta} Tg, SOX9 positive signals are detected around only ovarian medurally region. (**B**) On the other hand, in XO Tg ovaris, SOX9-positive signals are expand into the whole ovarian parenchyma. om: ovarian medulla.

Tables

Table 1	**Down-regulated pathways in 10d vs 0d**		
MAPP Name	**gene symbols**	**log fold**	**p value**
Dopminergic Neurogenesis:WP1498	Cdkn1c|Ddc|Msx1|Ret|Sox2	-2.65	0.026
Striated Muscle Contraction:WP216	Actn2|Myh6|Myh7|Tnni1|Tnnt1	-2.11	0.006
G1 to S cell cycle control:WP413	Ccne1|Cdk4|Cdkn1a|Cdkn1c|Mcm2|Mcm3	-1.55	0.016
Glycolysis and Gluconeogenesis:WP157	Aldoc|Eno3|Hk2|Pcx|Pdhb|Pfkl|Pkm2	-1.41	0.024

Table 2	Top 100 Down-regulated genes in 10d vs 0d			
Probesets	**Symbol**	**Definition**	**log fold**	**p value**
1450621_a_at	Hbb-y	hemoglobin Y, beta-like embryonic chain	-8.55	0.002
1436823_x_at	Hbb-y	hemoglobin Y, beta-like embryonic chain	-8.05	0.029
1436717_x_at	Hbb-y	hemoglobin Y, beta-like embryonic chain	-7.84	0.031
1448716_at	Hba-x	complex	-6.99	0.006
1437990_x_at	Hbb-bh1 /// LOC100044263	hemoglobin Z, beta-like embryonic chain /// hypothetical protein LOC100044263	-6.03	0.002
1450736_a_at	Hbb-bh1 /// LOC100044263	hemoglobin Z, beta-like embryonic chain /// hypothetical protein LOC100044263	-5.98	0.000
1437810_a_at	Hbb-bh1 /// LOC100044263	hemoglobin Z, beta-like embryonic chain /// hypothetical protein LOC100044263	-5.43	0.002
1416645_a_at	Afp	alpha fetoprotein	-5.34	0.011
1454737_at	Dusp9	dual specificity phosphatase 9	-5.00	0.004
1434502_x_at	Slc4a1	solute carrier family 4 (anion exchanger), member 1	-4.78	0.009
1424479_at	Cst8	cystatin 8 (cystatin-related epididymal spermatogenic)	-4.72	0.004
1425233_at	2210407C18Rik	RIKEN cDNA 2210407C18 gene	-4.59	0.001
1433845_x_at	Dusp9	dual specificity phosphatase 9	-4.57	0.005
1416967_at	Sox2	SRY-box containing gene 2	-4.40	0.035
1449071_at	Myl7	myosin, light polypeptide 7, regulatory	-4.38	0.010
1417504_at	Calb1	calbindin 1	-4.32	0.002
1420955_at	Vsnl1	visinin-like 1	-4.25	0.001
1454623_at	Cpa2	carboxypeptidase A2, pancreatic	-4.05	0.002
1426650_at	Myh8	myosin, heavy polypeptide 8, skeletal muscle, perinatal	-3.91	0.016
1439361_at			-3.84	0.005
1454159_a_at	Igfbp2	insulin-like growth factor binding protein 2	-3.82	0.007
1437631_at	Kcnip4	Kv channel interacting protein 4	-3.72	0.011
1429268_at	2610318N02Rik	RIKEN cDNA 2610318N02 gene	-3.71	0.004
1436879_x_at	Afp	alpha fetoprotein	-3.67	0.046
1417837_at	Phlda2	pleckstrin homology-like domain, family A, member 2	-3.66	0.023
1460084_at			-3.65	0.011
1420433_at	Taf7l	TAF7-like RNA polymerase II, TATA box binding protein (TBP)-associated factor	-3.65	0.027
1455223_at	Igf2bp1	insulin-like growth factor 2 mRNA binding protein 1	-3.65	0.013
1429074_at	1700026D08Rik	RIKEN cDNA 1700026D08 gene	-3.60	0.000
1437418_at	100041799	predicted gene, 100041799	-3.59	0.004
1435648_at	Lrrn4	leucine rich repeat neuronal 4	-3.58	0.021
1442379_at	EG574403	predicted gene, EG574403	-3.58	0.023
1418028_at	Dct	dopachrome tautomerase	-3.57	0.010
1454734_at	Lef1	lymphoid enhancer binding factor 1	-3.54	0.002
1457140_s_at	Rassf10	Ras association (RalGDS/AF-6) domain family (N-terminal) member 10	-3.52	0.004
1419147_at	Rec8	REC8 homolog (yeast)	-3.50	0.006
1439498_at	Igdcc3	immunoglobulin superfamily, DCC subclass, member 3	-3.48	0.005
1446308_at	1700106J16Rik	RIKEN cDNA 1700106J16 gene	-3.45	0.037
1460229_at	Stag3	stromal antigen 3	-3.44	0.045
1456035_at	Nxf3	nuclear RNA export factor 3	-3.42	0.024
1433707_at	Gabra4	gamma-aminobutyric acid (GABA-A) receptor, subunit alpha 4	-3.37	0.003
1419324_at	Lhx9	LIM homeobox protein 9	-3.37	0.010
1449865_at	LOC100044161 /// Sema3a	hypothetical protein LOC100044161 /// sema domain, immunoglobulin domain (Ig), short basic domain, secreted, (semaphorin) 3A	-3.36	0.009

Probesets	Symbol	Definition	log fold	p value
1429814_at	Pank1	pantothenate kinase 1	-3.35	0.016
1448326_a_at	Crabp1	cellular retinoic acid binding protein I	-3.33	0.017
1430520_at	Cpne8	copine VIII	-3.32	0.003
1450687_at	Igf2bp3	insulin-like growth factor 2 mRNA binding protein 3	-3.27	0.002
1422914_at	Sp5	trans-acting transcription factor 5	-3.26	0.001
1432031_at	4930563E18Rik	RIKEN cDNA 4930563E18 gene	-3.25	0.008
1449559_at	LOC100046255 /// Msx2	similar to homeobox protein /// homeobox, msh-like 2	-3.24	0.002
1436041_at	LOC100046086	similar to dHand protein	-3.24	0.016
1426243_at	Cth	cystathionase (cystathionine gamma-lyase)	-3.24	0.005
1423529_at	G6pc2	glucose-6-phosphatase, catalytic, 2	-3.23	0.000
1445679_at			-3.20	0.002
1450780_s_at	Hmga2	high mobility group AT-hook 2	-3.20	0.017
1450813_a_at	Tnni1	troponin I, skeletal, slow 1	-3.20	0.005
1435095_at	C030009O12Rik	RIKEN cDNA C030009O12 gene	-3.16	0.002
1460627_at	Thsd7b	thrombospondin, type I, domain containing 7B	-3.12	0.022
1420416_at	LOC100044161 /// Sema3a	hypothetical protein LOC100044161 /// sema domain, immunoglobulin domain (Ig), short basic domain, secreted, (semaphorin) 3A	-3.09	0.004
1458549_at			-3.08	0.013
1457429_s_at	Gm106	gene model 106, (NCBI)	-3.05	0.002
1457127_at	Defb42	defensin beta 42	-3.04	0.006
1427957_at	9530008L14Rik	RIKEN cDNA 9530008L14 gene	-3.02	0.001
1422851_at	Hmga2	high mobility group AT-hook 2	-3.00	0.010
1436398_at			-3.00	0.029
1429567_at	Rassf10	Ras association (RalGDS/AF-6) domain family (N-terminal) member 10	-2.99	0.011
1429905_at	Lhx9	LIM homeobox protein 9	-2.98	0.006
1435578_s_at	Dab1	disabled homolog 1 (Drosophila)	-2.94	0.013
1417388_at	Bex2	brain expressed X-linked 2	-2.93	0.009
1435314_at	Tph2	tryptophan hydroxylase 2	-2.92	0.005
1429813_at	Pank1	pantothenate kinase 1	-2.91	0.016
1429138_at	Npas3	neuronal PAS domain protein 3	-2.90	0.000
1422520_at	Nefm	neurofilament, medium polypeptide	-2.90	0.020
1434278_at	Mtm1	X-linked myotubular myopathy gene 1	-2.87	0.012
1456967_at	Trim66	tripartite motif-containing 66	-2.86	0.028
1431598_a_at	Lhx9	LIM homeobox protein 9	-2.85	0.017
1456335_at	Gm106	gene model 106, (NCBI)	-2.85	0.001
1422611_s_at	Igf2bp3	insulin-like growth factor 2 mRNA binding protein 3	-2.83	0.011
1422836_at	Mbnl3	muscleblind-like 3 (Drosophila)	-2.82	0.003
1424624_at	2900011O08Rik	RIKEN cDNA 2900011O08 gene	-2.80	0.003
1451191_at	Crabp2	cellular retinoic acid binding protein II	-2.78	0.002
1435182_at	Ccdc61	coiled-coil domain containing 61	-2.78	0.004
1423851_a_at	Shisa2	shisa homolog 2 (Xenopus laevis)	-2.78	0.003
1443913_at			-2.78	0.003
1433431_at	Pnlip	pancreatic lipase	-2.74	0.006
1429274_at	Lypd6b	LY6/PLAUR domain containing 6B	-2.74	0.005
1447655_x_at	Sox6	SRY-box containing gene 6	-2.74	0.003
1453084_s_at	Col22a1	collagen, type XXII, alpha 1	-2.72	0.004
1422610_s_at	Igf2bp3	insulin-like growth factor 2 mRNA binding protein 3	-2.72	0.001
1419719_at	Gabrb1	beta 1	-2.69	0.013
1419606_a_at	Tnnt1	troponin T1, skeletal, slow	-2.67	0.008
1444451_at	Pappa2	pappalysin 2	-2.67	0.003
1428923_at	Ppp1r3g	protein phosphatase 1, regulatory (inhibitor) subunit 3G	-2.66	0.016

Probesets	Symbol	Definition	log fold	p value
1417649_at	Cdkn1c	cyclin-dependent kinase inhibitor 1C (P57)	-2.66	0.004
1448688_at	Podxl	podocalyxin-like	-2.66	0.007
1449202_at	Sema4g	sema domain, immunoglobulin domain (Ig), transmembrane domain (TM) and short cytoplasmic	-2.66	0.024
1435577_at	Dab1	disabled homolog 1 (Drosophila)	-2.65	0.007
1417714_x_at	Hba-a1 /// Hba-a2	hemoglobin alpha, adult chain 1 /// hemoglobin alpha, adult chain 2	-2.64	0.008
1430943_at	6030498E09Rik	RIKEN cDNA 6030498E09 gene	-2.63	0.003
1430521_s_at	Cpne8	copine VIII	-2.63	0.009

Table 3	**Top 100 Down-regulated pre-granulosa genes in 10d vs 0**					
Probesets	**Symbol**	**Definition**	**log fold**	**p value**	**Sry-EGFP XX > XY**	**Genes independent of *Wnt4* and *Foxl2***
1416645_a_at	Afp	alpha fetoprotein	-5.34	0.011	-1.51	
1425233_at	2210407C18Rik	RIKEN cDNA 2210407C18 gene	-4.59	0.001	-4.30	3.25
1417504_at	Calb1	calbindin 1	-4.32	0.002	-4.11	5.4
1454623_at	Cpa2	carboxypeptidase A2, pancreatic	-4.05	0.002	-2.14	6.7
1454159_a_at	Igfbp2	insulin-like growth factor binding protein 2	-3.82	0.007	-2.57	8
1417837_at	Phlda2	pleckstrin homology-like domain, family A, member 2	-3.66	0.023	-1.40	
1420433_at	Taf7l	TAF7-like RNA polymerase II, TATA box binding protein (TBP)-associated factor	-3.65	0.027	-4.70	10.4
1429074_at	1700026D08Rik	RIKEN cDNA 1700026D08 gene	-3.60	0.000	-1.24	8.45
1437418_at	100041799	predicted gene, 100041799	-3.59	0.004	-3.02	
1442379_at	EG574403	predicted gene, EG574403	-3.58	0.023	-4.79	7.85
1454734_at	Lef1	lymphoid enhancer binding factor 1	-3.54	0.002	-2.66	
1419147_at	Rec8	REC8 homolog (yeast)	-3.50	0.006	-1.41	
1446308_at	1700106J16Rik	RIKEN cDNA 1700106J16 gene	-3.45	0.037	-5.22	
1456035_at	Nxf3	nuclear RNA export factor 3	-3.42	0.024	-1.61	
1433707_at	Gabra4	gamma-aminobutyric acid (GABA-A) receptor, subunit alpha 4	-3.37	0.003	-4.36	
1419324_at	Lhx9	LIM homeobox protein 9	-3.37	0.010	-4.13	
1449865_at	LOC100044161 /// Sema3a	hypothetical protein LOC100044161 /// sema domain, immunoglobulin domain (Ig), short basic domain, secreted, (semaphorin) 3A	-3.36	0.009	-2.20	
1429814_at	Pank1	pantothenate kinase 1	-3.35	0.016	-4.10	
1430520_at	Cpne8	copine VIII	-3.32	0.003	-2.32	
1422914_at	Sp5	trans-acting transcription factor 5	-3.26	0.001	-1.48	
1432031_at	4930563E18Rik	RIKEN cDNA 4930563E18 gene	-3.25	0.008	-5.60	
1423529_at	G6pc2	glucose-6-phosphatase, catalytic, 2	-3.23	0.000	-1.95	
1435095_at	C030009O12Rik	RIKEN cDNA C030009O12 gene	-3.16	0.002	-4.21	
1460627_at	Thsd7b	thrombospondin, type I, domain containing 7B	-3.12	0.022	-2.92	8.05
1420416_at	LOC100044161 /// Sema3a	hypothetical protein LOC100044161 /// sema domain, immunoglobulin domain (Ig), short basic domain, secreted, (semaphorin) 3A	-3.09	0.004	-3.19	
1429905_at	Lhx9	LIM homeobox protein 9	-2.98	0.006	-3.37	
1435578_s_at	Dab1	disabled homolog 1 (Drosophila)	-2.94	0.013	-4.09	
1435314_at	Tph2	tryptophan hydroxylase 2	-2.92	0.005	-5.35	4.45
1456967_at	Trim66	tripartite motif-containing 66	-2.86	0.028	-2.43	4.55
1431598_a_at	Lhx9	LIM homeobox protein 9	-2.85	0.017	-1.21	
1422836_at	Mbnl3	muscleblind-like 3 (Drosophila)	-2.82	0.003	-3.79	8.25
1424624_at	2900011O08Rik	RIKEN cDNA 2900011O08 gene	-2.80	0.003	-2.42	8.9
1435182_at	Ccdc61	coiled-coil domain containing 61	-2.78	0.004	-2.91	
1433431_at	Pnlip	pancreatic lipase	-2.74	0.006	-3.04	
1429274_at	Lypd6b	LY6/PLAUR domain containing 6B	-2.74	0.005	-1.94	5.2
1453084_s_at	Col22a1	collagen, type XXII, alpha 1	-2.72	0.004	-2.16	
1419719_at	Gabrb1	gamma-aminobutyric acid (GABA-A) receptor, subunit beta 1	-2.69	0.013	-4.22	6.25
1419606_a_at	Tnnt1	troponin T1, skeletal, slow	-2.67	0.008	-2.61	6.4
1428923_at	Ppp1r3g	protein phosphatase 1, regulatory (inhibitor) subunit 3G	-2.66	0.016	-2.03	6.35
1417649_at	Cdkn1c	cyclin-dependent kinase inhibitor 1C (P57)	-2.66	0.004	-2.37	9.8
1448688_at	Podxl	podocalyxin-like	-2.66	0.007	-2.87	11.4
1435577_at	Dab1	disabled homolog 1 (Drosophila)	-2.65	0.007	-3.52	
1430521_s_at	Cpne8	copine VIII	-2.63	0.009	-1.22	
1450624_at	Bhmt	betaine-homocysteine methyltransferase	-2.63	0.011	-1.18	
1458375_at	Klhl32	kelch-like 32 (Drosophila)	-2.60	0.006	-1.67	

Probesets	Symbol	Definition	log fold	p value	Sry-EGFP XX > XY	Genes independent of *Wnt4* and *Foxl2*
1419722_at	Klk8	kallikrein related-peptidase 8	-2.59	0.018	-1.88	
1436361_at	Vgll2	vestigial like 2 homolog (Drosophila)	-2.54	0.022	-3.94	
1421100_a_at	Dab1	disabled homolog 1 (Drosophila)	-2.51	0.025	-3.05	
1427308_at	Dab1	disabled homolog 1 (Drosophila)	-2.51	0.034	-2.93	
1448152_at	Igf2	insulin-like growth factor 2	-2.50	0.003	-2.28	7.25
1455851_at	Bmp5	bone morphogenetic protein 5	-2.47	0.006	-2.96	
1449064_at	Tdh	L-threonine dehydrogenase	-2.45	0.032	-2.56	
1442101_at	Elfn1	leucine rich repeat and fibronectin type III, extracellular 1	-2.45	0.010	-2.79	8.25
1440452_at	Drp2	dystrophin related protein 2	-2.43	0.007	-4.68	7.95
1455645_at	8030451F13Rik	RIKEN cDNA 8030451F13 gene	-2.41	0.007	-1.73	
1423635_at	Bmp2	bone morphogenetic protein 2	-2.40	0.002	-3.07	6.85
1441313_x_at	Lhx9	LIM homeobox protein 9	-2.40	0.002	-3.67	
1455991_at	Ccbl2	cysteine conjugate-beta lyase 2	-2.40	0.004	-2.77	5.9
1436853_a_at	Snca	synuclein, alpha	-2.37	0.043	-3.80	5.55
1434013_at	Ablim3	actin binding LIM protein family, member 3	-2.35	0.011	-1.28	7.95
1417553_at	Plac1	placental specific protein 1	-2.35	0.020	-1.12	
1449184_at	Pglyrp1	peptidoglycan recognition protein 1	-2.34	0.010	-2.03	
1435913_at	B4galnt4	beta-1,4-N-acetyl-galactosaminyl transferase 4	-2.33	0.007	-1.20	
1431146_a_at	Cpne8	copine VIII	-2.31	0.003	-1.74	
1435162_at	Prkg2	protein kinase, cGMP-dependent, type II	-2.30	0.018	-2.72	
1436739_at	Agtr1a	angiotensin II receptor, type 1a	-2.28	0.045	-2.62	5.35
1437085_at	D630039A03Rik	RIKEN cDNA D630039A03 gene	-2.28	0.000	-2.97	8.6
1457698_at	AI314831	expressed sequence AI314831	-2.27	0.009	-2.68	7.3
1448194_a_at	H19	H19 fetal liver mRNA	-2.26	0.005	-1.61	8.55
1417760_at	Nr0b1	nuclear receptor subfamily 0, group B, member	-2.25	0.034	-1.54	
1448783_at	Slc7a9	solute carrier family 7 (cationic amino acid transporter, y+ system), member 9	-2.23	0.029	-3.30	
1424638_at	Cdkn1a	cyclin-dependent kinase inhibitor 1A (P21)	-2.23	0.031	-2.50	7.55
1436789_at	Ccnjl	cyclin J-like	-2.22	0.020	-1.77	6.25
1423889_at	EG434402	predicted gene, EG434402	-2.20	0.006	-1.87	5.85
1421405_at	Zim1	zinc finger, imprinted 1	-2.17	0.011	-3.71	6.15
1421498_a_at	2010204K13Rik	RIKEN cDNA 2010204K13 gene	-2.13	0.017	-1.93	
1451461_a_at	Aldoc	aldolase C, fructose-bisphosphate	-2.13	0.003	-1.38	
1440436_at	328235	predicted gene, 328235	-2.12	0.029	-2.80	
1452889_at	2310007H09Rik	RIKEN cDNA 2310007H09 gene	-2.09	0.002	-2.64	5
1433977_at	Hs3st3b1	heparan sulfate (glucosamine) 3-O-sulfotransferase 3B1	-2.09	0.006	-2.19	7.2
1438745_at	ENSMUSG00000074178	predicted gene, ENSMUSG00000074178	-2.07	0.004	-2.35	
1451260_at	Aldh1b1	aldehyde dehydrogenase 1 family, member B1	-2.07	0.037	-2.36	7.25
1416077_at	Adm	adrenomedullin	-2.07	0.002	-3.54	
1450582_at	H2-Q5	histocompatibility 2, Q region locus 5	-2.06	0.004	-2.15	
1420430_a_at	2510048L02Rik	RIKEN cDNA 2510048L02 gene	-2.06	0.002	-1.90	
1419332_at	Egfl6	EGF-like-domain, multiple 6	-2.05	0.012	-3.15	6.9
1433988_s_at	C230098O21Rik	RIKEN cDNA C230098O21 gene	-2.03	0.007	-4.07	10.4
1420561_at	Trpc7	transient receptor potential cation channel, subfamily C, member 7	-2.03	0.004	-1.93	4
1448889_at	Slc38a4	solute carrier family 38, member 4	-2.02	0.016	-1.50	
1449641_at	Adk	adenosine kinase	-2.01	0.012	-3.71	
1428502_at	Actr6	ARP6 actin-related protein 6 homolog (yeast)	-2.00	0.008	-2.26	
1420521_at	Papln	papilin, proteoglycan-like sulfated glycoprotein	-1.99	0.015	-1.82	8.6
1456435_at	Morn1	MORN repeat containing 1	-1.99	0.040	-2.12	
1456161_at	0610040B10Rik	RIKEN cDNA 0610040B10 gene	-1.98	0.007	-1.43	3.5

Probesets	Symbol	Definition	log fold	p value	Sry-EGFP XX > XY	Genes independent of *Wnt4* and *Foxl2*
1455858_x_at	Pomc	pro-opiomelanocortin-alpha	-1.98	0.013	-2.33	3.65
1448601_s_at	Msx1	homeobox, msh-like 1	-1.96	0.023	-3.35	5.05
1447839_x_at	Adm	adrenomedullin	-1.95	0.009	-3.86	7.35
1418517_at	Irx3	Iroquois related homeobox 3 (Drosophila)	-1.95	0.013	-4.32	11.95
1440534_at	ENSMUSG00000056615	predicted gene, ENSMUSG00000056615	-1.95	0.013	-3.72	6.35
1454969_at	Lypd6	LY6/PLAUR domain containing 6	-1.95	0.002	-3.27	5.3

Table 4	**Candidate genes**					
Probesets	**Symbol**	**Definition**	**log fold**	**p value**	**Sry-EGFP XX > XY**	**Genes independent of *Wnt4* and *Foxl2***
1420433_at	Taf7l	binding protein (TBP)-associated factor	-3.65	0.027	-4.70	10.4
1454734_at	Lef1	lymphoid enhancer binding factor 1	-3.54	0.002	-2.66	
1419147_at	Rec8	REC8 homolog (yeast)	-3.50	0.006	-1.41	7.85
1419324_at	Lhx9	LIM homeobox protein 9	-3.37	0.010	-4.13	
1422914_at	Sp5	trans-acting transcription factor 5	-3.26	0.001	-1.48	
1429905_at	Lhx9	LIM homeobox protein 9	-2.98	0.006	-3.37	
1456967_at	Trim66	tripartite motif-containing 66	-2.86	0.028	-2.43	4.55
1431598_a_at	Lhx9	LIM homeobox protein 9	-2.85	0.017	-1.21	
1422836_at	Mbnl3	muscleblind-like 3 (Drosophila)	-2.82	0.003	-3.79	8.25
1417649_at	Cdkn1c	cyclin-dependent kinase inhibitor 1C (P57)	-2.66	0.004	-2.37	9.8
1448688_at	Podxl	podocalyxin-like	-2.66	0.007	-2.87	11.4
1436361_at	Vgll2	vestigial like 2 homolog (Drosophila)	-2.54	0.022	-3.94	
1448152_at	Igf2	insulin-like growth factor 2	-2.50	0.003	-2.28	7.25
1441313_x_at	Lhx9	LIM homeobox protein 9	-2.40	0.002	-3.67	
1417760_at	Nr0b1	nuclear receptor subfamily 0, group B, member 1	-2.25	0.034	-1.54	
1424638_at	Cdkn1a	cyclin-dependent kinase inhibitor 1A (P21)	-2.23	0.031	-2.50	7.55
1436789_at	Ccnjl	cyclin J-like	-2.22	0.020	-1.77	6.25
1421405_at	Zim1	zinc finger, imprinted 1	-2.17	0.011	-3.71	6.15
1448601_s_at	Msx1	homeobox, msh-like 1	-1.96	0.023	-3.35	5.05
1418517_at	Irx3	Iroquois related homeobox 3 (Drosophila)	-1.95	0.013	-4.32	11.95
1428402_at	Zcchc3	zinc finger, CCHC domain containing 3	-1.82	0.042	-1.01	
1436365_at	Zbtb7c	zinc finger and BTB domain containing 7C	-1.72	0.046	-2.05	10.25
1439506_at	Gm98	gene model 98, (NCBI)	-1.71	0.001	-1.34	4.6
1434678_at	Mbnl3	muscleblind-like 3 (Drosophila)	-1.70	0.003	-3.12	7.35
1428669_at	Bmyc	brain expressed myelocytomatosis oncogene	-1.66	0.032	-1.38	9.2
1432331_a_at	Prrx2	paired related homeobox 2	-1.63	0.001	-2.76	
1459978_x_at	Ccnjl	cyclin J-like	-1.61	0.016	-1.04	6.2
1420714_at	Lbx2	ladybird homeobox homolog 2 (Drosophila)	-1.55	0.014	-1.62	
1436845_at	Axin2	axin2	-1.45	0.029	-1.86	6.95
1455807_at	Tspyl5	testis-specific protein, Y-encoded-like 5	-1.41	0.016	-1.79	5.4
1420979_at	Pak1	p21 (CDKN1A)-activated kinase 1	-1.37	0.019	-1.98	5.8
1427176_s_at	AI428936	expressed sequence AI428936	-1.36	0.001	-1.78	
1425895_a_at	Id1	inhibitor of DNA binding 1	-1.32	0.010	-1.41	
1448664_a_at	Speg	SPEG complex locus	-1.31	0.007	-1.39	
1456258_at	Emx2	empty spiracles homolog 2 (Drosophila)	-1.28	0.033	-3.16	10.15
1418317_at	Lhx2	LIM homeobox protein 2	-1.28	0.004	-1.04	
1421267_a_at	Cited2	Cbp/p300-interacting transactivator, with Glu/Asp-rich carboxy-terminal domain, 2	-1.21	0.015	-1.14	
1451332_at	Zfp521	zinc finger protein 521	-1.18	0.017	-1.72	
1425428_at	Hif3a	hypoxia inducible factor 3, alpha subunit	-1.18	0.015	-1.28	
1434031_at	Zfp692	zinc finger protein 692	-1.13	0.002	-1.74	7.2
1451410_a_at	Crip3	cysteine-rich protein 3	-1.11	0.017	-1.53	
1452600_at	Taf6l	associated factor (PCAF)-associated factor	-1.11	0.009	-1.06	
1422771_at	Smad6	MAD homolog 6 (Drosophila)	-1.06	0.004	-1.30	
1439885_at	Hoxc5	homeo box C5	-1.05	0.039	-2.04	
1423401_at	Etv6	ets variant gene 6 (TEL oncogene)	-1.04	0.039	-1.41	

Chapter 3

Dynamic and temporal mechanism of XX sex reversal in mice.

Abstract

Sex determination is the most crucial activity for all living things. However, it has been known that there are surprising varieties in the mechanisms of sex determination among vertebrates and invertebrates. Although hormones, temperature and visual information have the key role in vertebrates except for mammals, mammals establish the strict genotypic sex determination systems. For instance, testis-specific genes such as *Sox8*, *Sox9* and *Dmrt1* and ovary-specific genes such as *Wnt4* and *Foxl2* play essential roles in respective sex determination. Despite such severe genotypic sex determination systems in mammals, some cases of genetically non-mutated XX sex reversal and disorders of sex development are sporadically reported. Elucidation of the cause and process of XX sex reversal has the enormous possibility for identifying the novel sex determination mechanisms, but until now, little is known. In the present study, by using experimental XX sex reversal system, I demonstrated the detailed morphological process and transitions in sex determination-related genes containing the novel gene, *Egr1*, *Egr2* and *Ctgf*, for the first time. Moreover, I indicated that even mammals had the possible conserved testis-forming pathway among vertebrates with steroid hormones, TGF-β signaling, *Dmrt1*, *Sox9* and *Amh*.

Introduction

Sex determination has the crucial role for reproduction and following survival of species in all of vertebrates and invertebrates. Especially, mammals are known to have typical genotypic sex determination system (GSD) (Nakamura, 2010; Munger and Capel, 2012). Initially, gonads arise from thickening of coelomic epithelia as a bipotential state. If one has Y chromosome, sex detemining gene on Y choromosome, *Sry*, is expressed to induce testis differentiation and to trigger the cascades of testis specific genes such as *Sox9*, *Amh*, *Sox8*, *Dhh*, and *Gdnf* (Behringer et al., 1990; Kent et al., 1996; Meng et al., 2000; Yao et al., 2002; Chaboissier et al., 2004). On the other hand, XX individuals without *Sry* develop ovaries by ovary-specific genes like *Dax1*, *Wnt4*, *Rspo1*, *Bmp2*, *Fst*, *Irx3*, *Foxl2* and *Ctnnb1* (Swain et al., 1998; Vainio et al., 1999, Ottolenghi et al., 2005; Parma et al., 2006; Liu et al., 2009; Kashimada et al., 2011; Kim et al., 2011). These sex determination-related genes are strictly orchestrated, and lack of any genes cause dysgenesis of ovaries or testes. Despite such severe mammalian GSD system, some examples of non-genetically mutated XX sex reversal are known. One case is bovine XX sex-reversal that I have reported recently (please see Chapter 1). Another is masculinization of XX ovaries transplanted under kidney capsule (Taketo et al., 1984; Taketo et al., 1986; please see Chapter 2). In addition, there are many DSDs (disorders of sex development) whose clear causes are not known (Vaiman and Pailhoux, 2000). Elucidation of detailed mechanisms of such genetically non-mutated XX sex reversal is necessary for understanding DSDs and mammalian sex determination further.

Other than mammals, strategies of sex determination have remarkable diversity. *Drosophila melanogaster* uses sex specific RNA splicing by SXL (Sex lethal) protein dependent on sex/autorsomal chromosome ratio (Kelley et al., 1997). In fish, in addition to unique sex

detemination mechanisms such as environment dependency, some spieces-specific various sex determining genes were discovered. For example, *Dmy* was discovered in *Oryzias latipes*, *GsdfY* in *Oryzias luzonensis*, *Amhy* in *Odontesthes hatcheri*, *Amhr2* in *Takifugu rubripes* and *sdY* in *Oncorhynchus mykiss* (Matsuda et al., 2002; Hattori et al., 2012; Kamiya et al., 2012; Myosho et al., 2012; Yano et al., 2012). Sex of *Oryzias latipes* is dependent on not only genetical determination but also on the presence or absence of germ cells (Nakamura et al., 2012). Many reptiles are classified into TSD (Temperature dependent sex determination) and might have no sex-determining genes, while it is indicated that hormones (androgen or aromatase) have the important role (Nakamura, 2010). Amphibian *Xenopus laevis* is reported to have ovarian sex determining gene *Dm-W* (Yoshimoto et al., 2008). Recently, it has been reported that chicken *Gallus domesticus* has cell-autonomous sex determination mechanism led by *DMRT1* (Smith et al., 2009) in addition to hormone dependent mechanisms. In mammals, sex-determining *Sry* gene is not conserved among other vertebrates and even marsupial *SRY* does not have the same role as that of mammals (Harry et al., 1995). Instead, marsupial is suggested to use *ATRY* or *SOX3* genes for sex determination (Foster and Graves, 1994; Pask et al., 2000). Besides, it is known that hormones, which have important roles in many vertebrates including marsupials, do not affect mammalian sex determination (Couse et al., 1999; Tsai et al., 2006). In spite of these diversity of sex determination mechanisms among vertebrates, the downstream genes have homologues in a much broader spectrum of species (Graham et al., 2003). Actually, *Sox9* is conserved from *Drosophila melanogaster* (*Sox100B*) to mammals (DeFalco et al., 2008), *Dmrt1* is also highly conserved even from *Caenorhabditis elegans* (*mab-3*) and *Drosophila melanogaster* (*doublesex*) (Raymond et al., 1998). Not only testis factors but also gonadogenesis and ovarian factors such as *Wt1, Gata4, Foxl2, Cyp19a1, Wnt4* and *Rspo1* are well conserved (Yao and Capel, 2005; Valenzuelaet al.,

in press). But, their order of expression and interaction is different between that of mammals and other vertebrates. Therefore, truly conserved sex determination mechanism throughout vertebrates remained to be elucidated.

In this study, I hypothesized that by means of the analyses of XX sex reversal (i.e. XX testicular formation without *Sry*, which is the same as that in other vertebrates), I could reveal 1) the mechanisms and causes of mammalian non-genetically mutated, unknown XX testicular formation or gonadal dysgenesis (DSDs); 2) the novel mammalian sex determination system conserved among vertebrates. For this purpose, I examined detailed morphological and temporal molecular changes throughout the formation of XX testis by the time series analysis. Results suggested that by the effects of TGF-β and/or steroid hormones, ovarian follicles degenerated and transdifferentiated into testicular structures without oocytes. In this process, I found that testicular factors were up-regulated in the norvel manner for mammlian testis-differentiation, while possibly conserved among vertebrates. By revealing the mammalian XX testicular formation, I could find out the cues for DSDs, and possible conserved testicular core-pathway among vertebrates.

Materials and methods

Animals

Male nude mice (8 weeks old; BALB/c, nu/nu, SLC Japan) were used as host mice for the transplantation of fetal ovaries.

Transplantation of Fetal Mouse Ovaries

Transplantation of fetal ovaries was carried out by the previously reported procedure (Taketo et al., 1984; Taketo et al., 1986; also see Chapter 2) .

Histology and Immunohistochemistry

The samples were fixed in 4% PFA-PBS at 4^{o}C for 16 hours, dehydrated, and then embedded in paraffin. Serial sagittal sections (approximately 4 μm in thickness) were cut. The sections were incubated with anti-AMH (1:200 dilution; Santa Cruz), and anti-SOX9 (1:250 dilution; Kidokoro et al., 2005; Kent et al., 1996) at 4 $^{\circ}$C for 12 hours. The reaction was visualized with biotin-conjugated secondary antibody in combination with Elite ABC kit (Vector Laboratories).

Quantitative RT-PCR

Total RNA was reverse-transcribed using random primer with a Superscript-III cDNA synthesis kit (Invitrogen). Specific primers and fluorogenic probes for *Sox9* (Mm00442795_m1), *Sox8* (Mm00803423_m1), *Egr2* (Mm00456650_m1), *Egr1* (Mm00656724_m1), *Ctgf* (Mm01192932_g1) and *Gapdh* (Taqman control reagents) were purchased from Applied Biosystems. PCR was performed using an Applied Biosystems Step

One Real Time PCR System. The expression levels represented the relative expression levels of each marker gene per *Gapdh* amplicon ratio (mean ± standard error).

Microarray processing and analysis

Total RNA of all samples was purified by NucleoSpin RNA XS kit (Macherey-Nagel) and along the protocols in GeneChip 3' IVT Express kit (Affymetrix), and fragmented aRNA was hybridized to mouse genome 430 2.0 arrays (Affymetrix). Chips were washed and stained in Fluidics Station 450 (Affymetrix). The arrays were scanned using a GeneChip scanner 3000 (Affymetrix) and the output was obtained by GeneChip Operating Software or Expression Console (Affymetrix). Data were normalized and further analyzed by RMA method using AltAnalyze software (http://www.altanalyze.org/). On unsupervised clustering, dChip was used (http://biosun1.harvard.edu/complab/dchip/). For 12.5 dpc somatic genes, I used cell files of Bouma et al. (2010) supported by GEO (GSE18211). To plot ovarian and testicular development on PCA analysis, I used cell files of GSE5334, GSE4818 and GSE6916. Genes related to *Foxl2* c-KO XX sex reversal are obtained from cell files of GSE16853 by Uhlenhaut et al. (2009).

Results

Histological temporal analyses of transplanted ovaries under male kidney capsule

To clarify what morphological changes occur and what pathways/factors are important for formation of XX testes without *Sry*, first I decided to induce experimental XX sex reversal by transplanting fetal ovaries at E13.5 (embryonic day 13.5; equal to 13.5 dpc) under the kidney capsule of male mice (Chapter 2, Fig. 2-8). I picked up transplanted grafts after 4, 7, 10, 15, 20 days for further analyses (Fig. 3-1A). At 4 days after transplantation, many germ cells and female-specific ovigerous cords were detected as normal age-matched E17.5 ovaries (Fig. 3-1B "4d"; please also see Chapter 2, Fig. 2-9). At 7 days, AMH positive follicular granulosa cells with oocytes, which seemed to mature at primary follicle stage, were observed, which is relatively earlier than normal follicular development of age-matched new-born ovaries. In addition, there were some clusters of AMH (a marker for immature Sertoli cells and mature granulosa cells) positive cells around which no oocytes were seen (Fig. 3-1B "7d", arrowheads). At 10 days, these clusters became larger and obvious (Fig. 3-1B "10d", arrowheads). In addition, a number of oocytes seemed to be decreased except for those in a few primary follicles. Subsequently, at 15 days, besides follicles, many AMH positive cord-like structures were observed throughout the whole parenchyma (Fig. 3-1B, "15d", arrowheads; Fig. 3-1C). No oocytes were detected in these cord-like structures. Finally, at 20 days after transplantation, I found that part of cord-like structures was not positive for AMH and instead became positive for SOX9 (a marker for Sertoli cells) (Fig. 3-1C, arrows), although it is well known that SOX9 does not localize at granulosa cells but at nuclei of Sertoli cells only. From 7 days to 20 days, it was found that some AMH positive clusters or

cord-like structures seemed to “bud” from follicles (Fig. 3-1C, white arrowheads) and actually cord-like structures had successive basement membranes with follicles (Chapter 2, Fig. 2-9). These observation strongly suggest that cord-like structures originated from regressed ovarian follicles.

In summary, by histological analyses of transplanted ovairan grafts under male kidney capsules, I demonstrated that SOX9 positive cord-like structures, that is, XX testicular cords were transdifferenriated from XX ovaries. In this process, first, AMH positive small cords appeared and grew. In contrary to fast growing of follicles and cord-like structures, a number of oocytes seemed to be decreased.

Comprehensive gene profile analysis of XX sex reversal by microarray

In order to further analyze the molecular mechanisms of XX sex reversal and identify major expression profiles, I conducted microarray analyses by using time-series transplanted grafts and fetal gonads (transplanted ovaries at 0d, 4d, 7d, 10d, 15d and 20d; fetal gonads at E12.5 XX and E12.5 XY). As a result, unsupervised sample clustering approaches showed that all transplanted grafts were clustred into the same group with E12.5 “XY” (Fig. 3-2A, clustering tree; based on 1431 genes differently expressed between E12.5 XY and XX *Sry*-EGFP positive somatic cells, $|fold| > 2$, $p < 0.05$). Especially, among transplanted grafts, 15d samples had relatively the nearest profiles with those of E12.5 XY (Fig. 3-2A, sample correlation matrix). In gene clustering, 1431 genes were clustered into approximately 4 large groups (Fig. 3-2B, group A-D). Genes more exclusively expressed in 12.5 XX somatic cell than XY were contained in clusters A, B and C. In cluster A, there were some ovarian genes down-regulated

by XX sex reversal (E12.5 XX>XY and 0d>10d, 15d and 20d; also see Chapter 2). In clusters B and C, there seemed to be genes up-regulated by techniques of transplantation (up-regulated only from 4d to 20d grafts) and genes presumptively involving meiosis (up-regulated only in 0d to 20d grafts). Remarkably, genes up-regulated in all of 10d , 15d and 20d grafts and E12.5 XY somatic cells were present in part of cluster D.

Next, to compare major expression profiles associated with transplanted grafts and ovarian/testicular development, I used principal component analysis (PCA). Garcia-Ortiz et al. (2009) clearly show the process of development in normal ovaries and testes by PCA. Therefore, I gained the same 47 files as those of Garcia-Ortiz et al. (2009) from GEO and tried to traject transplanted grafts (0d, 4d, 7d, 10d, 15d and 20d) to normal ovarian or testicular “life history” (Fig. 3-2C). As expected, at bipotential E11 gonads, sets of XX and XY genes were mutually close. From E12, however, XX ovaries came to demonstrate high PC2, while XY testes came to get high PC1 value. This trend was indicated to lead two fates to diverge sharply (Garcia-Ortiz et al., 2009). In XX transplanted grafts, contrary to 0d grafts (E13.5 ovaries without mesonephroi) near to E13-E14 profiles predictably, 4d to 20d grafts mapped consistently far from age-matched control ovaries (4d corresponds to E17.5; 7d to P0; 10d to P3; 15d to P8; 20d to P13 ovaries, respectively) along PC1 axis (Fig. 3-2C). In addition, PCA showed increase of PC2 values from 0d to 7d and sudden decrease from 7d to 15d. These high PC1/low PC2 values showed the clear trends toward testis (Garcia-Ortiz et al., 2009).

In summary, these unsupervised analyses (gene, sample clustering and PCA) confirm my histological observations that transplanted XX ovaries come to transdifferentiate into XX

testis approximately from 10 day after transplantation under male environment.

Following unsupervised analyses, I examined supervised analyses to know what genes, factors or pathways are involved in XX testicular formation exactly. Among up- and down-regulated probes (baseline: 0d; fold>1.5, p<0.05), I picked up a number of pre-granulosa specific and Sertoli-specific probes by using data of Bouma et al. (2010) and plotted them to the graph (Fig. 3-2D). Consistent with above unsupervised analyses, the graph apparently demonstrated that pre-granulosa probes were down-regulated especially from 4d to 10d and Sertoli probes were up-regulated from 10d to 20d. Because probes in 15d had the least pre-granulosa ones among transplanted grafts and a similar number of up-regulated Sertoli-specific probes with 20d, I decided to focus on up-regulated 487 genes (619 probe sets) in 0d vs 15d as candidate genes for having important roles in fomration and/or maintenance of non-genetically mutated XX testes (fold>1.5; Figure 3-2D).

New candidate genes including *Egr1, Egr2* and *Ctgf* suggest the novel testis-forming/DSDs pathway without *Sry* and the presence of the presumable conserved pathway in mammalian testis-differentiation.

On comparing gene expression profiles of 15d with 0d, I found that almost all famous female genes such as *Rspo1, Wnt4, Fst, Irx3, Dax1/Nr0b1* and *Bmp2* were significantly down-regulated (Fig. 3-3A; also see Chapter 2) (*Foxl2* and *Ctnnb1* did not change their expression level throughout 0d to 20d). In contrary, famous male genes, *Ptgds, Gdnf, Sox8, Dhh, Amh* and *Sox9* were up-regulated (Fig. 3-3A, B; Table 3-1). Graphs demonstrated that down-regulation of female factor and up-regulation of male factor exclusively occurred from

7d to 15d.

Top 100 up-regulated gene lists showed that in addition to these known factors, there were novel male factors whose precise functions in mammalian testis determination were not known (Table 3-1; common genes in 0d<15d and E12.5 XY>XX). Especially, zinc finger transcription factors *Egr2* and *Egr1,* basic helix-loop-helix transcription factor *Bhlhe40,* an orphan nuclear receptor *Nr4a1* and a TGF-β soluble factor *Ctgf* were highly up-regulated from 10d (Fig. 3-3A, Table 3-1). Real-time PCR also confirmed the up-regulated expression of *Sox9, Sox8, Egr1*, *Egr2* and *Ctgf* in 15d (Fig. 3-3B). It is noteworthy that expression of *Sox9* occurs at later period from 15d, and *Sox8* and *Gdnf* expresses from early peiod, which is apparently different from normal XY testis-forming pathway. Considering it is from 7d to 15d that almost all female or male factors changed their expression and sexually bipotential granulosa cells were reaquired at that timing (Fig. 3-3A, white arrowheads; see Chapter 2, Fig. 2-8), next, I examined GO pathways up-regulated between 0d and 10d to reveal the causes of XX testis formation, because I thought that soluble factors and/or hormones might be important, considering the cases of freemartin and kidney transplantation (see Chapter 1). As a result, in addition to inflammatory response, eicosanoid synthesis or retinol metabolism which was thought to be up-regulated by technique of transplantation or maturation of oocytes, GO analysis showed up-regulation of “nuclear receptors” and “TGF beta signaling pathway” (Table 3-2). It was notable that androgen receptor was highly up-regulated in nuclear receptor pathways.

Taken together, for the first time, I could demonstrate that pathways such as TGF-β soluble factors and steroid hormones including androgens were up-regulated, then, major ovarian

factors were down-regulated and testicular factor were up-regulated in the norvel manner throughout XX testis formation. In this process, I also identified up-regulation of the novel testicular genes that were suggested to be important for testicular formation even without *Sry*.

Discussion

In order to clarify the mechanisms of XX sex reversal in detail, I tried histological and comprehensive gene profile analyses by time series (0, 4, 7, 10, 15 and 20 days after transplantation). On histology, transplanted ovaries seemed to mature normally until day 4 and AMH-positive primary follicles started to be observed from day 7. However, continuously, an accute decrease in the number of oocytes began, and AMH-positive clusters/ cord-like structures were seen widely across the gonads. Among them, there were some SOX9-, the Sertoli cell-specific protein, positive cords. The presence of AMH-positive testis cord-like structures at day 7 is demonstrated also by Taketo et al. (1993). This fact suggests the transdifferentiation of XX ovaries into XX testes under transplantation, and in fact, these histological observations are consistent with the results by gene profile analyses that clearly showed the same clustering of transplanted grafts with E12.5 XY testes (Fig. 3-2A), temporal shift to the trends of XY testes (Fig. 3-2B-D), and down-regulation of ovarian factors/ up-regulation of testicular factors (Fig. 3-3A). In summary, I could demonstrate the model of the temporal process on the formation of XX testis (Fig. 3-4A). 1) from 0d to 4d, transplanted ovaries normally develop. 2) from 7d, granulosa cells around oocytes begin to express AMH. 3) from 7d to 10d, oocytes are drastically lost from follicles. 4) from 15d to 20d, most of the round shaped follicles change into testis cord-like structures and some epithelia come to express SOX9. At the same time, FOXL2, which is normally localized at only granulosa cells, disappeared from the SOX9-positive epithelium (see Chapter 2, Fig. 2-8). Because I did not observe the same follicles throughout the time series continuously, this model has a little expectation. But, the “budding” form of testis cord-like structures successive with follicles could apparently support my model (Fig. 3-1C).

To find out molecular mechanisms of XX sex reversal further, I examined supervised analyses. Along with down-regulation of female factors such as *Bmp2, Dax1, Irx3, Fst, Wnt4* and *Rspo1*, all of which are known to be essential for ovarian sex determination and ovarian fertility, male factors such as *Sox8, Gdnf, Dhh, Amh* and *Sox9* were gradually up-regulated from 7d to 15d (Fig. 3-3; Fig. 3-4B). Moreover, plotted graphs showed obviously that female genes were down-regulated especially from 4d to 10d, although male genes were not so much increased during these periods (Figs. 3-2D; 3-3A). This result could be considered that from 4d to 10d, transplanted grafts move toward bipotential states. Previously, I reported the existence of granulosa cells with sexual bipotency/plasticity. It was also demonstrated that these bipotential granulosa cells were reaquired at 10d and contributed to or had relationship with following XX sex-reversal (see Chapter 2). My present results are consistent with previous findings and also strongly indicate that 10d grafts are near to bipotential situation. Therefore, I could conclude that transdifferentiation of XX ovaries occurs via the bipotential states.

Among up-regulated male factors, I identified genes *Egr1, Egr2, Ctgf, Bhlhe40* and *Nr4a1* (Fig. 3-3; Table 3-1). Until now, transcription factor *Egr1* is known to regulate luteinizing hormone beta subunit (LHbeta) gene expression in the pituitary gland and *Egr4-Egr1* double mutant male mice is reported to have low levels of serum LH and testosterone, and atrophy of whole testes especially in Leydig cells (Tourtellotte et al., 2000). In Sertoli cells, *Egr1* is indicated to act with *Sp1* to up-regulate *Dmrt1*, the conserved sex determination factor (Lei and Hackert, 2002). *Bhlhe40* and *Nr4a1* is reported to act with GDNF, which is essential for maintenance of spermatogonial stem cells (Schmidt et al., 2009; Ding et al., 2011). Testes of

transgenic mice that overproduce CTGF under the control of mouse type XI collagen promoter are shown to be much smaller than normal ones and infertile (Nakanishi et al., 2001). However, nothing is yet reported about precise functions, involvement and importance of these genes in testis determination pathways. It is desired to reveal these functions further. Uhlenhaut et al. (2009) reported 854 genes related to XX sex reversal by using *Foxl2* conditional KO sex reversed adult ovaries. Among my up-regulated 487 genes in 0d vs 15d, 86 genes including *Dhh*, *Sox8* and *Sox9* are common with Uhlenhaut's results and thought to be the most important genes for XX sex reversal, although there is the difference from my present study in the aspect of the lack of *Foxl2*. Especially, *Sox8* has been recently reported about its indispensability in formation and maintenance of testicular stuructures (Barrionuevo et al., 2009). Moreover, *Sox8* has been shown to have inhibitory effects against ovarian gene *Foxl2* (Georg et al., 2012). I also checked *Dmrt1*, another important factor for testis determination, and unfortunately could not find it neither in 0d vs 15d up-regulated nor down-regulated gene lists. Throughout from 4d to 20d, real-time PCR showed that *Dmrt1* kept higher expression level than that of corresponding non-transplanted ovaries (data not shown) and immunohistochemistry demonstrated the up-regulation of DMRT1 from 15d (Fig. 2-8, Chapter 2). Therefore, it is suggested that *Sox8* and continuous high *Dmrt1* expression may also contribute to XX sex reversal.

As for the cause of genetically non-mutated XX sex reversal including freemartin and some DSDs, many scientists have debated for long time (Ottolenghi et al., 2007b). Taketo-Hosotani (1987) reported the cause of sex reversal in transplanted grafts is the soluble factors that could pass through semipermeable membrane (Taketo-Hosotani. 1987). In freemartin, it has been suggested that TGF-β signaling factor secreted from Sertoli cells of XY co-twin, AMH, is the

main cause and actually rat gonads co-cultured with AMH are known to be masculinized (Vigier et al., 1987). In my study, by GO analysis, I demonstrated the up-regulation of receptors of steroid hormones and TGF-β signaling (Table 3-2; Fig. 3-4B). Because I checked "affected" pathways, my observation is indirect to find out the cause. But, early growth of primordial to primary follicles I could observed are known to be the unique characteristic of ovaries under excess androgen (Fig. 3-1B) (Abbott et al., 2002). Therefore, ectopic androgens and TGF-β signaling may be the main cause for non-genetically mutated XX sex reversal and DSDs.

In mammalian testicular sex determination, very complicate pathways have been known recently. In short, *Sry* is the master switch and directly or indirectly, induces downstream factors such as *Sox9, Gdnf, Amh, Dhh, Dmrt1* and *Sox8* (Fig. 3-4B). Stages of the expression of these factors are strictly determined and delay of *Sry* or *Sox9* expression is known to result in incomplete testes (Hiramatsu et al., 2009; Gregoire et al., 2011; Correa et al., 2012). On the other hand, my present study showed that during transplantation, until 10d, *Sox8* and *Gdnf* were up-regulated and then, *Amh* was expressed. *Sox9* was expressed at last from 15d. These results are consistent with histological observation, although timings of protein localization are a little different from RNA expression (Figs. 3-1B, C; 3-3; 3-4A, B; also see Chapter 2). Notably, this XX testicular formation is apparently different from normal XY testicular formation. To my knowledge, it is the first time to report this "strange" process of mammalian XX testis. However, it is common among other vertebrates. Until now, reserchers find out that genes involving sex determination, their orders (i.e. *Dmrt1-Amh-Sox9*) and hormone/environment-dependent mechanisms are relatively conserved among vertebrates except for mammals (Oréal et al., 2002; Yao and Capel, 2005; Klüver et al., 2007) (Fig. 3-4C).

In this study, I demonstrated that mammalian XX testis without *Sry* was formed in order of *Amh/Dmrt1-Sox9* which is the same with other vertebrates without *Sry*. Moreover, TGF-β signaling and steroid hormones are indicated to be important for mammalian XX sex reversal as well as testicular formation of other vertebrates (Fig. 3-4C). Therefore, I could demonstrate the potential presence of conserved mechanism of testicular formation among vertebrates including even mammals for the first time. In addition, male genes we newly identified in XX testis formation, such as *Egr1*, *Egr2*, *Ctgf*, *Bhlhe40* and *Nr4a1*, are suggested to have potential conserved and important mechanisms also in XY testis formation.

The presence of conserved testis-foming pathway gives new insights into non-conserved testis-determining gene *Sry* and its cascades in XY testis. Why do mammals aquire *Sry* ? This might be due to the testis-determination under maternal environment, which is a specific characteristic in mammals. With the acquisition of viviparity, it is necessary for mammals to differentiate testis by new genetic manner instead of old environment-dependent manner. This fact is apparently consistent with the lack of functional *Sry* gene in marsupials which determine sex in mother's pouch after birth (Sekido and Lovell-Badge, 2009).

To my knowledge, for the first time, I successfully identified temporal morphological changes and molecular mechanisms of genetically non-mutated mammalian XX testis. My study contributes not only to the elucidation of the mechanisms or diagonsis of animal and human DSDs, but also to revealing novel important genes and mechanisms conserved among vertebrate sex deteremination.

Figures and Legends

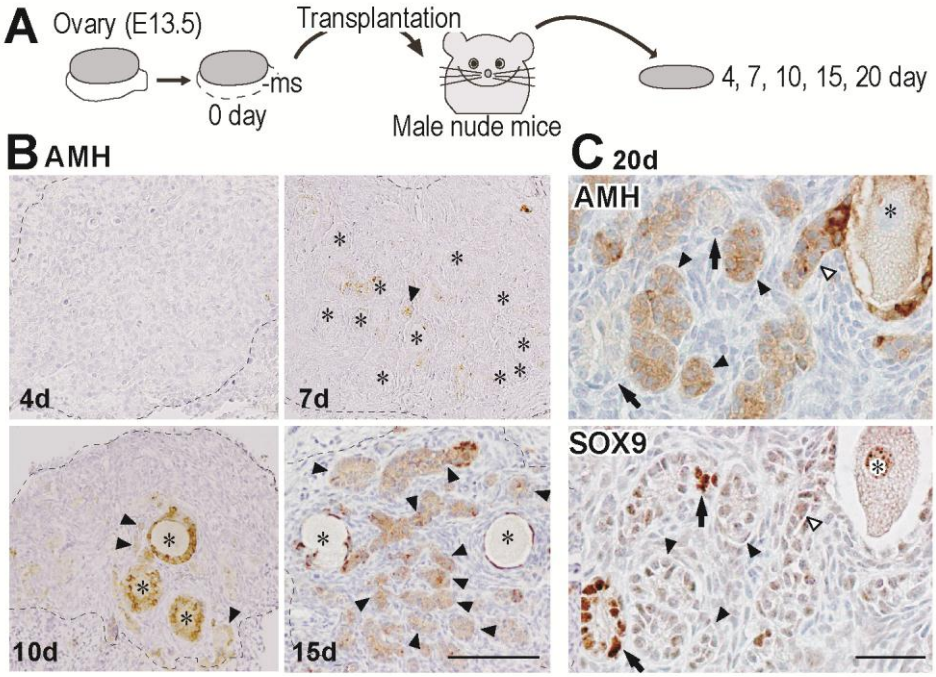
A
Ovary (E13.5)
0 day
Transplantation
Male nude mice
4, 7, 10, 15, 20 day
B AMH
4d
7d
10d
15d
C 20d
AMH
SOX9

FIGURE 3-1

Figure 3-1. Histological observation of XX testicular formation in time-series transplanted ovaries.

(**A**) The fetal ovaries at E13.5 were transplanted under the kidney capsule of male nude mice from 4 to 20 days and picked up at 4, 7, 10, 15 and 20 days after transplantation. Transplanted ovaries were fixed and stained for immunohistochemistry. (**B**) anti-AMH immunostaining of transplanted grafts at 4, 7, 10 and 15 days after transplantation (4d, 7d, 10d and 15d). In 4d, there are many oocytes in whole parenchyma. From 7d, in addition to primary follicles (AMH-positive granulosa cells with oocytes marked by asterisks), AMH-positive cord-like structures without oocytes are observed (arrowheads). Over time, the number of primary follicles seemed to be decreased, while that of cord-like structures is apparently increased. (**C**) At 20 days, some AMH-positive cord-like structures appear to “bud” from follicles (white arrowheads). Part of cord-like structures is positive for SOX9 (arrows). Asterisks, germ cells/oocytes. Scale bar: 100 μm in B, 10μm in C.

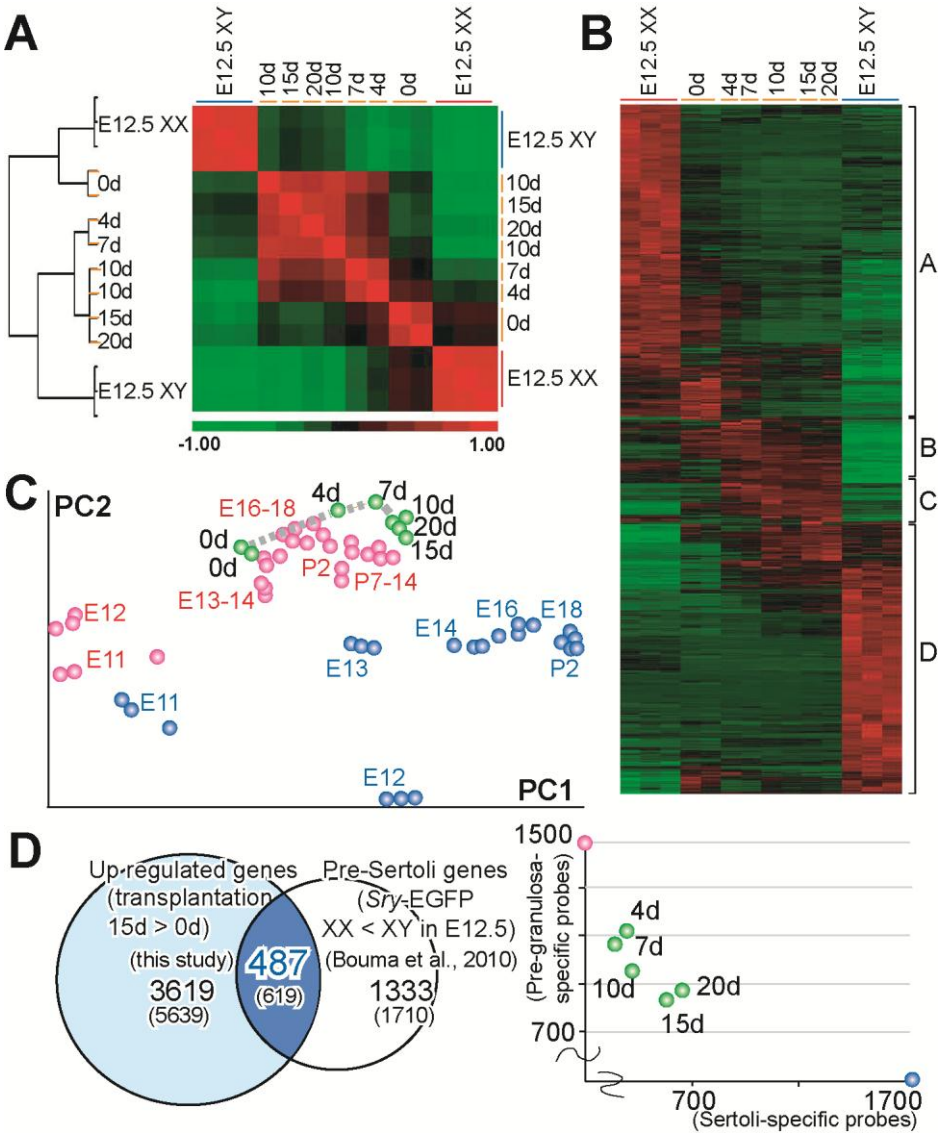
A
E12.5 XY
10d
15d
20d
10d
7d
4d
0d
E12.5 XX
E12.5 XX
0d
4d
7d
10d
10d
15d
20d
E12.5 XY
E12.5 XY
10d
15d
20d
10d
7d
4d
0d
E12.5 XX
-1.00
1.00
B
E12.5 XX
0d
4d
7d
10d
15d
20d
E12.5 XY
A
B
C
D
C
PC2
PC1
E16-18
4d
7d
10d
20d
15d
0d
0d
P2
P7-14
E13-14
E12
E11
E11
E12
E13
E14
E16
E18
P2
D
Up-regulated genes
(transplantation
15d > 0d)
(this study)
3619
(5639)
487
(619)
Pre-Sertoli genes
(Sry-EGFP
XX < XY in E12.5)
(Bouma et al., 2010)
1333
(1710)
1500
700
(Pre-granulosa-specific probes)
4d
7d
10d
20d
15d
700
1700
(Sertoli-specific probes)

FIGURE 3-2

Figure 3-2. Comprehensive gene profile analysis demonstrating the process of XX sex reversal in transplanted ovaries.

(**A**) Unsupervised sample clustering (A) and gene clustering (B) show transplanted ovaries are classified into the same group with XY testis and thus, proceeding sex-reversal. Especially, grafts at 15d have the nearest correlation with E12.5 XY testes. Part of cluster D contains presumptive candidates (B). (**C**) Several published microarray data are mapped onto the PCA with time-series transplanted ovaries. Pink points for XX datasets, blue points for XY datasets and green points for transplanted ovaries. A broken lined trajectory shows high PC1 value in transplanted grafts. (**D**) 487 genes (619 probe sets) significantly up-regulated in 15d compared with 0d and commonly expressed in E12.5 Sertoli cells are obtained. Up-regulated Sertoli-specific probes and down-regulated granulosa-specific probes are plotted onto the graph. Toward 10d, granulosa-specific probes are decreased, and then, Sertoli-specific ones are increased. Pink points for E12.5 XX datasets, blue points for E12.5 XY datasets and green points for transplanted ovaries. (E12.5 XX; 1437 probes, E12.5 XY; 1711 probes. 4d; 351 down-regulated pre-granulosa specific probes and 345 up-regulated Sertoli-specific probes. 7d; 397 down and 310 up, 10d; 504 down and 360 up, 15d; 642 down and 620 up, 20d; 615 down and 640 up.)

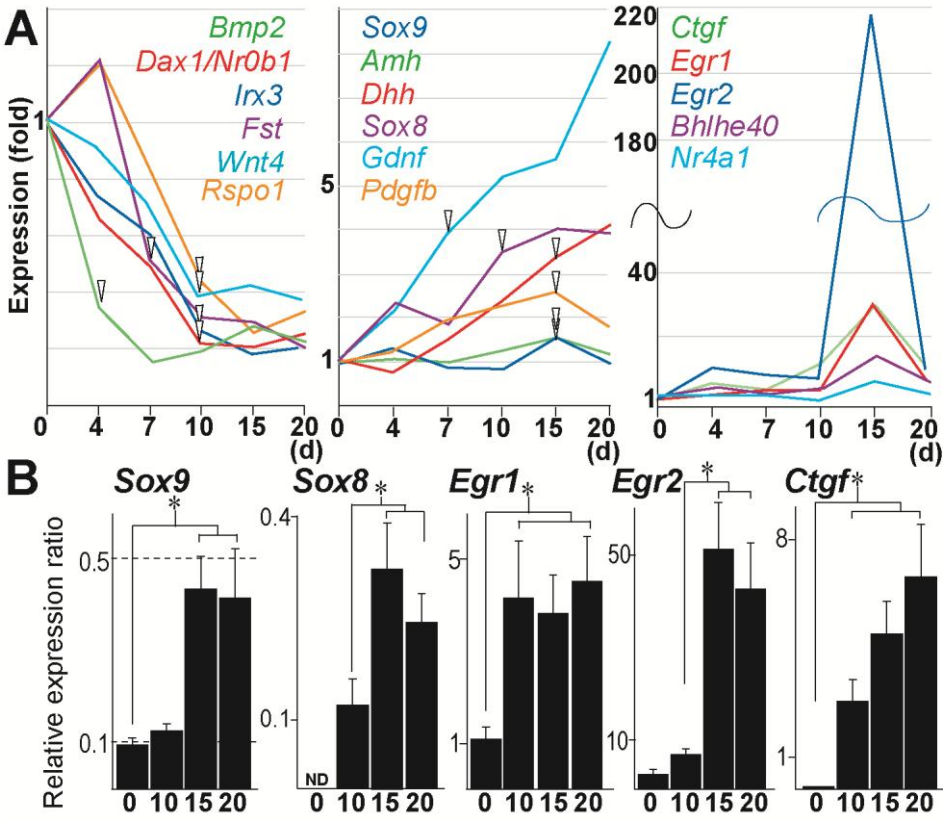
A
Expression (fold)
Bmp2
Dax1/Nr0b1
Irx3
Fst
Wnt4
Rspo1
Sox9
Amh
Dhh
Sox8
Gdnf
Pdgfb
Ctgf
Egr1
Egr2
Bhlhe40
Nr4a1
(d)
B
Sox9
Sox8
Egr1
Egr2
Ctgf
Relative expression ratio
ND

FIGURE 3-3

Figure 3-3. Many well-known ovarian genes are down-regulated and testicular genes including both well-known and the novel ones are up-regulated throughout XX sex reversal. (**A**) Temporal expression values of well-known ovarian genes, testicular genes and the novel testicular genes are plotted onto the graphs. Each value is gained by microarray experiments. Ovarian genes are most significantly reduced from 7d to 10d, except for *Bmp2* (from 0d and 4d) and *Fst* (from 4d to 7d). To the contrary, testicular genes are much increased from 10d to 15d, except for *Gdnf* (from 4d and 7d) and *Sox8* (from 7d to 10d). *Ctgf*, *Egr1*, *Egr2*, *Bhlhe40* and *Nr4a1* are highly up-regulated in 15d. White arrowheads show the point where the value changed the most exclusively. (**B**) Real-time RT-PCR analysis showing transcript levels of the *Sox9*, *Sox8*, *Egr1*, *Egr2* and *Ctgf* genes relative to *Gapdh* (the mean values ± standard error; n= 4-5) in the ovarian transplants at days 0, 10, 15 and 20 after transplantation (*$p<0.05$, as compared with each transcript level at day 0; Only in *Sox8*, compared with days 10).

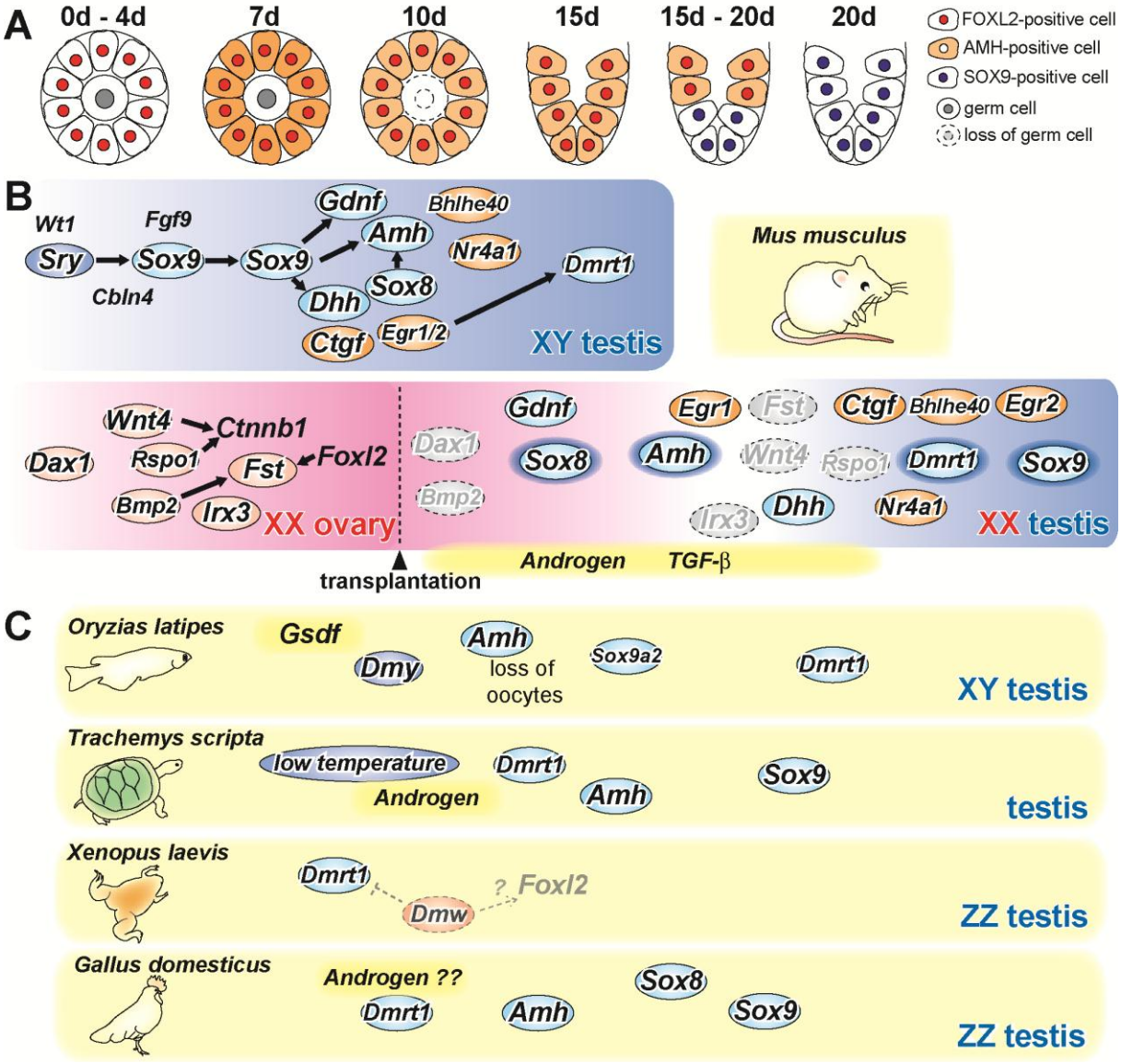
A
0d - 4d
7d
10d
15d
15d - 20d
20d
FOXL2-positive cell
AMH-positive cell
SOX9-positive cell
germ cell
loss of germ cell
B
Wt1
Fgf9
Sry
Sox9
Sox9
Cbln4
Gdnf
Bhlhe40
Amh
Nr4a1
Dmrt1
Sox8
Dhh
Ctgf
Egr1/2
XY testis
Mus musculus
Wnt4
Ctnnb1
Dax1
Rspo1
Fst
Foxl2
Bmp2
Irx3
XX ovary
Dax1
Bmp2
Gdnf
Sox8
Egr1
Fst
Ctgf
Bhlhe40
Egr2
Amh
Wnt4
Rspo1
Dmrt1
Sox9
Irx3
Dhh
Nr4a1
XX testis
transplantation
Androgen
TGF-β
C
Oryzias latipes
Gsdf
Dmy
Amh
loss of oocytes
Sox9a2
Dmrt1
XY testis
Trachemys scripta
low temperature
Androgen
Dmrt1
Amh
Sox9
testis
Xenopus laevis
Dmrt1
Dmw
? Foxl2
ZZ testis
Gallus domesticus
Androgen ??
Dmrt1
Amh
Sox8
Sox9
ZZ testis

FIGURE 3-4

Figure 3-4. Morphological changes and temporal shift of genes related with XX sex reversal. (**A**) In the transplanted ovary, primordial follicles and germ cells seem to mature normally until about day 7, and granulosa cells express AMH. After 10d, many germ cells/oocytes appear to be lost from primordial follicles and many cord-like structures are observed at day 15. At day 20, SOX9 localizes in the epithelia of cord-like structures, leading to formation of XX testis. (**B**) In mammalian XY gonads, *Sry* triggers expression of many down-stream genes, represented by *Sox9*, *Amh*, *Sox8*, *Dmrt1* and so on, to differentiate bipotential gonads into testis. While in XX gonads, no ovarian determining genes is discovered yet, but some ovarian genes such as *Dax1*, *Wnt4*, *Rspo1* and *Foxl2* are thought to have a key role in differentiation and following follicle formation. When ovaries are transplanted during fetal period and affected by ectopic androgen and/or TGF-β signaling, which are supposed causes for XX testis (XX DSDs), many ovarian genes come to lose their expression (broken gray ellipses). Instead, expression of some testicular genes like *Gdnf*, *Sox8*, *Dhh*, *Dmrt1*, *Amh* and *Sox9* is increased. Among them, the novel genes including *Ctgf*, *Egr1/2*, *Bhlhe40* and *Nr4a1* are observed, suggesting their important roles in testicular differentiation in both XY and XX. Genes with orange ellipses are the novel ones I identified in this study and those with blue flames are presumptive conserved genes among vertebrates. (**C**) Sex-determiming cascades in various animals, clearly demonstrating conserved relationship of *Dmrt1*/*Amh*-*Sox9* and hormone/environment-dependent manner. GSDF in in *Oryzias latipes* is a TGF-β soluble factor. *Dmy* is produced by gene duplication of *Dmrt1*. Please compare genes with blue flames and soluble factors in yellow flames in B.

Tables

Table 1	**Top 100 Up-regulated Sertoli genes in 15d vs 0d**				
Probesets	**Symbol**	**Definition**	**log fold 15d vs 0d**	**log fold 20d vs 0d**	**Sry-EGFP XX > XY**
1427683_at	Egr2	early growth response 2	7.77	3.71	1.87
1427682_a_at	Egr2	early growth response 2	7.14	3.06	2.25
1449396_at	Aoc2 /// Aoc3	amine oxidase, copper containing 2 (retina-specific) /// amine oxidase, copper containing 3	5.09	5.08	3.20
1417065_at	Egr1	early growth response 1	4.89	2.74	1.50
1416953_at	Ctgf	connective tissue growth factor	4.89	3.47	2.37
1417408_at	F3	coagulation factor III	4.69	3.36	4.34
1416460_at	Miox	myo-inositol oxygenase	4.69	4.38	1.78
1436712_at	Pla2g4c	phospholipase A2, group IVC (cytosolic, calcium-independent)	4.63	5.24	1.61
1415935_at	Smoc2	SPARC related modular calcium binding 2	4.60	4.98	3.72
1423584_at	Igfbp7	insulin-like growth factor binding protein 7	4.45	4.59	2.18
1426663_s_at	Slc45a3	solute carrier family 45, member 3	4.15	4.73	1.15
1440339_at	Enpp1	ectonucleotide pyrophosphatase/phosphodiesterase 1	3.98	3.67	4.80
1455224_at	Angptl1	angiopoietin-like 1	3.95	4.46	1.30
1449392_at	Hsd17b1	hydroxysteroid (17-beta) dehydrogenase 1	3.88	4.25	2.32
1459546_s_at	Enpp1	ectonucleotide pyrophosphatase/phosphodiesterase 1	3.86	3.36	2.24
1418572_x_at	Tnfrsf12a	tumor necrosis factor receptor superfamily, member 12a	3.85	0.87	2.40
1419276_at	Enpp1	ectonucleotide pyrophosphatase/phosphodiesterase 1	3.79	3.49	2.14
1426808_at	Lgals3	lectin, galactose binding, soluble 3	3.78	4.63	1.61
1451236_at	Rerg	RAS-like, estrogen-regulated, growth-inhibitor	3.76	4.16	4.82
1434494_at	Zar1	zygote arrest 1	3.73	4.09	2.20
1418025_at	Bhlhe40	basic helix-loop-helix family, member e40	3.73	2.18	1.34
1443823_s_at	Atp1a2	ATPase, Na+/K+ transporting, alpha 2 polypeptide	3.70	3.96	3.98
1418061_at	Ltbp2	latent transforming growth factor beta binding protein 2	3.63	3.84	1.76
1434628_a_at	Rhpn2	rhophilin, Rho GTPase binding protein 2	3.57	4.07	2.82
1418571_at	Tnfrsf12a	tumor necrosis factor receptor superfamily, member 12a	3.49	0.58	1.93
1431805_a_at	Rhpn2	rhophilin, Rho GTPase binding protein 2	3.46	3.96	1.86
1455610_at	Synm	synemin, intermediate filament protein	3.45	3.56	2.96
1454681_at	Rbm35a	RNA binding motif protein 35A	3.43	3.55	2.47
1421172_at	Adam12	a disintegrin and metallopeptidase domain 12 (meltrin alpha)	3.41	3.27	2.32
1428896_at	Pdgfrl	platelet-derived growth factor receptor-like	3.41	2.89	2.60
1449533_at	Tmem100	transmembrane protein 100	3.37	3.91	3.43
1435486_at	Pak3	p21 (CDKN1A)-activated kinase 3	3.31	2.87	5.49
1416666_at	Serpine2	serine (or cysteine) peptidase inhibitor, clade E, member 2	3.28	3.34	4.98
1437318_at	Pak3	p21 (CDKN1A)-activated kinase 3	3.28	2.85	2.73
1436568_at	Jam2	junction adhesion molecule 2	3.27	3.34	3.38
1450652_at	Ctsk	cathepsin K	3.25	2.70	1.23
1431362_a_at	Smoc2	SPARC related modular calcium binding 2	3.25	3.65	1.63
1437247_at	Fosl2 /// LOC6344	fos-like antigen 2 /// similar to fos-like antigen 2	3.24	2.71	2.52
1417785_at	Pla1a	phospholipase A1 member A	3.22	2.57	1.76
1436528_at	Kazald1	Kazal-type serine peptidase inhibitor domain 1	3.21	3.23	3.65
1436870_s_at	Afap1l2	actin filament associated protein 1-like 2	3.20	3.26	5.47
1416039_x_at	Cyr61	cysteine rich protein 61	3.20	1.69	1.50
1420965_a_at	Enc1	ectodermal-neural cortex 1	3.18	1.96	1.40
1448470_at	Fbp1	fructose bisphosphatase 1	3.16	2.76	1.81

Probesets	Symbol	Definition	log fold 15d vs 0d	log fold 20d vs 0d	Sry-EGFP XX > XY
1434537_at	Slco3a1	solute carrier organic anion transporter family, member 3a1	3.16	3.40	3.97
1424649_a_at	Tspan8	tetraspanin 8	3.13	3.89	2.26
1426438_at	Ddx3y	DEAD (Asp-Glu-Ala-Asp) box polypeptide 3, Y-linked	3.08	3.34	6.25
1450061_at	Enc1	ectodermal-neural cortex 1	3.05	1.96	1.46
1438133_a_at	Cyr61	cysteine rich protein 61	3.05	1.50	2.39
1418106_at	Hey2	hairy/enhancer-of-split related with YRPW motif 2	3.04	2.94	2.19
1433579_at	Tmem30b	transmembrane protein 30B	3.03	4.05	2.04
1422124_a_at	Ptprc	protein tyrosine phosphatase, receptor type, C	3.03	4.29	1.67
1428547_at	Nt5e	5' nucleotidase, ecto	3.02	2.56	3.20
1417625_s_at	Cxcr7	chemokine (C-X-C motif) receptor 7	3.00	2.48	2.19
1425841_at	Slc26a7	solute carrier family 26, member 7	2.97	2.76	1.11
1421114_a_at	Epyc	epiphycan	2.92	2.98	4.72
1454795_at	Cobll1	Cobl-like 1	2.91	3.27	2.64
1435387_at	Slc2a13	solute carrier family 2 (facilitated glucose transporter), member 13	2.87	2.41	3.00
1433847_at	Fam40b	family with sequence similarity 40, member B	2.81	3.00	1.86
1429682_at	Fam46c	family with sequence similarity 46, member C	2.80	3.55	4.11
1435554_at	Tmcc3	transmembrane and coiled coil domains 3	2.77	3.29	5.07
1423091_a_at	Gpm6b	glycoprotein m6b	2.76	2.93	3.64
1421040_a_at	Gsta2	glutathione S-transferase, alpha 2 (Yc2)	2.74	3.04	1.21
1417923_at	Pak3	p21 (CDKN1A)-activated kinase 3	2.72	2.31	3.93
1449408_at	Jam2	junction adhesion molecule 2	2.71	2.54	3.88
1421106_at	Jag1	jagged 1	2.70	3.16	1.39
1434070_at	Jag1	jagged 1	2.69	3.00	2.31
1456321_at	Npal1	NIPA-like domain containing 1	2.69	3.48	1.96
1416505_at	Nr4a1	nuclear receptor subfamily 4, group A, member 1	2.69	0.82	1.06
1434647_at	Egflam	EGF-like, fibronectin type III and laminin G domains	2.67	2.32	1.41
1436196_at	C030046G05	hypothetical protein C030046G05	2.66	2.36	2.22
1445669_at	Spry4	sprouty homolog 4 (Drosophila)	2.65	1.73	4.30
1425506_at	Mylk	myosin, light polypeptide kinase	2.63	2.90	2.31
1449109_at	Socs2	suppressor of cytokine signaling 2	2.59	2.85	2.04
1438654_x_at	Mmd2	monocyte to macrophage differentiation-associated 2	2.56	2.67	5.12
1422706_at	Pmepa1	prostate transmembrane protein, androgen induced 1	2.54	2.03	2.73
1425336_x_at	H2-K1	histocompatibility 2, K1, K region	2.54	3.46	1.42
1426774_at	Parp12	poly (ADP-ribose) polymerase family, member 12	2.51	2.90	1.65
1419080_at	Gdnf	glial cell line derived neurotrophic factor	2.47	3.05	5.86
1428485_at	Car12	carbonic anyhydrase 12	2.46	2.10	2.51
1454974_at	LOC672215 /// Ntn1	similar to Netrin-1 precursor /// netrin 1	2.46	2.14	1.11
1448918_at	Slco3a1	solute carrier organic anion transporter family, member 3a1	2.43	2.66	1.62
1434252_at	Tmcc3	transmembrane and coiled coil domains 3	2.41	3.01	2.87
1428853_at	Ptch1	patched homolog 1	2.41	2.91	2.17
1453345_at	Npal1	NIPA-like domain containing 1	2.40	3.15	2.28
1448895_a_at	Ctnna2	catenin (cadherin associated protein), alpha 2	2.39	2.13	1.74
1427257_at	Vcan	versican	2.38	2.21	2.70
1455538_at	6330403M23Rik	RIKEN cDNA 6330403M23 gene	2.38	2.40	2.30
1429809_at	Tmtc2	transmembrane and tetratricopeptide repeat containing 2	2.37	2.52	1.82
1434510_at	Papss2	3'-phosphoadenosine 5'-phosphosulfate synthase 2	2.35	2.31	1.96

Probesets	Symbol	Definition	log fold 15d vs 0d	log fold 20d vs 0d	Sry-EGFP XX > XY
1436501_at	Mtus1	mitochondrial tumor suppressor 1	2.33	2.47	1.88
1418507_s_at	Socs2	suppressor of cytokine signaling 2	2.33	2.44	2.73
1415834_at	Dusp6	dual specificity phosphatase 6	2.32	0.27	2.63
1455833_at	Afap1l2	actin filament associated protein 1-like 2	2.32	2.42	2.79
1434342_at	S100b	S100 protein, beta polypeptide, neural	2.23	3.40	2.84
1418936_at	Maff	v-maf musculoaponeurotic fibrosarcoma oncogene family, protein F (avian)	2.22	0.73	1.92
1451031_at	Sfrp4	secreted frizzled-related protein 4	2.22	1.73	1.86
1436502_at	Mtus1	mitochondrial tumor suppressor 1	2.21	2.53	1.91
1418492_at	Grem2	gremlin 2 homolog, cysteine knot superfamily (Xenopus laevis)	2.20	2.32	3.14

Table 2	**Up-regulated pathways in 10d vs 0d**		
MAPP Name	**gene symbols**	**log fold**	**p value**
Ovarian Infertility Genes:WP273	Egr1|Inha|Nrip1|Pgr|Prlr|Ptger2|Smad3|Syne2|Zp2|Zp3	3.28	0.019
Nuclear Receptors:WP509	Ar|Esr1|Nr1d2|Nr3c1|Nr5a2|Pgr|Pparg|Rora	2.64	0.012
Small Ligand GPCRs:WP353	Lpar1|Ptger2|Ptger4|S1pr3	2.58	0.013
Prostaglandin Synthesis and Regulation:WP374	Anxa1|Anxa3|Hsd11b2|Ptger2|Ptger4|Ptgis|S100a6	2.52	0.018
Complement Activation, Classical Pathway:WP200	C1qa|C1qb|C1ra|C1s|C2|C3|C4a|C4b|Cd55	2.44	0.011
Complement and Coagulation Cascades:WP449	C1qa|C1qb|C1ra|C1s|C2|C3|C4a|C4b|Cd55|Cfb|Cfh|F3|Plau|Pros1|Serping1|Tfpi|Thbd	2.30	0.010
Inflammatory Response Pathway:WP458	Col1a1|Col1a2|Col3a1|Thbs1|Thbs3|Tnfrsf1b|Vtn	2.08	0.012
Myometrial Relaxation and Contraction Pathways:WP385	Acta2|Adcy5|Adcy7|Adcy9|Camk2d|Cnn1|Corin|Cxcr7|Ets2|Fos|Gnb4|Gng4|Igfbp3|Igfbp6|Lpar1|Pkia|Prkar2b|Ramp1|Rgs18|Rgs2|Rgs4|Rgs5|Slc8a1	2.05	0.014
Eicosanoid Synthesis:WP318	Alox5ap|Dpep1|Ptges|Ptgis	2.05	0.013
Type II interferon signaling (IFNG):WP1253	Cxcl10|Cxcl9|Cybb|Ifngr1|Irf8|Jak1|Psmb9|Stat1	2.02	0.010
selenium:WP1272	Ptges|Ptgis|Sepp1|Xdh	1.94	0.016
Senescence and Autophagy:WP1267	Bmi1|Col1a1|Cxcl14|Gsn|Igf1|Igf1r|Igfbp7|Il6ra|Pten|Rnasel|Sparc|Thbs1|Vtn	1.93	0.013
Endochondral Ossification:WP1270	Adamts4|Adamts5|Bmp6|Ddr2|Enpp1|Frzb|Igf1|Igf1r|Mgp|Plau|Ptch1|Stat1	1.92	0.010
Retinol metabolism:WP1259	Aldh1a1|Cd36|Cyp2e1|Lpl|Lrat|Rbp4|Sult1a1	1.91	0.018
TGF Beta Signaling Pathway:WP113	Fos|Inhba|Jak1|Smad3|Stat1|Tgfbr2|Tgfbr3|Thbs1|Zeb2	1.88	0.017
Focal Adhesion:WP85	Bcl2|Birc3|Cav2|Col11a1|Col1a1|Col1a2|Col3a1|Col4a1|Col4a2|Col4a4|Col5a1|Col5a2|Col5a3|Col6a2|Egfr|Hck|Igf1|Itga9|Itgal|Itgb2|Itgb3|Itgb8|Lama2|Mylk|Pak3|Pdgfb|Pdgfd|Pdgfra|Pgf|Pik3r1|Pten|Sepp1|Thbs1|Thbs3|Thbs4|Tnc|Tnxb|Vtn	1.87	0.016
Iron Homeostasis:WP1596	Hfe|Il6ra|Slc40a1|Trf	1.80	0.011
Osteoclast:WP454	Ctsk|Itgb3|Pdgfb|Tnfrsf11b	1.78	0.022
Adipogenesis:WP447	Agt|Ebf1|Egr2|Epas1|Frzb|Igf1|Klf15|Klf6|Lmna|Lpl|Mbnl1|Nr3c1|Nrip1|Pparg|Ppargc1a|Prlr|Ptgis|Rora|Smad3|Stat1|Stat5a|Twist1	1.73	0.015
Apoptosis:WP1254	Bcl2|Birc3|Casp1|Casp4|Igf1|Igf1r|Irf6|Mapk10|Myc|Pik3r1|Tnfrsf1b|Tnfsf10	1.70	0.015

General Discussion

In the present study, first I demonstrated almost complete sex-reversed XX freemartin gonads not only morphological level but also molecular level (Chapter 1). Although freemartin gonads did not have *SRY* but have XX sex chromosome, differentiated Sertoli cells, Leydig cells and peritubular myoid cells were identified and ovarian structures were almost non-existent (Figure of General Discussion, "Sertoli-like cells"). Existence of such complete XX sex reversal without testis-determining gene *SRY* strongly supports the idea that there are unknown anti-testis/ovary-determining factor, so-called "*Od/Z* genes", which has been proposed in recent years (i.e., ovaries differentiate *positively*), and the lack of these genes leads to XX sex-reversal (McElreavey et al., 1993; Ottolenghi et al, 2007b). At the same time, XX sex reversal raises the question about long-believed "ovary default hypothesis" that ovarian state is nealy equal to a bipotential state and gonads differentiate into ovaries autonomously/*passively* under non-*Sry* condition. Which is true for ovarian sex determination, "*Od/Z* gene hypothesis" or "ovary default hypothesis" and how does ovary determine ??

In order to answer this question, I observed temporal changes of a sexually bipotential state in ovaries throughout fetal to adult stage by using the forced expression of *Sry* (Chapter 2). As a result, I conclude that both "*Od/Z* gene hypothesis" and "ovary default hypothesis" are mutually correct. That is, bipotential gonads at early stages rapidly lose sexual bipotency and differentiate into ovaries by anti-*Sry*/ovary-determining genes (i.e., *Od/Z* genes) which I identified by microarray analysis (Figure of General Discussion, "anti-testis/ovary determining genes"). After ovarian differentiation, these anti-*Sry*/ovary-determining genes might contribute to maintain normal ovarian structures or differentiated states. At the same time, however, not all ovarian somatic cells are differentiated, but small amounts of ovarian somatic cells keep sexual bipotency even after birth (Figure of General Discussion,

"bipotential granulosa cells"). Because the bipotency is a default setting for both XY and XX gonads, it can be thought for some populations of ovarian granulosa cells to retain the default state (i.e., "ovary is default"). This fact is clearly consistent with the experiment that the bipotential state is originally tending toward female (Jameson et al., 2012). Without anti-*Sry*/ ovary-determining genes under special circumstances like excess androgens or ectopic TGF-β signaling, ovary reaquires sexual bipotency and transdifferentiates into XX testis, such as freemartin (Chapter 3; Figure of General Discussion, "XX testis"). This is surely equal for testis to differentiate into ovary without *Sry*. That is to say, it is clearly revealed that sex of ovary is not determied by *default*, but is maintained by delicate *balance* between ovarian genes and testicular genes.

The cause and process of XX sex-reversal are thought to have key roles for not only exploring the mechanism of ovarian differentiation further, but also revealing unexplained human and livestock sex-reversed syndrome. Next I conducted detailed morphological and comprehensive gene profile analyses of XX sex reversal by using experimental mouse model (Chapter 3). Results showed that effects of steroid hormones, especially excess androgens, and TGF-β signaling triggered XX ovarian follicles toward rapid growing, following dysgenesis, loss of oocytes and down-regulation of ovarian genes. Degenerative follicles gradually transform themselves into testicular cord-like structures with up-regulation of testicular genes including the novel testicular genes, *Egr1*, *Egr2* and *Ctgf* (Figure of General Discussion, "XX testis"). Interestingly, the way to up-regulate testicular genes is different from XY testis-forming pathway. This new testis-forming pathway without *Sry* is the possible conserved cascades among vertebrates and may be the most important "core-cascades" for vertebrate testis determination (Figure of General Discussion, "conserved testis forming

pathway"). I can not clearly explain why ovary differentiates with such high heterogeneity/sexual plasticity yet, but bipotential granulosa cells in ovarian medullary region might also be potential remnants of characteristics conserved among vertebrates. Actually, the female gonads of moles (genus Talpa) are composed of a cortex, functioning as an ovary, and a medulla, which is structurally similar to that of the testis (Jiménez et al., 1993; Beolchini et al., 2000).

I believe my present study is very unique in the respect of using genetically non-mutated XX sex reversed gonads for study of mammalian sex determination system, and has the strong impact on ovarian and testicular sex determination. My study must have important roles for future researches of sex determination.

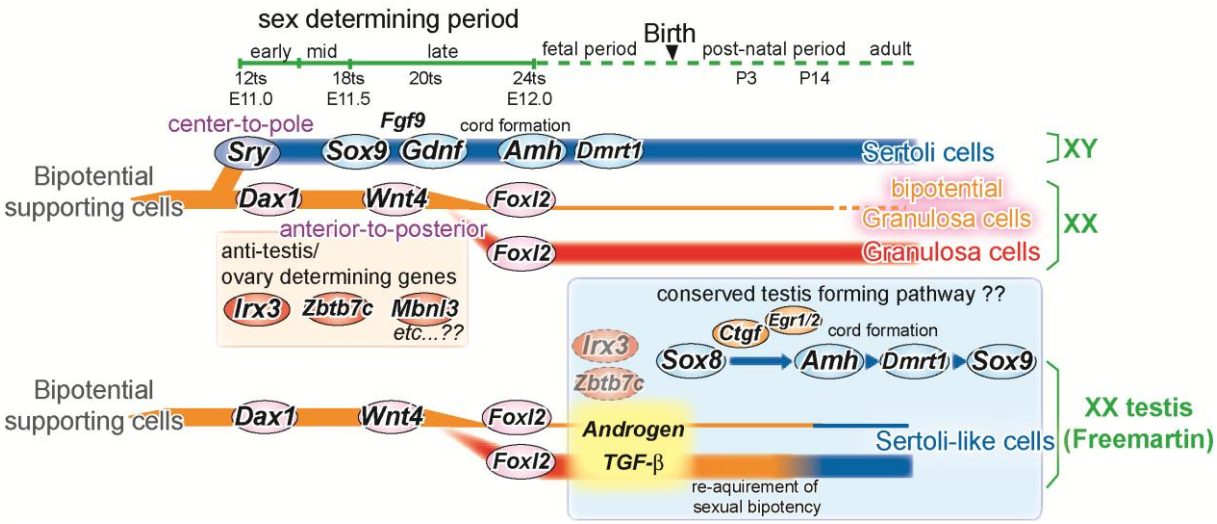

FIGURE OF GENERAL DISCUSSION

Figure of General Discussion

In normal development, sex of gonadal somatic cells is determined from E11.0 to approximately E12.0 during fetal period. From E11.0, *Sry* is first expressed in a center-to-pole mannar in XY gonads and leads the expression of subsequent downstream genes such as *Sox9*, *Fgf9*, *Gdnf*, *Amh* and *Dmrt1*, which make characteristics of Sertoli cells (blue bar). Around E12.0, testis-specific cord-like structures are formed. The timing or order of expression of each gene is severely fixed on "ts" (tail somite stages, passage of 2 hour corresponds to increase of 1 ts) bases. In normal differentiation of XX ovary, some ovary-specific genes such as *Dax1* or *Wnt4* are already expressed in early gonadal somatic cells, but ovary clearly loses its bipotency from 20ts in an anterior-to-posterior mannar by anti-testis/ovary-determining genes including *Irx3*, *Zbtb7c* or *Mbnl3* etc. (light orange box; red bar in "XX") (Chapter 2). On the other hand, some cells locating at ovarian medullary region retain sexual bipotency from fetal to even postnatal preiod (orange bar in "XX") (Chapter 2). If fetal XX ovaries are exposed to ectopic androgens or male TGF-β signaling, granulosa cells rapidly reaquire their sexual bipotency and testis cord-like structures are formed, leading transdifferentiation of ovarian pre-granulosa cells into Sertoli cells (orange and blue bar in "XX testis") (Chapters 1 and 3). In the process of transdifferentiation, ovarian genes disappear and instead, testis-specific genes including *Sox8*, *Amh*, *Dmrt1*, *Sox9* and the novel genes come to express. The order of these genes is highly conserved among vertebrates, implying the presence of conserved testis forming pathway even in mammals (light bule box) (Chapter 3).

Acknowledgements

I would like to deeply appreciate Drs. Shohei Toda and Kunio Yokouchi (Maebashi Institute of Animal Science, Livestock Improvement Association of Japan, Inc.) for technical assistance and significant discussion in Chapter 1. I would like to appreciate also Drs. Toshiaki Noce (MVH antibody; Advanced Research Centers, Keio University, Japan), Ken-ichirou Morohashi (SF1/Ad4BP, 3β-HSD, DAX1/NR0B1 and EMX2 antibody; Department of Molecular Biology, Graduate School of Medical Sciences, Kyushu University, Japan), David Shlessinger (FOXL2 antibody; Laboratory of Genetics, Biomedical Research Center, National Institute on Aging, USA), Dagmar Wilhelm (SOX9 antibody and critical reading of Chapter 2; Department of Anatomy and Developmental Biology, Monash University, Australia) and Peter Koopman (*Sox9* probe and SRY antibody; Institute for Molecular Bioscience, The University of Queensland, Australia) for providing antibodies, probes and meaningful advices.

Next, I wish to also greatly appreciate Drs. Kurohmaru Masamichi, Yoshiakira Kanai, Naoki Tsunekawa (Department of Veterinary Anatomy, The University of Tokyo, Japan) and Masami Kanai-Azuma (Department of Experimental Animal Model for Human Disease, Center for Experimental Animal, Tokyo Medical and Dental University, Japan) for giving me exciting environment for reseach, huge number of important advices and many supports. I am very happy to study for 7 years under these wonderful mentors.

I am also greatly thankful to my seniors, Drs. Ryuji Hiramatsu (Department of Safety

Research on Blood and Biological Products, National Institute of Infectious Diseases, Japan) and Shogo Matoba (Harvard Medical School, USA) for not only giving me advices or teaching me many techniques but also cheering me up every time. They are special and great seniors for me. Furthermore, I am deeply greatful for Ms. Itsuko Yagihashi for her secretarial assistance and Mr. Yoh-ichiro Mori for technical assistance of microarray. I would like to give special thanks to Drs. Masayoshi Kuwahara and Koichi Ito at University of Tokyo, and my precious classmates at veterinary medical science for their warm encouragement and cheer.

Lastly but definitly not least, I would deeply thank my beloved family. Dr. Kenshiro Hara (Division of Germ Cell Biology, National Institute for Basic Biology, National Institutes of Natural Sciences, Japan) is my husband, my senior and the most respectable researcher. He always encourages me, stands by me and gives me special advices. Without him, I would not finish my Ph.D course. Needless to say, my parents, Mr. Ken Harikae and Miss. Nachiko Harikae, also cheer and support me every day. I am very happy to be their children. And two more cats that I should not forget are Don and Saba. Don lived for 18 years and died May 28th 2012. From my childhood, he was always my best friend. Thanks to him, I decided to be a researcher of veterinary science.

I wish to give great thanks to all of them.

December, 2012

Kyoko Harikae, D.V.M.

References

1. **Abbott DH, Dumesic DA, Franks S.** (2002) Developmental origin of polycystic ovary syndrome - a hypothesis. *J Endocrinol*. **174**:1-5.
2. **Albrecht, K. H. and Eicher, E. M. (**2001) Evidence that Sry is expressed in pre-Sertoli cells and Sertoli and granulosa cells have a common precursor. *Dev. Biol*. **240**, 92-107.
3. **Aponte PM, Soda T, Teerds KJ, Mizrak SC, van de Kant HJ, de Rooij DG.** (2008) Propagation of bovine spermatogonial stem cells in vitro. *Reproduction*. **136**:543-557.
4. **Avilion AA, Nicolis SK, Pevny LH, Perez L, Vivian N, Lovell-Badge R.** (2003) Multipotent cell lineages in early mouse development depend on SOX2 function. *Genes Dev*. **17**:126-140.
5. **Barrionuevo F, Georg I, Scherthan H, Lécureuil C, Guillou F, Wegner M, Scherer G.** (2009) Testis cord differentiation after the sex determination stage is independent of Sox9 but fails in the combined absence of Sox9 and Sox8. *Dev Biol*. **327**:301-312.
6. **Behringer RR, Cate RL, Froelick GJ, Palmiter RD, Brinster RL.** (1990) Abnormal sexual development in transgenic mice chronically expressing müllerian inhibiting substance. *Nature.* **345**:167-170.
7. **Beolchini F, Rebecchi L, Capanna E, Bertolani R.** (2000) Female gonad of moles, genus Talpa (Insectivora, mammalia): ovary or ovotestis? *J Exp Zool*. 286:745-754.
8. **Beverdam, A. and Koopman, P.** (2006) Expression profiling of purified mouse gonadal somatic cells during the critical time window of sex determination reveals novel candidate genes for human sexual dysgenesis syndromes. *Hum. Mol. Genet*. **15**, 417-431.
9. **Bouma, G. J., Hudson, Q. J., Washburn, L. L., Eicher, E. M.** (2010) New candidate genes identified for controlling mouse gonadal sex determination and the early stages of granulosa and Sertoli cell differentiation. *Biol Reprod*. **82**, 380-389.
10. **Cabianca G, Rota A, Cozzi B, Ballarin C.** (2007) Expression of AMH in female fetal intersex gonads in the bovine. *Anat Histol Embryol*. **36**:24-26.
11. **Capel B, Coveney D**. (2004) Frank Lillie's freemartin: illuminating the pathway to 21st century reproductive endocrinology. *J Exp Zoolog A Comp Exp Biol*. **301**:853-856.
12. **Chaboissier MC, Kobayashi A, Vidal VI, Lützkendorf S, van de Kant HJ, Wegner M, de Rooij DG, Behringer RR, Schedl A.** (2004) Functional analysis of Sox8 and Sox9 during sex determination in the mouse. *Development*. **131**:1891-1901.
13. **Chassot A. A, Ranc F., Gregoire E. P., Roepers-Gajadien H. L., Taketo M. M., Camerino, G., de Rooij, D. G., Schedl, A., Chaboissier, M. C.** (2008) Activation of beta-catenin signaling by Rspo1 controls differentiation of the mammalian ovary. *Hum Mol Genet.* **17**, 1264-1277.
14. **Chen, H., Palmer, J.S., Thiagarajan, R.D., Dinger, M.E., Lesieur, E., Chiu, H., Schulz, A., Spiller, C., Grimmond, S.M., Little, M.H. et al.** (2012) Identification of novel markers of mouse fetal ovary development. *PLoS One*. **7**:e41683.
15. **Colvin, J. S., Green, R. P., Schmahl, J., Capel, B. and Ornitz, D. M.** (2001) Male-to-female sex reversal in mice lacking fibroblast growth factor 9. *Cell* **104**, 875-889.
16. **Correa SM, Washburn LL, Kahlon RS, Musson MC, Bouma GJ, Eicher EM, Albrecht KH.** (2012) Sex reversal in C57BL/6J XY mice caused by increased expression of ovarian genes and insufficient activation of the testis determining pathway. *PLoS Genet*.

8:e1002569.

17. **Couse, J. F., Hewitt, S. C., Bunch, D. O., Sar, M., Walker, V. R., Davis, B. J., Korach, K. S.** (1999) Postnatal sex reversal of the ovaries in mice lacking estrogen receptors alpha and beta. *Science.* **286**, 2328-2331.
18. **Curtis SK, Amann RP.** (1981) Testicular development and establishment of spermatogenesis in Holstein bulls. *J Anim Sci.* **53**:1645-1657.
19. **DeFalco T, Camara N, Le Bras S, Van Doren M.** (2008) Nonautonomous sex determination controls sexually dimorphic development of the Drosophila gonad. *Dev Cell*. **14**: 275-286.
20. **Devkota B, Sasaki M, Matsui M, Amaya Montoya C, Miyake Y.** (2006) Alterations in the immunohistochemical localization patterns of alpha-smooth muscle actin (SMA) and vimentin in the postnatally developing bovine cryptorchid testis. *J Reprod Dev.* **52**:329-334.
21. **Ding LJ, Yan GJ, Ge QY, Yu F, Zhao X, Diao ZY, Wang ZQ, Yang ZZ, Sun HX, Hu YL.** (2011) FSH acts on the proliferation of type A spermatogonia via Nur77 that increases GDNF expression in the Sertoli cells. *FEBS Lett*. **585**:2437-2444.
22. **Dominguez MM, Liptrap RM, Croy BA, Basrur PK.** (1990) Hormonal correlates of ovarian alterations in bovine freemartin fetuses. *Anim Reprod Sci.* **22**:181-201.
23. **Dupont, S., Dennefeld, C., Krust, A., Chambon, P., Mark, M.** (2003) Expression of Sox9 in granulosa cells lacking the estrogen receptors, ERalpha and ERbeta. *Dev Dyn.* **226**, 103-106.
24. **Foster JW, Dominguez-Steglich MA, Guioli S, Kwok C, Weller PA, Stevanovic M, Weissenbach J, Mansour S, Young ID, Goodfellow PN, et al.** (1994) Campomelic dysplasia and autosomal sex reversal caused by mutations in an SRY-related gene. *Nature.* **372**:525-530.
25. **Foster JW, Graves JA.** (1994) An SRY-related sequence on the marsupial X chromosome: implications for the evolution of the mammalian testis-determining gene. *Proc Natl Acad Sci U S A*. 91:1927-1931.
26. **Garcia-Ortiz, J. E., Pelosi, E., Omari, S., Nedorezov, T., Piao, Y., Karmazin, J., Uda, M., Cao, A., Cole, S. W., Forabosco, A., et al.** (2009) Foxl2 functions in sex determination and histogenesis throughout mouse ovary development. *BMC Dev Biol*. **9**, 36-57.
27. **Georg I, Barrionuevo F, Wiech T, Scherer G.** (2012) Sox9 and Sox8 Are Required for Basal Lamina Integrity of Testis Cords and for Suppression of FOXL2 During Embryonic Testis Development in Mice. *Biol Reprod*. **87**:99.
28. **Ghanem ME, Nakao T, Nishibori M.** (2006) Deficiency of uridine monophosphate synthase (DUMPS) and X-chromosome deletion in fetal mummification in cattle. *Anim Reprod Sci.* **91**:45-54.
29. **Ghanem ME, Yoshida C, Nishibori M, Nakao T, Yamashiro H.** (2005) A case of freemartin with atresia recti and ani in Japanese Black calf. *Anim Reprod Sci*. **85**:193-199.
30. **Graham P, Penn JK, Schedl P.** (2003) Masters change, slaves remain. Bioessays. **25**:1-4.
31. **Gregoire EP, Lavery R, Chassot AA, Akiyama H, Treier M, Behringer RR, Chaboissier MC.** (2011) Transient development of ovotestes in XX Sox9 transgenic mice. *Dev Biol*. **349**:65-77.
32. **Guigon CJ, Magre S.** (2006) Contribution of germ cells to the differentiation and

maturation of the ovary: insights from models of germ cell depletion. *Biol Reprod*. **74**:450-458.

33. **Harry JL, Koopman P, Brennan FE, Graves JA, Renfree MB.** (1995) Widespread expression of the testis-determining gene SRY in a marsupial. *Nat Genet*. **11**:347-349.
34. **Hatano O, Takayama K, Imai T, Waterman MR, Takakusu A, Omura T, Morohashi K.** (1994) Sex-dependent expression of a transcription factor, Ad4BP, regulating steroidogenic P-450 genes in the gonads during prenatal and postnatal rat development. *Development.* **120**:2787-2797.
35. **Hattori RS, Murai Y, Oura M, Masuda S, Majhi SK, Sakamoto T, Fernandino JI, Somoza GM, Yokota M, Strüssmann CA.** (2012) A Y-linked anti-Müllerian hormone duplication takes over a critical role in sex determination. *Proc Natl Acad Sci U S A.* **109**:2955-2959.
36. **Hiramatsu, R., Harikae, K., Tsunekawa, N., Kurohmaru, M., Matsuo, I., Kanai, Y.** (2010) FGF signaling directs a center-to-pole expansion of tubulogenesis in mouse testis differentiation. *Development.* **137**, 303-312.
37. **Hiramatsu, R., Kanai, Y., Mizukami, T., Ishii, M., Matoba, S., Kanai-Azuma, M., Kurohmaru, M., Kawakami, H., Hayashi, Y.** (2003) Regionally distinct potencies of mouse XY genital ridge to initiate testis differentiation dependent on anteroposterior axis. *Dev Dyn*. **228**, 247-253.
38. **Hiramatsu, R., Matoba, S., Kanai-Azuma, M., Tsunekawa, N., Katoh-Fukui, Y., Kurohmaru, M., Morohashi, K., Wilhelm, D., Koopman, P., Kanai, Y.** (2009) A critical time window of Sry action in gonadal sex determination in mice. *Development.* **136**, 129-138.
39. **Ikeda, Y., Takeda, Y., Shikayama, T., Mukai, T., Hisano, S., Morohashi, K.** (2001) Comparative localization of Dax-1 and Ad4BP/SF-1 during development of the hypothalamic-pituitary-gonadal axis suggests their closely related and distinct functions. *Dev. Dyn*. **220**, 363-376.
40. **Jameson, S.A., Natarajan, A., Cool, J., DeFalco, T., Maatouk, D.M., Mork, L., Munger, S.C., Capel, B.** (2012) Temporal transcriptional profiling of somatic and germ cells reveals biased lineage priming of sexual fate in the fetal mouse gonad. *PLoS Genet*. **8**:e1002575.
41. **Jiménez R, Burgos M, Sánchez A, Sinclair AH, Alarcón FJ, Marín JJ, Ortega E, Díaz de la Guardia R.** (1993) Fertile females of the mole Talpa occidentalis are phenotypic intersexes with ovotestes. *Development*. 118:1303-1311.
42. **Jorgensen JS, Gao L.** (2005) Irx3 is differentially up-regulated in female gonads during sex determination. *Gene Expr Patterns*. **5**, 756-762.
43. **JOST A.** (1947) The age factor in the castration of male rabbit fetuses. *Proc Soc Exp Biol Med*. **66**:302.
44. **Jost A, Vigier B, Prepin J.** (1972) Freemartins in cattle: the first steps of sexual organogenesis. *J Reprod Fertil*. **29**:349-379.
45. **Kamiya T, Kai W, Tasumi S, Oka A, Matsunaga T, Mizuno N, Fujita M, Suetake H, Suzuki S, Hosoya S. et al.** (2012) A trans-species missense SNP in Amhr2 is associated with sex determination in the tiger pufferfish, Takifugu rubripes (fugu). *PLoS Genet*. **8**:e1002798.
46. **Karl, J. and Capel, B.** (1998). Sertoli cells of the mouse testis originate from the coelomic epithelium. *Dev. Biol.* **203**, 323-333.
47. **Kashimada K, Pelosi E, Chen H, Schlessinger D, Wilhelm D, Koopman P.** (2011)

FOXL2 and BMP2 act cooperatively to regulate follistatin gene expression during ovarian development. Endocrinology. **152**:272-280.

48. Kelley RL, Wang J, Bell L, Kuroda MI. (1997) Sex lethal controls dosage compensation in Drosophila by a non-splicing mechanism. *Nature*. **387**:195-199.

49. Kent, J., Wheatley, S. C., Andrews, J. E., Sinclair, A. H. and Koopman, P. (1996) A male-specific role for SOX9 in vertebrate sex determination. *Development* **122**, 2813-2822.

50. Khan MZ, Foley GL. (1994) Retrospective studies on the measurements, karyotyping and pathology of reproductive organs of bovine freemartins. *J Comp Pathol*. **110**:25-36.

51. Kidokoro, T., Matoba, S., Hiramatsu, R., Fujisawa, M., Kanai-Azuma, M., Taya, C., Kurohmaru, M., Kawakami, H., Hayashi, Y., Kanai, Y., et al. (2005) Influence on spatiotemporal patterns of a male-specific Sox9 activation by ectopic Sry expression during early phases of testis differentiation in mice. *Dev. Biol*. **278**, 511-525.

52. Kim, B., Kim, Y., Cooke, P.S., Rüther, U., Jorgensen, J.S. (2011) The fused toes locus is essential for somatic-germ cell interactions that foster germ cell maturation in developing gonads in mice. *Biol Reprod.* **84**, 1024-1032.

53. Kim, Y., Kobayashi, A., Sekido, R., DiNapoli, L., Brennan, J., Chaboissier, M. C., Poulat, F., Behringer, R. R., Lovell-Badge, R., Capel, B. (2006) Fgf9 and Wnt4 act as antagonistic signals to regulate mammalian sex determination. *PLoS Biol*. **4**, e187.

54. Koopman P, Gubbay J, Vivian N, Goodfellow P, Lovell-Badge R. (1991) Male development of chromosomally female mice transgenic for Sry. *Nature*. **351**:117-121.

55. Klüver N, Pfennig F, Pala I, Storch K, Schlieder M, Froschauer A, Gutzeit HO, Schartl M. (2007) Differential expression of anti-Müllerian hormone (amh) and anti-Müllerian hormone receptor type II (amhrII) in the teleost medaka. *Dev Dyn*. **236**:271-281.

56. Lee, H. J., Pazin, D. E., Kahlon, R. S., Correa, S. M., Albrecht, K. H. (2009) Novel markers of early ovarian pre-granulosa cells are expressed in an Sry-like pattern. *Dev Dyn.* **238**, 812-825.

57. Lei N, Heckert LL. (2002) Sp1 and Egr1 regulate transcription of the Dmrt1 gene in Sertoli cells. *Biol Reprod*. **66**:675-684.

58. Lillie FR. (1917) Sex-Determination and Sex-Differentiation in Mammals. *Proc Natl Acad Sci U S A*. **3**:464-470.

59. Liu, C. F., Bingham, N., Parker, K., Yao, H. H. (2009) Sex-specific roles of beta-catenin in mouse gonadal development. *Hum Mol Genet.* **18**, 405-417.

60. Ludbrook, L.M., Bernard, P., Bagheri-Fam, S., Ryan, J., Sekido, R., Wilhelm, D., Lovell-Badge, R., Harley, V.R. (2012) Excess DAX1 Leads to XY Ovotesticular Disorder of Sex Development (DSD) in Mice by Inhibiting Steroidogenic Factor-1 (SF1) Activation of the Testis Enhancer of SRY-box-9 (Sox9). *Endocrinology*. in press

61. Maatouk, D. M., DiNapoli, L., Alvers, A., Parker, K. L., Taketo, M. M., Capel, B. (2008) Stabilization of beta-catenin in XY gonads causes male-to-female sex-reversal. *Hum Mol Genet*. **17**, 2949-2955.

62. Marcum JB. (1974) The freemartin syndrome. *Anim. Breed. Abstr*. **42**: 227-242.

63. Matoba, S., Kanai, Y., Kidokoro, T., Kanai-Azuma, M., Kawakami, H., Hayashi, Y., Kurohmaru, M. (2005) A novel Sry-downstream cellular event which preserves the readily available energy source of glycogen in mouse sex differentiation. *J. Cell Sci*. **118**,

1449-1459.

64. **Matoba, S., Hiramatsu, R., Kanai-Azuma, M., Tsunekawa, N., Harikae, K., Kawakami, H., Kurohmaru, M., Kanai, Y.** (2008). Establishment of testis-specific SOX9 activation requires high-glucose metabolism in mouse sex differentiation. *Dev. Biol.* **324**, 76-87.
65. **Matson, C.K., Murphy, M.W., Sarver, A.L., Griswold, M.D., Bardwell, V.J., Zarkower, D.** (2011) DMRT1 prevents female reprogramming in the postnatal mammalian testis. *Nature.* **476**, 101-104.
66. **Matsuda M, Nagahama Y, Shinomiya A, Sato T, Matsuda C, Kobayashi T, Morrey CE, Shibata N, Asakawa S, Shimizu N, Hori H, Hamaguchi S, Sakaizumi M.** (2002) DMY is a Y-specific DM-domain gene required for male development in the medaka fish. *Nature.* **417**:559-563.
67. **Mawaribuchi S, Yoshimoto S, Ohashi S, Takamatsu N, Ito M.** (2012) Molecular evolution of vertebrate sex-determining genes. *Chromosome Res*. **20**:139-151.
68. **McElreavey K, Vilain E, Abbas N, Herskowitz I, Fellous M.** (1993) A regulatory cascade hypothesis for mammalian sex determination: SRY represses a negative regulator of male development. *Proc Natl Acad Sci U S A*. **90**:3368-3372.
69. **Meng X, Lindahl M, Hyvönen ME, Parvinen M, de Rooij DG, Hess MW, Raatikainen-Ahokas A, Sainio K, Rauvala H, Lakso M, Pichel JG, Westphal H, Saarma M, Sariola H.** (2000) Regulation of cell fate decision of undifferentiated spermatogonia by GDNF. *Science.* **287**:1489-1493.
70. **Miller JR, Koopman M.** (1990) Isolation and characterization of two male-specific DNA fragments from the bovine gene. *Anim Genet.* **21**:77-82.
71. **Mizusaki, H., Kawabe, K., Mukai, T., Ariyoshi, E., Kasahara, M., Yoshioka, H., Swain, A., Morohashi, K.** (2003) Dax-1 (dosage-sensitive sex reversal-adrenal hypoplasia congenita critical region on the X chromosome, gene 1) gene transcription is regulated by wnt4 in the female developing gonad. *Mol. Endocrinol*. **17**, 507-519.
72. **Morais da Silva, S., Hacker, A., Harley, V., Goodfellow, P., Swain, A., Lovell-Badge, R.** (1996) Sox9 expression during gonadal development implies a conserved role for the gene in testis differentiation in mammals and birds. *Nat Genet.* **14**, 62-68.
73. **Mork, L., Maatouk, D.M., McMahon, J.A., Guo, J.J., Zhang, P., McMahon, A.P., Capel, B.** (2012) Temporal differences in granulosa cell specification in the ovary reflect distinct follicle fates in mice. *Biol Reprod.* in press
74. **Munger, S. C., Aylor, D. L., Syed, H. A., Magwene, P. M., Threadgill, D. W., Capel, B.** (2009) Elucidation of the transcription network governing mammalian sex determination by exploiting strain-specific susceptibility to sex reversal. *Genes Dev.* **23**, 2521-2536.
75. **Munger SC, Capel B.** (2012) Sex and the circuitry: progress toward a systems-level understanding of vertebrate sex determination. *Wiley Interdiscip Rev Syst Biol Med*. **4**:401-412.
76. **Myosho T, Otake H, Masuyama H, Matsuda M, Kuroki Y, Fujiyama A, Naruse K, Hamaguchi S, Sakaizumi M.** (2012) Tracing the emergence of a novel sex-determining gene in medaka, Oryzias luzonensis. *Genetics*. 191:163-170.
77. **Nakamura M.** (2010) The mechanism of sex determination in vertebrates-are sex steroids the key-factor? *J Exp Zool A Ecol Genet Physiol*. **313**:381-398.
78. **Nakamura S, Watakabe I, Nishimura T, Picard JY, Toyoda A, Taniguchi Y, di Clemente N, Tanaka M.** (2012) Hyperproliferation of mitotically active germ cells due to defective anti-Müllerian hormone signaling mediates sex reversal in medaka.

Development. 139:2283-2287.

79. Nakanishi T, Yamaai T, Asano M, Nawachi K, Suzuki M, Sugimoto T, Takigawa M. (2001) Overexpression of connective tissue growth factor/hypertrophic chondrocyte-specific gene product 24 decreases bone density in adult mice and induces dwarfism. *Biochem Biophys Res Commun*. 281:678-681.

80. Nef, S., Schaad, O., Stallings, N. R., Cederroth, C. R., Pitetti, J. L., Schaer, G., Malki, S., Dubois-Dauphin, M., Boizet-Bonhoure, B., Descombes, P., et al. (2005) Gene expression during sex determination reveals a robust female genetic program at the onset of ovarian development. *Dev. Biol*. **287**, 361-377.

81. Oréal E, Mazaud S, Picard JY, Magre S, Carré-Eusèbe D. (2002) Different patterns of anti-Müllerian hormone expression, as related to DMRT1, SF-1, WT1, GATA-4, Wnt-4, and Lhx9 expression, in the chick differentiating gonads. *Dev Dyn*. **225**:221-232.

82. Ottolenghi, C., Omari, S., Garcia-Ortiz, J. E., Uda, M., Crisponi, L., Forabosco, A., Pilia, G., Schlessinger, D. (2005) Foxl2 is required for commitment to ovary differentiation. *Hum. Mol. Genet*. **14**, 2053-2062.

83. Ottolenghi, C., Pelosi, E., Tran, J., Colombino, M., Douglass, E., Nedorezov, T., Cao, A., Forabosco, A., Schlessinger, D. (2007a) Loss of Wnt4 and Foxl2 leads to female-to-male sex reversal extending to germ cells. *Hum. Mol. Genet*. **16**, 2795-2804.

84. Ottolenghi C, Uda M, Crisponi L, Omari S, Cao A, Forabosco A, Schlessinger D. (2007b) Determination and stability of sex. *Bioessays.* **29**:15-25.

85. Padula AM. (2005) The freemartin syndrome: an update. *Anim Reprod Sci*. **87**:93-109.

86. Pailhoux E, Vigier B, Chaffaux S, Servel N, Taourit S, Furet JP, Fellous M, Grosclaude F, Cribiu EP, Cotinot C, Vaiman D. (2001) A 11.7-kb deletion triggers intersexuality and polledness in goats. *Nat Genet.* **29**:453-458.

87. Parma, P., Radi, O., Vidal, V., Chaboissier, M. C., Dellambra, E., Valentini, S., Guerra, L., Schedl, A., Camerino, G. (2006) R-spondin1 is essential in sex determination, skin differentiation and malignancy. *Nat Genet.* **38**, 1304-1309.

88. Pask A, Renfree MB, Marshall Graves JA. (2000) The human sex-reversing ATRX gene has a homologue on the marsupial Y chromosome, ATRY: implications for the evolution of mammalian sex determination. *Proc Natl Acad Sci U S A*. **97**:13198-13202.

89. Payan-Carreira R, Pires MA, Quaresma M, Chaves R, Adega F, Guedes Pinto H, Colaco B, Villar V. (2008) A complex intersex condition in a Holstein calf. *Anim Reprod Sci*. **103**:154-163.

90. Probst FJ, Cooper ML, Cheung SW, Justice MJ. (2008) Genotype, phenotype, and karyotype correlation in the XO mouse model of Turner Syndrome. *J Hered*. **99**:512-517

91. Raymond CS, Shamu CE, Shen MM, Seifert KJ, Hirsch B, Hodgkin J, Zarkower D. (1998) Evidence for evolutionary conservation of sex-determining genes. *Nature*. **391**:691-695.

92. Rota A, Ballarin C, Vigier B, Cozzi B, Rey R. (2002) Age dependent changes in plasma anti-Mullerian hormone concentrations in the bovine male, female, and freemartin from birth to puberty: relationship between testosterone production and influence on sex differentiation. *Gen Comp Endocrinol*. **129**:39-44.

93. Sato T, Aiyama Y, Ishii-Inagaki M, Hara K, Tsunekawa N, Harikae K, Uemura-Kamata M, Shinomura M, Zhu XB, Maeda S, Kuwahara-Otani S, Kudo A, Kawakami H, Kanai-Azuma M, Fujiwara M, Miyamae Y, Yoshida S,

Seki M, Kurohmaru M, Kanai Y. (2011) Cyclical and patch-like GDNF distribution along the basal surface of Sertoli cells in mouse and hamster testes. *PLoS One.* **6**:e28367.

94. Schmahl, J., Capel, B. (2003) Cell proliferation is necessary for the determination of male fate in the gonad. *Dev Biol*. **258**, 264-276.

95. Schmahl, J., Eicher, E. M., Washburn, L. L. and Capel, B. (2000) Sry induces cell proliferation in the mouse gonad. *Development* **127**, 65-73.

96. Schmidt, D., Ovitt, C. E., Anlag, K., Fehsenfeld, S., Gredsted, L., Treier, A. C., Treier, M. (2004) The murine winged-helix transcription factor Foxl2 is required for granulosa cell differentiation and ovary maintenance. *Development* **131**, 933-942.

97. Schmidt JA, Avarbock MR, Tobias JW, Brinster RL. (2009) Identification of glial cell line-derived neurotrophic factor-regulated genes important for spermatogonial stem cell self-renewal in the rat. *Biol Reprod*. **81**:56-66.

98. Sekido, R., Bar, I., Narvaez, V., Penny, G. and Lovell-Badge, R. (2004) SOX9 is up-regulated by the transient expression of SRY specifically in Sertoli cell precursors. *Dev. Biol*. **274**, 271-279.

99. Sekido, R. and Lovell-Badge, R. (2008) Sex determination involves synergistic action of SRY and SF1 on a specific Sox9 enhancer. *Nature* **453**, 930-934.

100. Sekido R, Lovell-Badge R. (2009) Sex determination and SRY: down to a wink and a nudge? *Trends Genet*. 25:19-29.

101. Sinclair AH, Berta P, Palmer MS, Hawkins JR, Griffiths BL, Smith MJ, Foster JW, Frischauf AM, Lovell-Badge R, Goodfellow PN. (1990) A gene from the human sex-determining region encodes a protein with homology to a conserved DNA-binding motif. *Nature*. 346:240-244.

102. Sinowatz F, Amselgruber W. (1986) Postnatal development of bovine Sertoli cells. *Anat Embryol*. **174**:413-423.

103. Smith CA, Roeszler KN, Ohnesorg T, Cummins DM, Farlie PG, Doran TJ, Sinclair AH. (2009) The avian Z-linked gene DMRT1 is required for male sex determination in the chicken. *Nature.* **461**:267-71.

104. Smith KC, Parkinson TJ, Pearson GR, Sylvester L, Long SE. (2003) Morphological, histological and histochemical studies of the gonads of ovine freemartins. *Vet Rec.* **152**:164-169.

105. Swain, A., Narvaez, V., Burgoyne, P., Camerino, G., Lovell-Badge, R. (1998) Dax1 antagonizes Sry action in mammalian sex determination. *Nature.* **391**, 761-767.

106. Taketo-Hosotani T. (1987) Factors involved in the testicular development from fetal mouse ovaries following transplantation. *J Exp Zool*. **241**:95-100.

107. Taketo T, Saeed J, Manganaro T, Takahashi M, Donahoe PK. (1993) Müllerian inhibiting substance production associated with loss of oocytes and testicular differentiation in the transplanted mouse XX gonadal primordium. *Biol Reprod*. **49**:13-23.

108. Taketo, T., Merchant-Larios, H. (1986) Gonadal sex reversal of fetal mouse ovaries following transplantation into adult mice. *Prog Clin Biol Res.* **217A**,171-174.

109. Taketo, T., Merchant-Larios, H., Koide, S. S. (1984) Induction of testicular differentiation in the fetal mouse ovary by transplantation into adult male mice. *Proc Soc Exp Biol Med.* **176**, 148-153.

110. Tomizuka, K., Horikoshi, K., Kitada, R., Sugawara, Y., Iba, Y., Kojima, A., Yoshitome, A., Yamawaki, K., Amagai, M., Inoue, A., et al. (2008) R-spondin1 plays an essential role in ovarian development through positively regulating Wnt-4 signaling.

Hum Mol Genet. **17**, 1278-1291.

111. Tourtellotte WG, Nagarajan R, Bartke A, Milbrandt J. (2000) Functional compensation by Egr4 in Egr1-dependent luteinizing hormone regulation and Leydig cell steroidogenesis. *Mol Cell Biol*. 20:5261-5268.

112. Toyooka Y, Tsunekawa N, Takahashi Y, Matsui Y, Satoh M, Noce T. (2000) Expression and intracellular localization of mouse Vasa-homologue protein during germ cell development. *Mech Dev.* **93**:139-149.

113. Tsai MY, Yeh SD, Wang RS, Yeh S, Zhang C, Lin HY, Tzeng CR, Chang C. (2006) Differential effects of spermatogenesis and fertility in mice lacking androgen receptor in individual testis cells. *Proc Natl Acad Sci U S A.* **103**:18975-18980.

114. Uda, M., Ottolenghi, C., Crisponi, L., Garcia, J. E., Deiana, M., Kimber, W., Forabosco, A., Cao, A., Schlessinger, D., Pilia, G. (2004) Foxl2 disruption causes mouse ovarian failure by pervasive blockage of follicle development. *Hum. Mol. Genet*. **13**, 1171-1181.

115. Uhlenhaut, N. H., Jakob, S., Anlag, K., Eisenberger, T., Sekido, R., Kress, J., Treier, A.C., Klugmann, C., Klasen, C., Holter, N. I., et al. (2009) Somatic sex reprogramming of adult ovaries to testes by FOXL2 ablation. *Cell.* **139**, 1130-1142.

116. Vaiman D, Pailhoux E. (2000) Mammalian sex reversal and intersexuality: deciphering the sex-determination cascade. *Trends Genet*. **16**:488-494.

117. Vainio, S., Heikkila, M., Kispert, A., Chin, N. and McMahon, A. P. (1999) Female development in mammals is regulated by Wnt-4 signalling. *Nature* **397**, 405-409.

118. Valenzuela N, Neuwald JL, Literman R. Transcriptional evolution underlying vertebrate sexual development. *Dev Dyn.* in press

119. Vidal VP, Chaboissier MC, de Rooij DG, Schedl A. (2001) Sox9 induces testis development in XX transgenic mice. *Nat Genet.* **28**:216-217.

120. Vigier B, Tran D, Legeai L, Bezard J, Josso N. (1984) Origin of anti-Mullerian hormone in bovine freemartin fetuses. *J Reprod Fertil.* **70**:473-479.

121. Vigier B, Watrin F, Magre S, Tran D, Josso N. (1987) Purified bovine AMH induces a characteristic freemartin effect in fetal rat prospective ovaries exposed to it in vitro. *Development.* **100**:43-55.

122. Wagner T, Wirth J, Meyer J, Zabel B, Held M, Zimmer J, Pasantes J, Bricarelli FD, Keutel J, Hustert E, et al. (1994) Autosomal sex reversal and campomelic dysplasia are caused by mutations in and around the SRY-related gene SOX9. *Cell.* **79**:1111-1120.

123. Wilhelm, D., Martinson, F., Bradford, S., Wilson, M. J., Combes, A. N., Beverdam, A., et al. (2005) Sertoli cell differentiation is induced both cell-autonomously and through prostaglandin signaling during mammalian sex determination. *Dev. Biol*. **287**, 111-124.

124. Wilson EB. (1902) MENDEL'S PRINCIPLES OF HEREDITY AND THE MATURATION OF THE GERM-CELLS. *Science.* **16**:991-993.

125. Yano A, Guyomard R, Nicol B, Jouanno E, Quillet E, Klopp C, Cabau C, Bouchez O, Fostier A, Guiguen Y. (2012) An immune-related gene evolved into the master sex-determining gene in rainbow trout, Oncorhynchus mykiss. *Curr Biol*. 22:1423-1428.

126. Yao HH, Capel B. (2005) Temperature, genes, and sex: a comparative view of sex determination in Trachemys scripta and Mus musculus. *J Biochem.* **138**:5-12.

127. Yao HH, Whoriskey W, Capel B. (2002) Desert Hedgehog/Patched 1 signaling

specifies fetal Leydig cell fate in testis organogenesis. *Genes Dev*. 16:1433-1440.

128. Yoshimoto S, Okada E, Umemoto H, Tamura K, Uno Y, Nishida-Umehara C, Matsuda Y, Takamatsu N, Shiba T, Ito M. (2010) A W-linked DM-domain gene, DM-W, participates in primary ovary development in Xenopus laevis. *Proc Natl Acad Sci U S A*. **105**:2469-2474.